ROLE OF WHOLE-BODY MRI IN LYMPHOMA STAGING: A COMPARISON WITH COMPOSITE REFERENCE STANDARD, INCLUDING ^{18}F-FDG PET/CT

THESIS

Submitted to

ALL INDIA INSTITUE OF MEDICAL SCIENCES, JODHPUR

In partial fulfilment of the requirement for the degree of

DOCTOR OF MEDICINE (MD)

(RADIOLOGY)

JULY 2020

AIIMS, JODHPUR   **DR. LUNAVATH VEERANNA**

All India Institute of Medical Sciences, Jodhpur

CERTIFICATE

This is to certify that the thesis titled **"ROLE OF WHOLE-BODY MRI IN LYMPHOMA STAGING: A COMPARISON WITH COMPOSITE REFERENCE STANDARD INCLUDING ^{18}F-FDG-PET/CT"** is the bona fide work of Dr. L. Veeranna carried out under our guidance and supervision, in the Department of Diagnostic and Interventional Radiology, All India Institute of Medical Sciences, Jodhpur.

GUIDE

Dr. Taruna Yadav
Associate Professor
Department of Diagnostic and Interventional Radiology
AIIMS, Jodhpur

Dr. Pushpinder Singh Khera
Professor & Head
Department of Diagnostic and
Interventional Radiology,
AIIMS, Jodhpur.

Dr. Rajesh Kumar
Professor & Head
Department of Nuclear
Medicine,
AIIMS, Jodhpur.

Dr. Siyaram Didel
Associate Professor
Department of Pediatrics,
AIIMS, Jodhpur.

Dr. Puneet Pareek
Additional Professor & Head
Department of Radiation
Oncology,
AIIMS, Jodhpur

Dr. Binit Sureka
Additional Professor
Department of Diagnostic and
Interventional Radiology,
AIIMS, Jodhpur.

Dr. Poonam Elhence
Professor & Head
Department of Pathology and
Lab Medicine,
AIIMS, Jodhpur.

All India Institute of Medical Sciences, Jodhpur

<u>DECLARATION</u>

I hereby declare that the thesis titled **"ROLE OF WHOLE-BODY MRI IN LYMPHOMA STAGING: A COMPARISON WITH COMPOSITE REFERENCE STANDARD INCLUDING ^{18}F-FDG PET/CT"** embodies the original work carried out by the undersigned.

Dr. Lunavath Veeranna

Junior Resident

Department of Diagnostic and Interventional Radiology

All India Institute of Medical Sciences

Jodhpur

ACKNOWLEDGEMENT

INDEX

ABBREVIATIONS

^{18}F-FDG PET/ CT	F-18 fluoro-deoxy-glucose Positron Emission Tomography/ Computed Tomography
WB-MRI	Whole-Body MRI
STIR	Short Inversion tau recovery
DWI	Diffusion Weighted Imaging
T1W	T1 Weighted imaging
T2W	T2 Weighted
CT	Computed Tomography
CECT	Contrast enhanced computed tomography
FNAC	Fine Needle Aspiration Cytology
ADC	Apparent Diffusion Coefficient
TPR	True Positive Rate
FPR	False Positive Rate
HL	Hodgkin's lymphoma
NHL	Non-Hodgkin's lymphoma
NK	Natural killer
AJCC	American joint committee on cancer
PS	Parotid space
EAC	External Auditory Canal
RPS	Retropharyngeal space
IJV	Internal jugular vein
ICA	Internal carotid artery
IJC	Internal jugular chain
LN'S	Lymph nodes
SAC	Spinal accessory chain
TCC	Transverse cervical chain
EJV	External jugular vein
SCM	Sternocleidomastoid
CA	Carotid arteries
IASLC	International association of study by lung cancer
TEC	Thymic epithelial cell
MALT	Mucosa-associated lymphoid tissue
KSHV	Kaposi's sarcoma associated herpesvirus
HHV	Human herpes virus
NOS	Not otherwise specified
iAMP21	Intra chromosomal amplification of chromosome21
BCR	Breakpoint cluster region
ALK	Anaplastic lymphoma kinase

POEMS syndrome	Polyneuropathy, Organomegaly, Endocrinopathy, Monoclonal gammopathy, Skin changes
TEMPI	The telangiectasias, Elevated erythropoietin and Erythrocytosis, Monoclonal gammopathy, peripheral fluid collections, and intrapulmonary shunting
AESOP	Adenopathy and extensive skin patch overlying a plasmacytoma
CD	Cluster of differentiation
TFH	T-follicular helper
EBV	Epstein-Barr virus
CNS	Central nervous system
DLBCL	Diffuse large B-cell lymphoma
MIP	Maximum intensity projection
AIDS	Acquired Immunodeficiency syndrome.
HIV	Human Immunodeficiency Virus
IWG	International working group
MOPP	Mechlorethamine hydrochloride, Vincristine sulfate (oncovin), Procarbazine hydrochloride and Prednisone.
ABVD	Doxorubicin hydrochloride (Adriamycin), Bleomycin sulfate, Vinblastine sulfate and Dacarbazine.
BEACOPP	Bleomycin-etoposide-adriamycin-cyclophosphamide-oncovin-procarbazide-prednisone regimen.
R-CHOP	Rituximab, Cyclophosphamide, hydroxydaunorubicin hydrochloride (Doxorubicin hydrochloride), Vincristine (oncovin) and prednisone
R-CVP	Rituximab, Cyclophosphamide, Vincristine, and prednisone.
R-EPOCH	Rituximab, Etoposide phosphate, Prednisone, Vincristine sulfate (oncovin), Cyclophosphamide and Doxorubicin hydrochloride (hydroxydaunorubicin).

LIST OF TABLES

LIST OF FIGURES

ANNEXURES

Annexures No.	Title	Page no.
I	Ethical clearance certificate	108
II	Patient information sheet (English)	109
3	Patient information sheet (Hindi)	110
4	Participant informed consent form (English)	111
5	Participant informed consent form (Hindi)	112
6	Patient proforma	113
7	Master chart	

INTRODUCTION

The use of the terms lymphocytic leukaemia and lymphoma can be confusing in relation to lymphoid neoplasms. Leukaemia refers to neoplasms that manifest as widespread bone marrow and (often, but not always) peripheral blood involvement. The term "lymphoma" refers to proliferations that manifest as distinct tissue masses. These terms are often used interchangeably as lymphoma can present like leukaemia in incurable form and leukaemia can present as localized lymphomatous form[1].

Lymphomas are a heterogeneous group of blood cancers caused by the clonal proliferation of B or T lymphocytes. The two main types of lymphomas are Hodgkin's lymphoma and Non-Hodgkin's lymphomas. HL is classified into classical and non-classical types whereas NHL is further classified into B-cell, T-cell and natural killer (NK) cell types[2]. The Ann Arbor Staging System was originally designed for HL, but it is also used for NHL. Lymphoma constitutes about 5% to 6% of all malignancies[3]. Together Hodgkin lymphoma (HL) and non-Hodgkin lymphoma (NHL) are the third most common cancers in children[4].

The global age-standardized incidence rate of non-Hodgkin's lymphoma is 5.8 per 100000 and the age-standardized mortality rate of 2.6 per 100000. The global age-standardized incidence rates of non-Hodgkin lymphoma by sex in 2020, are 6.9 per 100000 in males and 4.8 per 100000 in females. Globally, Non-Hodgkin lymphoma accounted for 2.8% and 2.6% of all newly reported cancer-related cases and deaths in 2020[5]. The global incidence and mortality rates of Hodgkin lymphoma were 0.98 and 0.26 per 100,000 in 2020. Globally, Hodgkin lymphoma accounted for 0.4% and 0.2% of all newly reported cancer-related cases and deaths in 2020[6]. In India, the projected number of newly diagnosed cases of lymphoma was 52,942, out of which 1,320 cases were of Hodgkin lymphoma and 41,607 cases were of non-Hodgkin lymphoma. The projected crude incidence rate was 3.8 per 100000[7]. The incidence of HL peaks in the 20–30 age group, with a further peak in the elderly population. After 20 years, the risk of NHL rises dramatically with age[8].

Most of the cases of lymphoma are idiopathic however a number of etiological factors have been described including environmental factors, occupational exposure to

herbicides and pesticides (like Agent Orange), infectious agents (eg: HTLV, EBV, CMV, Campylobacter jejuni, H.pylori, Hep-C), immunodeficiency states (HIV) and genetic factors[2].

Patients with lymphoma, usually present with painless swelling of lymph nodes in the neck, armpits or groin, persistent fatigue, fever (more than 101°F), chills, night sweats, pruritus and unexplained weight loss of more than 10% of body mass over 6 months[9]. The clinical symptoms of lymphoma are illustrated in figure 1.
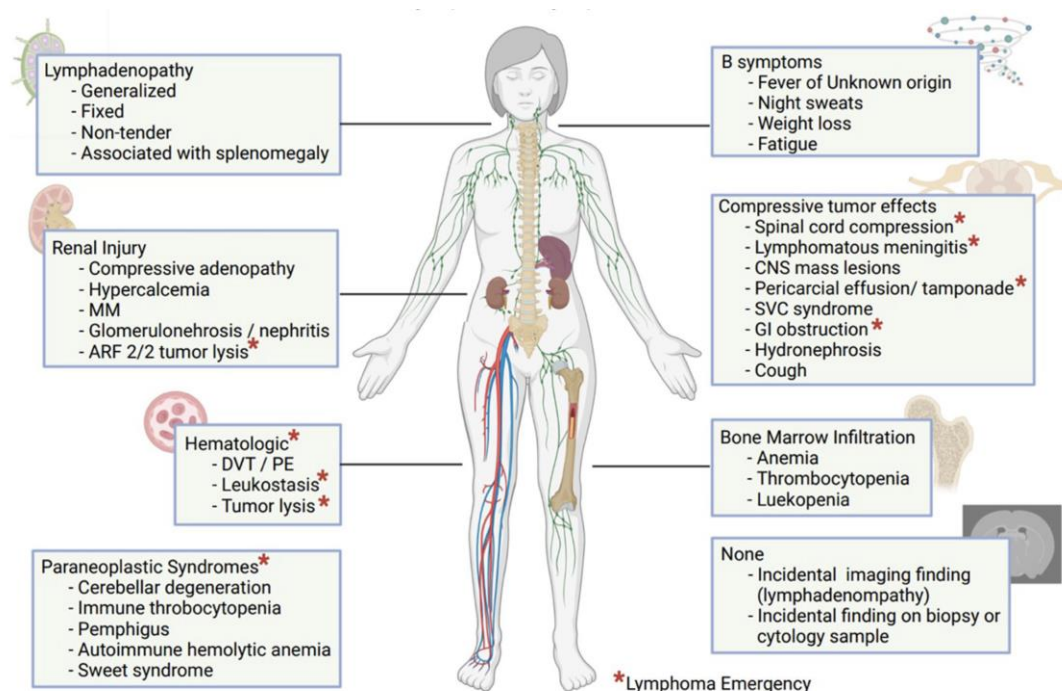
Figure 1: Clinical presentation of lymphoma[10]

Diagnosis of lymphoma depends on the morphology, immunohistochemistry, and flow cytometry. It is based on tissue samplings like FNAC, core biopsy, incision/ wedge biopsy, and excisional biopsy, among which excisional biopsy is considered the standard of care for initial diagnosis[11]. However, other modalities like ultrasound, CECT, PET/CT, and WB-MRI are also used in diagnosis, staging and interim response assessment.

On ultrasonography, involved lymph nodes will be enlarged and will show homogenous echotexture. They are usually round with a hypoechoic pseudocyst appearance due to the replacement of the node with lymphomatous tissue[12].

On computed tomography (CT), involved lymph nodes will be commonly enlarged with homogeneous density and the involved abdominal solid organs often manifest as multiple solid masses frequently demonstrating mild enhancement[13].

WB-MRI provides images from head to toe of the body including the patient's arms. In lymphoma, WB-MRI images can be acquired with various sequences including unenhanced T1- and T2-weighted, short tau inversion recovery and diffusion-weighted imaging (DWI). DWI sequence is based on the visualization and quantification of the random Brownian motion of water molecules in the biological tissues, assessed by apparent diffusion coefficient (ADC) – providing the functional evaluation of the tissue[14]. Lymphoma shows high cellularity and increased nuclear-to-cytoplasm ratio causing restricted diffusion of water molecules compared to normal tissues. This produces high signal intensity on DWI and low ADC values, which help in identifying the sites of disease[15].

^{18}F-FDG PET/CT provides functional and anatomical characteristics by mapping glucose metabolism using fluorine-18-fluoro-2-deoxy-d-glucose and anatomical correlations provided by CT. Since lymphomas have high FDG avidity and chemosensitivity, ^{18}F-FDG PET/CT has emerged as a promising tool for imaging-adapted treatment strategies[16]. Advances in molecular imaging with ^{18}F-FDG, have led to the use of ^{18}F-FDG PET/CT imaging for diagnosis, staging as well as response assessment in lymphoma patient[13]. Whole-body PET/CT scanning comes with significant radiation exposure and an increased risk of cancer. As a result, tests should be clinically necessary, and dosage reduction measures should be done[17]. The practice of surveillance computed tomography in lymphoma patients is associated with the risk of developing second primary malignancies, particularly those who undergo more than 8 CT scans during treatment and after primary tumours are in remission[18].

EMBRYOLOGY

During the embryological period, a number of endothelium-lined *lymph sacs develop*. Six major, recognizable lymph sacs, namely right and left *jugular sacs*, right and left *posterior (or iliac)* sacs, one *retroperitoneal sac* and the *cisterna chyli*. Lymphatic vessels then develop either via extension from the lymphatic sacs or they can develop de novo and spread into different tissues. These lymphatic channels also connect the lymphatic sacs and drain lymph from the head, neck, body wall and limbs. The *thoracic duct* and *right lymphatic duct* will develop from these lymphatic channels. As the growth progresses, these lymphatic sacs will be invaded by connective tissue and lymphocytes and are transformed into groups of lymph nodes[19].

RELEVANT ANATOMY

LYMPH NODE STATIONS.

1. **CERVICAL LYMPH NODES[20]**: Cervical lymph nodes are classified into different groups based on fundamental anatomic location or according to the AJCC surgical level criteria which are used for cancer management.

The anatomic descriptions include the following lymph node groups (other than those included in AJCC classification)

Parotid lymph nodes	Intra glandular nodes within the fascia circumscribing the PS
Periauricular lymph nodes	Pre-auricular – Nodes in subcutaneous plane anterior to EAC Post-auricular – Nodes in subcutaneous plane posterior to EAC
Retropharyngeal space (RPS) lymph nodes	Medial RPS nodes – in paramedian RPS in suprahyoid neck Lateral RPS nodes – lateral to pre-vertebral muscle & medial to IJV and ICA within the RPS.
Facial nodes	Mandibular nodes – superficial to mandible Buccinator nodes – within subcutaneous tissues of cheek Infra-orbital nodes – below orbits Malar nodes – along the mala eminence Zygomatic nodes – superficial to zygomatic arch
Occipital nodes	Within subcutaneous tissues posterior and inferior to calvarium

Cervical soft tissue nodes as 3 linear chains of LNs	Anteriorly, IJC nodes – surround IJV from skull base to thoracic inlet Posteriorly, SAC nodes – along course of spinal accessory nerve across the posterior cervical neck space Inferiorly, TCC nodes – along transverse cervical artery in supra-clavicular fossa connecting the inferior aspects of IJC and SAC
Anterior cervical lymph nodes	Pre-laryngeal chain– superficial midline cervical neck chain Pre-tracheal chain – follows EJV in superficial fascia of neck outside of the strap muscles. Para-tracheal chain - follows tracheoesophageal groove in visceral space of infra hyoid neck.
Supra-clavicular lymph nodes	Nodes within subclavian / Ho's triangle (Outlined by sternal & lateral clavicular ends and junction of neck and shoulder)

Table 1: Simple anatomic description of cervical lymph nodes.
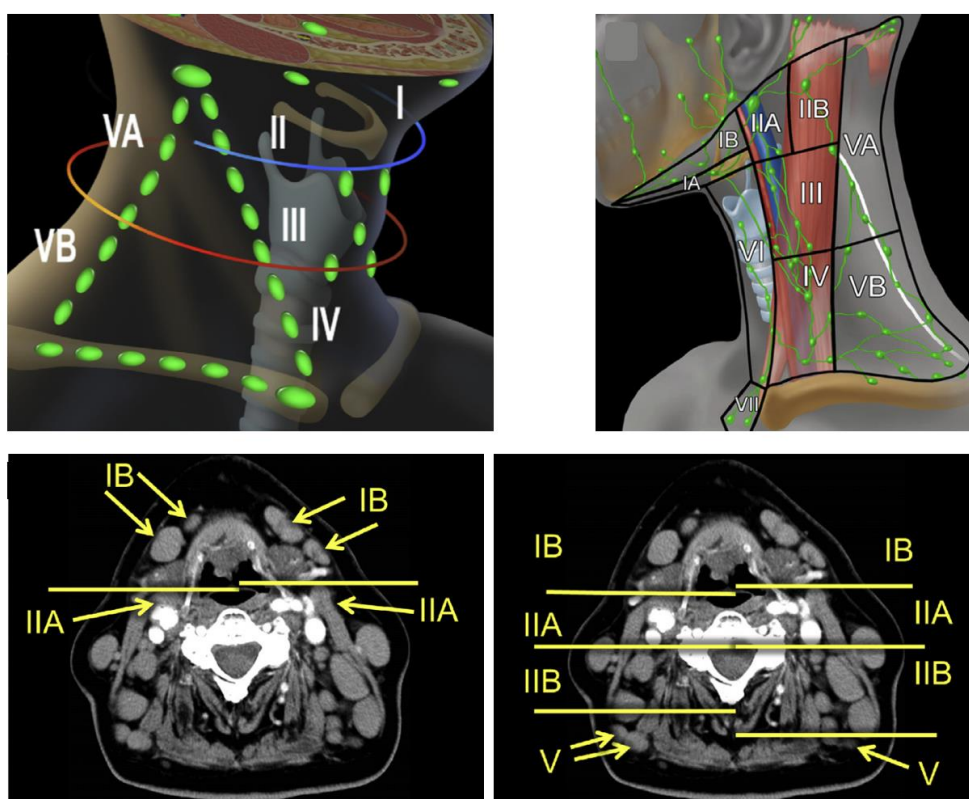
Figure 2: AJCC map of Cervical Lymph nodes[20]

Based on the surgical landmarks, the AJCC criteria classified the cervical lymph nodes into seven levels (Table 2).

Table 2: Cervical lymph node stations according to AJCC

Level	Location
Level I	
IA	Submental group – Nodes between anterior bellies of right & left digastric muscle, below the mandible.
IB	Submandibular group – nodes anterior to submandibular gland & lateral to anterior bellies of digastric muscle, in submandibular space.
Level II	Nodes in the upper portions of internal jugular chain and spinal accessory chain from the posterior belly of digastric muscle / skull base to the level of the hyoid bone
IIA	Nodes posterior to the posterior border of submandibular gland, may be located anterior, medial lateral or immediately posterior & adjacent to the internal jugular vein without a visible fat plane in between the node and IJV.
IIB	Nodes posterior to the internal jugular vein (IJV) with a fat plane between the node and IJV and center of node should be located anterior to the posterior margin of sternocleidomastoid (SCM).
Level III	Nodes along the internal jugular chain between the hyoid bone and the inferior margin of cricoid cartilage
Level IV	Nodes along the internal jugular chain, between the inferior margin of cricoid cartilage to supra clavicular fossa
Level V	Nodes of posterior cervical space corresponding to spinal accessory chain (SAC), lying posterior to posterior margin of sterno-cleido-mastoid (SCM) in coronal plane.
VA	Nodes in upper spinal accessory chain from the skull base to lower border of cricoid cartilage.
VB	Nodes in the lower spinal accessory chain from the lower border of cricoid cartilage to the supra clavicular fossa.
Level VI	Nodes in the visceral compartment of infra hyoid neck, from the hyoid bone superiorly to the suprasternal notch / upper border of manubrium

	inferiorly. The pre-laryngeal, pre-tracheal, para-tracheal (roughly all neck nodes inferior to thyroid) and trachea-esophageal nodes are included in this group. On each side the lateral border is formed by the medial border of the carotid sheath.
Level VII	Nodes in the superior mediastinum, from the superior border of manubrium sterni to the innominate vein and are located between the carotid arteries (CA).

THORACIC LYMPH NODES [21,22,23]: -

Fourteen distinct lymph node stations are identified by the "International Association of study by lung cancer" (IASLC) lymph node map, which can be grouped into seven zones

Zone 1 - Supra-clavicular Nodes

Station 1

- Includes right (1R) and left (1L) low cervical , supra-clavicular and sternal notch nodes
- From lower margin of cricoid to clavicles & upper border of the manubrium
- Divided into 1R & 1L with midline of the trachea as border in-between.

Zone 2 - Superior Mediastinal Nodes

Station 2 - Upper Paratracheal Nodes

- 2R - From the apex of right lung & pleural space and in midline upper border of manubrium to intersection of caudal margin of the innominate (left brachiocephalic) vein with trachea.
- 2L - From the apex of left lung & pleural space and in midline upper border of manubrium to superior border of the aortic arch.
- The boundary between 2R & 2L is left lateral tracheal wall (not midline of body).

Station 3 - Pre-vascular Nodes

- Anterior to the vessels
- From chest apex to carina.
- Sternum to anterior aspect of SVC on right side and anterior aspect of left common carotid artery on the left side.

Station 3P - Pre-vertebral / Retro-tracheal Nodes

- From chest apex to carina
- In retro-tracheal region / posterior to trachea / oesophagus

Station 4 - Lower Paratracheal Nodes

- 4R - From the intersection of the caudal margin of innominate (left brachiocephalic) vein with the trachea to the lower border of the azygous vein.
- 4L – From the superior border of the aortic arch to upper border of left main pulmonary artery & located medial to ligamentum arteriosum.
- The boundary between 4R & 4L is left lateral tracheal wall (not midline of body).

Zone 3 - Aorto-pulmonary Nodes

Station 5 – Subaortic (Aortopulmonary window) Nodes

- From the lower border of the aortic arch to upper border of left main pulmonary artery & located lateral to ligamentum arteriosum.

Station 6 – Para-aortic Nodes

- Located anterior & lateral to ascending aorta and aortic arch.
- From upper to lower border of aortic arch.

Zone 4 - Subcarinal Nodes

Station 7 - Subcarinal Nodes

- Carina to upper border of lower lobe bronchus on left and lower border of bronchus intermedius on right

Zone 5 - Inferior Mediastinal Nodes

Station 8 - Paraesophageal Nodes

- Lie adjacent to the wall of oesophagus and to the right & let of the midline.
- From upper border of lower lobe bronchus on left and lower border of bronchus intermedius on right to the diaphragm.

Station 9 - Pulmonary Ligament Nodes

- Nodes lying within the pulmonary ligaments (inferior pulmonary vein to diaphragm)

Zone 6 - Hilar and Interlobar Nodes

Station 10 – Hilar Nodes

, Lobar and (sub) segmental nodes 10-14

- Adjacent to main stem bronchus and hilar vessels.
- They extend from lower rim of azygous vein on the right and upper rim of the pulmonary artery on the left to the interlobar regions on both sides

Station 11 - Interlobar Nodes: between lobar bronchi origins

11s: between upper lobe bronchus and bronchus intermedius

11i: between middle and lower lobe bronchi

Zone 7 - Peripheral Nodes

Station 12: Adjacent to lobar bronchi

Station 13: Adjacent to segmental bronchi

Station 14: Adjacent to subsegmental bronchi
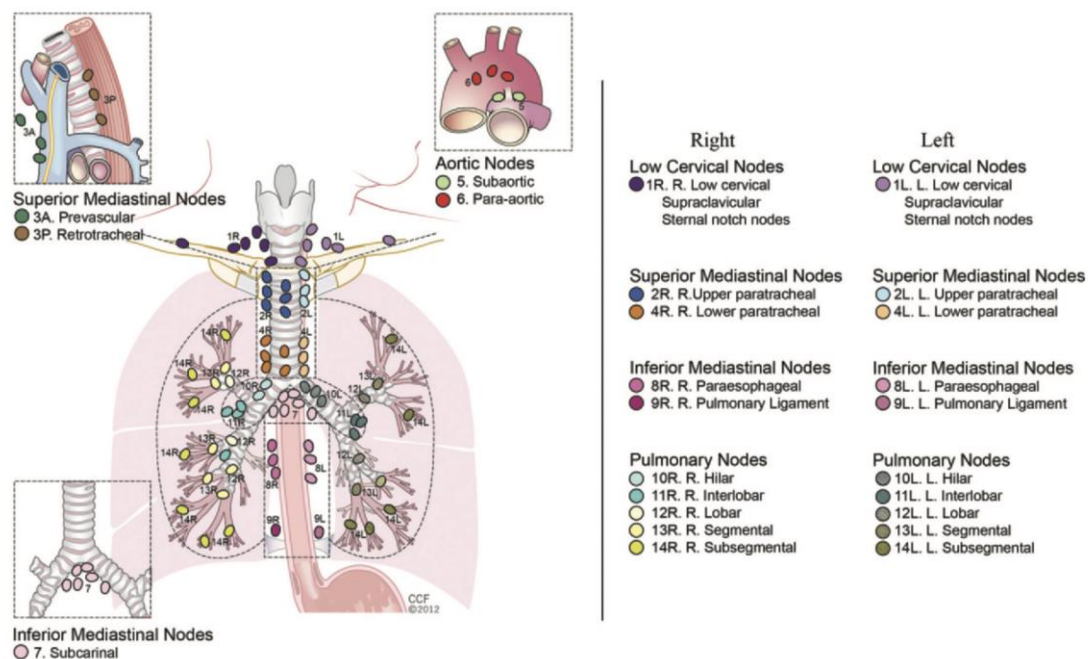
Figure 3: IASLC lymph node map illustration[23]

Other thoracic lymph nodes include internal mammary nodes, deep pectoral nodes, and cardio-phrenic nodes. Axillary nodes are also commonly involved in lymphoma.

ABDOMINOPELVIC LYMPHNODES[24,25].

Anatomically important abdominopelvic lymph nodes can be described in gastric, pancreatic, hepatic, small bowel & colonic, retroperitoneal, pelvic, peri vesicle, inguinal, abdominal wall and diaphragmatic stations. The perigastric lymph nodes can be further grouped into those located along the lesser curvature, greater curvature and second-tier perigastric lymph nodes. The important nodes along lesser curvature are right paracardial lymph nodes, lesser curvature nodes along branches of left & right gastric arteries and supra pyloric nodes. The important nodes along lesser curvature are

left paracardial lymph nodes, greater curvature nodes along the short gastric artery, left gastroepiploic artery & right distal gastroepiploic artery and infra pyloric artery. The second-Tier peri gastric lymph nodes are left gastric artery nodes, common hepatic artery nodes, celiac trunk artery nodes, hepato-duodenal ligament nodes, left hepato-duodenal ligament nodes, posterior hepato-duodenal ligament nodes and omental foramen nodes. The peripancreatic lymph node group includes anterior pancreaticoduodenal lymph nodes, posterior pancreaticoduodenal / retro-pancreatic lymph nodes, inferior pancreaticoduodenal lymph nodes, nodes along the dorsal pancreatic artery & splenic artery and splenic hilar lymph nodes. The superficial lymphatic drainage of the liver is through the gastro-hepatic, hepatoduodenal ligament nodes, and diaphragmatic lymph node plexus. The deep lymphatic drainage of the liver is through cystic nodes and hepato-duodenal ligament lymph nodes. The lymph nodes draining the small bowel are juxta intestinal nodes, intermediate mesenteric nodes and central superior mesenteric nodes. The colic lymph nodes and superior mesenteric nodes drain the ascending colon and proximal two-thirds of the transverse colon. The inferior mesenteric and colic lymph nodes drain the distal one-third of the transverse colon, the descending colon, the sigmoid colon and the upper rectum. The internal iliac nodes drain the lower rectum and anal canal above the pectinate line while superficial inguinal nodes drain the anal canal below the pectinate line.
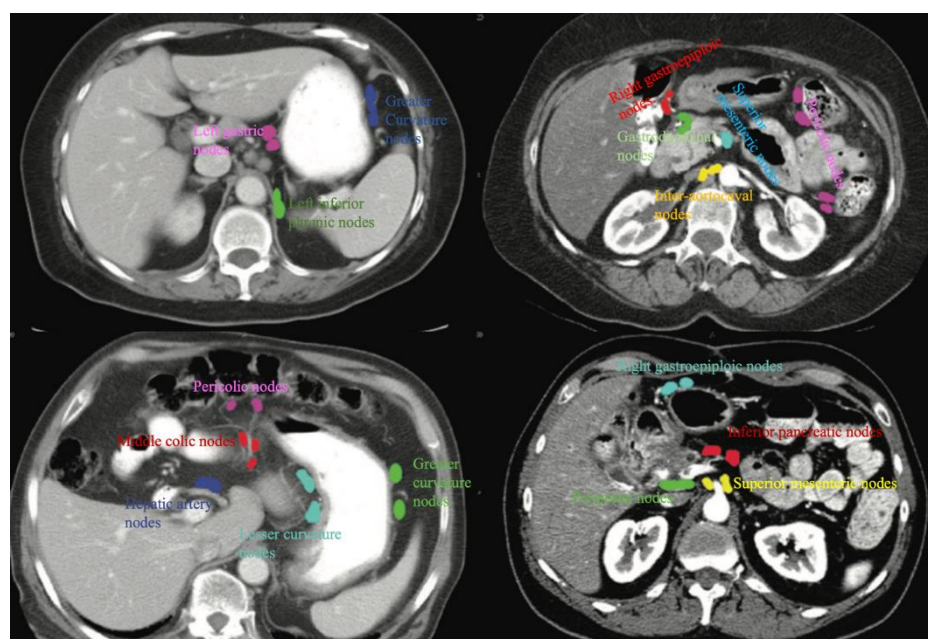
Figure 4: Axial images showing the location of abdominal lymph nodes[24].
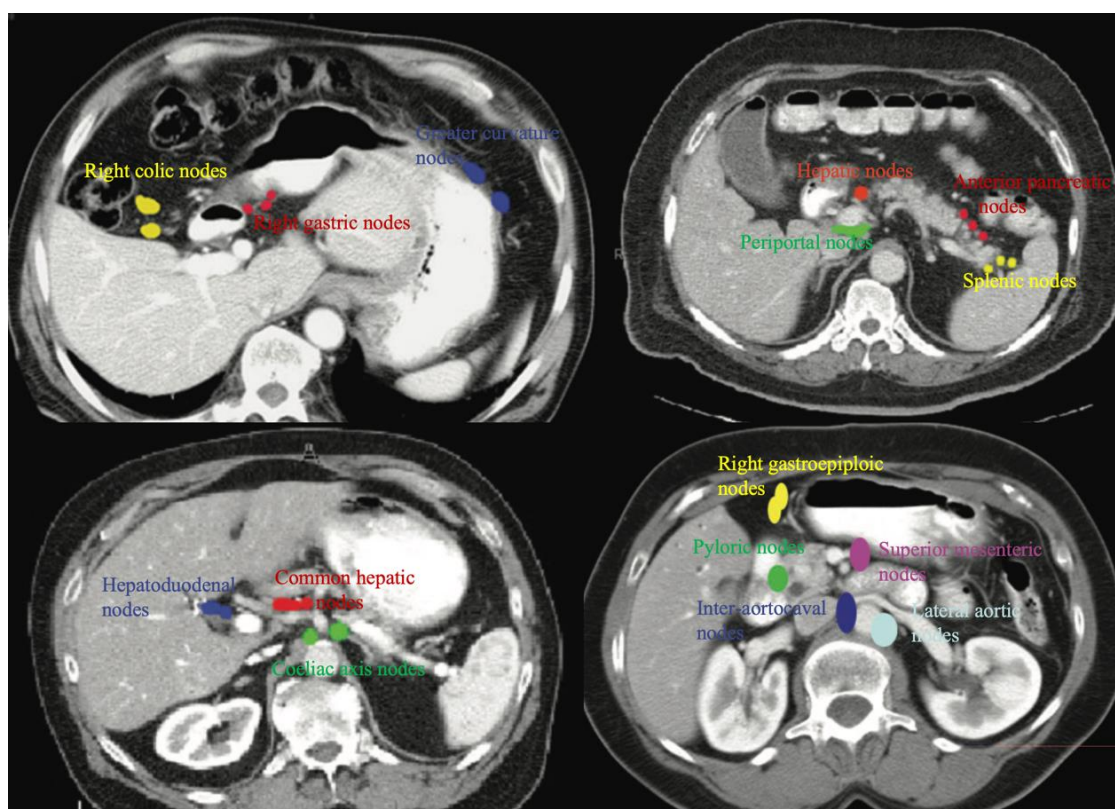
Figure 5: Axial images showing the location of abdominal lymph nodes[cntd].
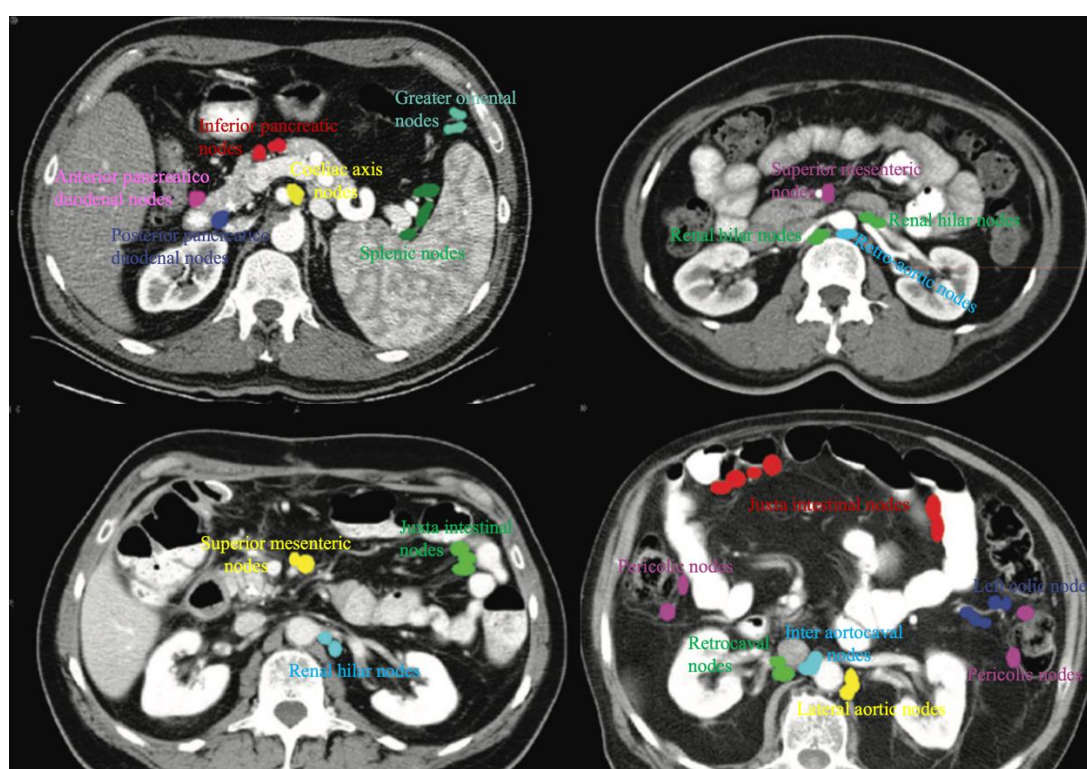
Figure 6: Axial images showing the location of abdominal lymph nodes[cntd].
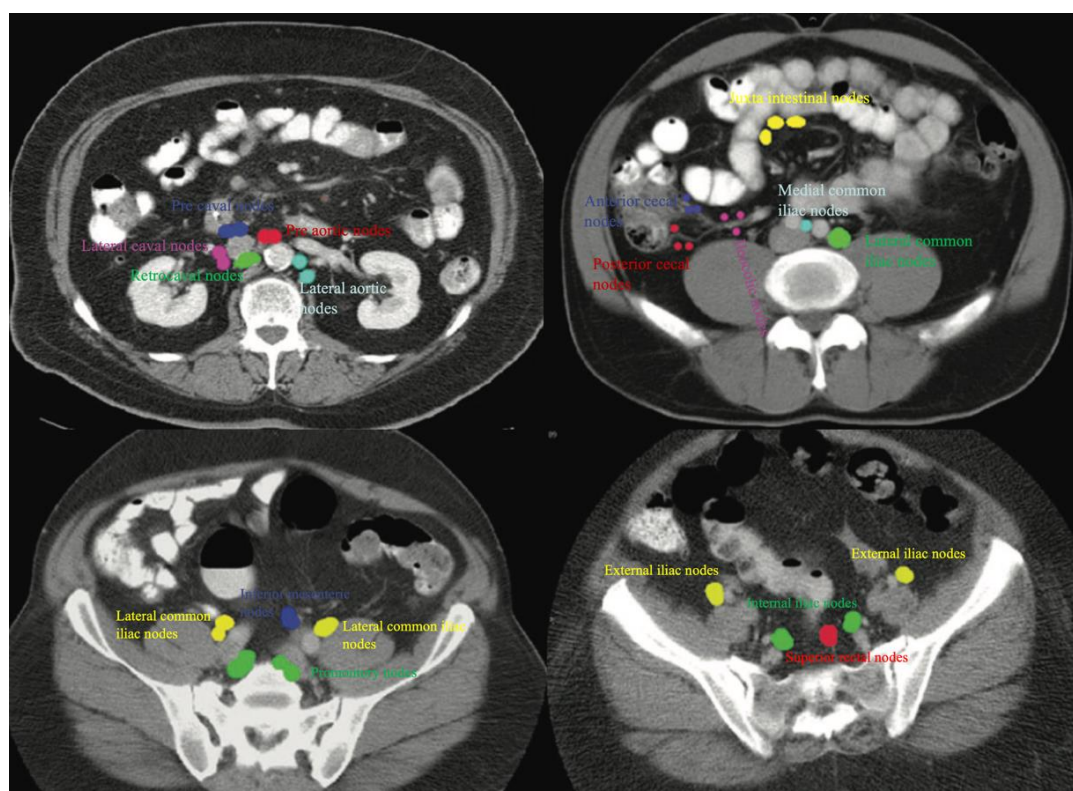
Figure 7: Axial images showing the location of abdominal lymph nodes[cntd].

The five major groups of the retroperitoneal and pelvic LNs are paraaortic, common iliac, internal iliac, external iliac, and inguinal. Based on their connections to the aorta and IVC, paraaortic LNs can be further categorised into seven groups: retrocaval, precaval, latero-caval, aortocaval, pre-aortic, retro aortic, and lateral aortic groups. The perivisceral lymph nodes include perirectal, peri vesical, and peri prostatic lymph nodes. The inguinal lymph nodes include superficial inguinal lymph nodes and deep inguinal lymph nodes. The superficial femoral vein and saphenous vein are accompanied by the superficial inguinal nodes, which are situated in the subcutaneous tissue anterior to the inguinal ligament. Deep inguinal LNs are visible posterior to the inguinal ligament and inferior to the beginnings of the inferior epigastric and iliac circumflex arteries. The lymph nodes of the anterior abdominal wall include supra & infra umbilical lymph nodes which constitute the superficial system of the anterior abdominal wall lymph nodes. The superior & inferior epigastric lymph nodes constitute the deep system of the anterior abdominal wall lymph nodes. The posterior abdominal wall lymph node group includes the nodes along the superficial circumflex vessels & the lumbar arteries or deep circumflex iliac artery. The diaphragmatic lymph node

group constitute the anterior & middle diaphragmatic lymph nodes and retro rural lymph nodes.

HISTOLOGY

Lymphocytes are first generated in primary lymphoid organs (the thymus and bone marrow), but secondary lymphoid organs are where most lymphocyte activation and proliferation take place (the lymph nodes, the spleen, and diffuse lymphoid tissue found in the mucosa of the digestive system, including the tonsils, Peyer patches, and appendix)[26].

The red bone marrow is where all lymphocyte stem cells are found in adults. The lymphoid stem cells mature and become functional in central or primary lymphoid organs. The stem cells that are destined to become B lymphocytes remain in the bone marrow and undergo differentiation to become mature and functional while the stem cells that are destined to become T lymphocytes migrate to the thymus via circulation and develop into mature and functional T lymphocytes.

The *spleen* is a sizable lymphoid organ that lacks a cortex/medulla structure and has two intertwined but functionally distinct regions: the white pulp and the red pulp. Only 20% of the spleen is made up of white pulp, which is secondary lymphoid tissue linked to tiny central arterioles that are likewise surrounded by periarteriolar lymphoid sheaths of T cells. Splenic cords containing macrophages, blood cells of all types, and splenic sinusoids make up the red pulp, which filters blood, eliminates damaged erythrocytes, and recycles haemoglobin iron.

The thymus is a bilobed structure located in the mediastinum. It has a vascularized connective tissue capsule and contains multiple lobules separated by the septa which are extensions of the connective tissue capsule. Each lobule has an outer darkly staining cortex and a lightly staining inner medulla. The cortex has a huge population of T lymphocytes (thymocytes) macrophages and thymic epithelial cells(TECs). The TECs in the medulla aggregate to form Hassall corpuscles. The thymus is the site where T lymphocytes undergo maturation and differentiation. Thymus also plays an important role in the selective removal of T cells that are reactive against self-antigens which is a part of inducing central self-tolerance.

The term "*mucosa-associated lymphoid tissue*" (MALT) refers to the immune cells that are dispersed across the mucosae of the gastrointestinal, respiratory, or urogenital systems. However, it is well organised in certain areas and is referred to as palatine, lingual and pharyngeal tonsils, Peyer patches and the appendix. In MALT the proliferating B lymphocytes are organised in the form of "small spherical lymphoid nodules".

In contrast to MALT, *lymph nodes* are fully encapsulated, located along lymphatic channels, and have many afferent lymphatics as well as one efferent lymphatic. Each lymph node filters the lymph and offers a location for B-cell activation and differentiation into plasma cells that secrete antibodies. Three functional, but not visually distinct, components make up a lymph node: an outer cortex, a paracortex beneath it, and an inner medulla next to the hilum and efferent lymphatic. Lymphatics enter the node's cortex, where B lymphocytes come into contact with antigens, multiply in lymphoid nodules, and subsequently proceed into the lymph node's deeper sections. The majority of the lymphocytes that reach the lymph cortex are T helper cells, which are solely present in that area.
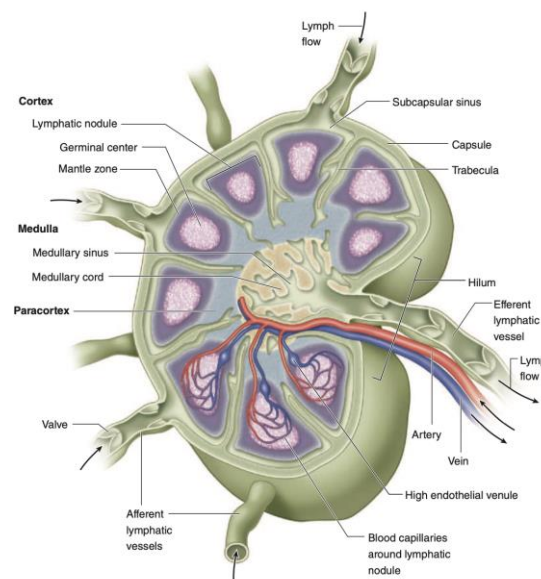
Figure 8: Structure of Lymph Node[26]

The medulla comprises medullary cords that are made of reticular fibres and contain densely packed plasma cells, macrophages, and other leukocytes. Between the cords are medullary sinuses that drain lymph, which converge at the efferent lymphatic vessel[26].

PATHOGENESIS OF LYMPHOMA[27]

The pathogenesis of lymphoid neoplasms is multifactorial. Multiple etiological agents and chromosomal aberrations lead to the development of lymphoid neoplasms. Multiple tumours contain mutations that primarily influence maturation or promote self-renewal, promote growth, or inhibit apoptosis.
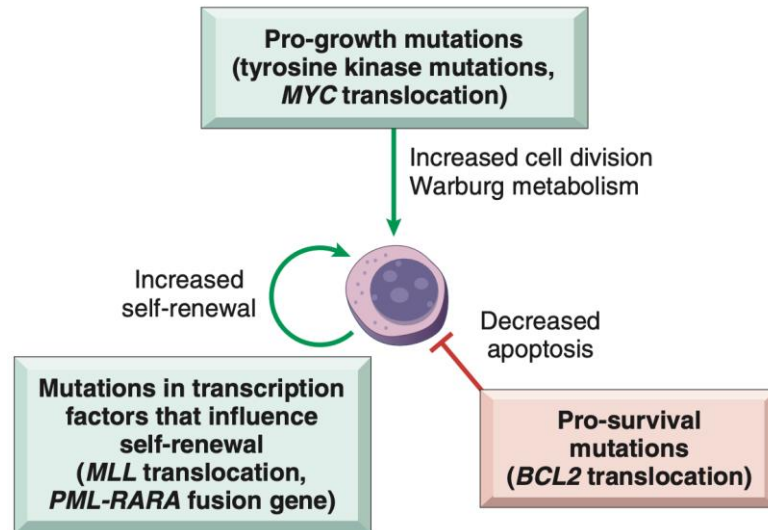
Figure 9: Pathogenesis of lymphoid neoplasms[1]

The various etiologic factors and chromosomal aberrations together lead to arrest in the normal development of lymphoid progenitors and lead to abnormal proliferation, thus resulting in neoplasms.
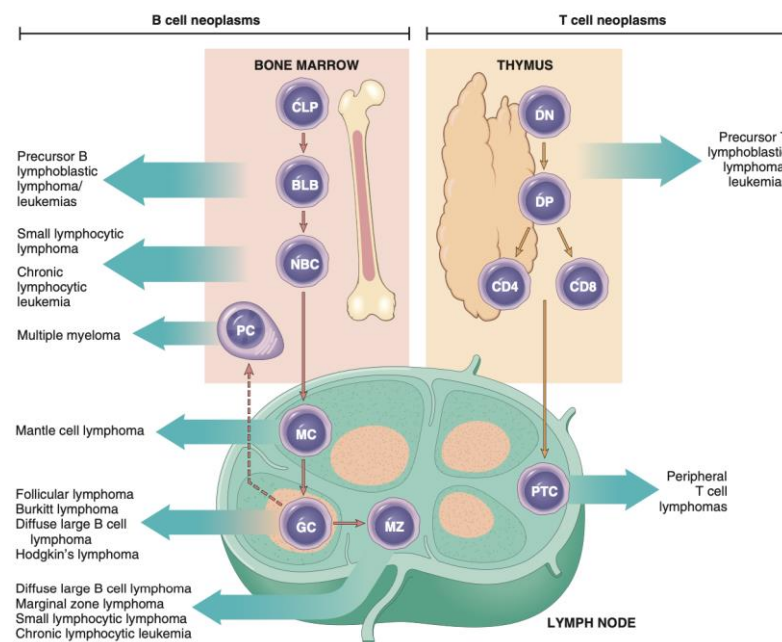
Figure 10: Origin of Various Lymphoid Neoplasms[1]

CLASSIFICATION OF LYMPHOMA

With increasing knowledge of cell biology, immunophenotyping, molecular genetics, and recognition of new lymphoma entities, a census for universal lymphoma classification came in 1994 in the form of the revised European-American classification of lymphoid neoplasms. Stratification of disease on basis of cell lineage and maturity, clinical, morphological, immunophenotypic and molecular data were major principles of WHO 2001 classification that was adapted from revised European-American classification[28]. In this classification, NHL was categorized into more than 20 subtypes based on cell of origin (B- or T-cell precursor), immunophenotypic and morphologic data[29]. WHO classification of 2008 refined the definitions of well-recognized diseases, identified new entities and variants, and incorporated new emerging concepts in the understanding of lymphoid neoplasms[30]. An advisory Committee discussing 2001 and 2008 classifications were held in 2014 to obtain advice and consent of clinical oncologists/haematologists and other physicians critical to the revision. Additional editorial meetings and consultations followed leading to the updated 2022 WHO classification[31].

Table 3: 5th Edition of WHO classification of hemato-lymphoid tumours, 2022[31]

B-CELL LYMPHOID PROLIFERATIONS AND LYMPHOMAS.	
Tumour-like lesions with B-cell predominance	
Reactive B-cell-rich lymphoid proliferations that can mimic lymphoma	IgG4-related disease
Unicentric Castleman disease	Idiopathic multicentric Castleman disease
KSHV/HHV8-associated multicentric Castleman disease	
Precursor B-cell neoplasms	
B-cell lymphoblastic leukaemias / lymphomas	
B-lymphoblastic leukaemia/lymphoma, NOS	B-lymphoblastic leukaemia/lymphoma with high hyper diploidy

B-lymphoblastic leukaemia/lymphoma with hypodiploidy	B-lymphoblastic leukaemia/lymphoma with iAMP21
B-lymphoblastic leukaemia/lymphoma with BCR::ABL1 fusion	B-lymphoblastic leukaemia/lymphoma with BCR::ABL1-like features
B-lymphoblastic leukaemia/lymphoma with KMT2A rearrangement	B-lymphoblastic leukaemia/lymphoma with ETV6:: RUNX1 fusion
B-lymphoblastic leukaemia/lymphoma with ETV6::RUNX1-like features	B-lymphoblastic leukaemia/lymphoma with TCF3::PBX1 fusion
B-lymphoblastic leukaemia/lymphoma with IGH::IL3 fusion	B-lymphoblastic leukaemia/lymphoma with TCF3::HLF fusion
B-lymphoblastic leukaemia/lymphoma with other defined genetic abnormalities	
Mature B-cell neoplasms	
Pre-neoplastic and neoplastic small lymphocytic proliferations	
Monoclonal B-cell lymphocytosis	Chronic lymphocytic leukaemia/small lymphocytic lymphoma
Splenic B-cell lymphomas and leukaemias	
Hairy cell leukaemia	Splenic diffuse red pulp small B-cell lymphoma
Splenic marginal zone lymphoma	Splenic B-cell lymphoma/leukaemia with prominent nucleoli
Lymphoplasmacytic lymphoma	
Lymphoplasmacytic lymphoma	
Marginal zone lymphoma	
Extra nodal marginal zone lymphoma of mucosa-associated lymphoid tissue	Primary cutaneous marginal zone lymphoma
Nodal marginal zone lymphoma	Paediatric marginal zone lymphoma

Follicular lymphoma	
In situ follicular B-cell neoplasm	Follicular lymphoma
Paediatric-type follicular lymphoma	Duodenal-type follicular lymphoma
Cutaneous follicle centre lymphoma	
Primary cutaneous follicle centre lymphoma	
Mantle cell lymphoma	
In situ mantle cell neoplasm In situ mantle cell neoplasia	Mantle cell lymphoma
Leukaemic non-nodal mantle cell lymphoma	
Transformations of indolent B-cell lymphomas	
Transformations of indolent B-cell lymphomas Not previously included	
Large B-cell lymphomas	
Diffuse large B-cell lymphoma, NOS	Diffuse large B-cell lymphoma/ high grade B-cell lymphoma with MYC and BCL2 rearrangements
ALK-positive large B-cell lymphoma	Large B-cell lymphoma with IRF4 rearrangement
High-grade B-cell lymphoma with 11q aberrations	Lymphomatoid granulomatosis EBV-positive diffuse large B-cell lymphoma
Diffuse large B-cell lymphoma associated with chronic inflammation	Fibrin-associated large B-cell lymphoma
Fluid overload-associated large B-cell lymphoma	Plasmablastic lymphoma
Primary large B-cell lymphoma of immune-privileged sites	Primary cutaneous diffuse large B-cell lymphoma, leg type

Intravascular large B-cell lymphoma	Primary mediastinal large B-cell lymphoma
Mediastinal grey zone lymphoma BHigh-grade B-cell lymphoma, NOS	
Burkitt lymphoma	
Burkitt lymphoma	
KSHV/HHV8-associated B-cell lymphoid proliferations and lymphomas	
Primary effusion lymphoma	KSHV/HHV8-positive diffuse B-cell lymphoma HHV8-positive diffuse large B-cell lymphoma, NOS
KSHV/HHV8-positive germinotropic lymphoproliferative HHV8-positive germinotropic lymphoproliferative disorder	
Lymphoid proliferations and lymphomas associated with immune deficiency and dysregulation	
Hyperplasia's arising in immune deficiency/dysregulation	Polymorphic lymphoproliferative disorders arising in immune deficiency / dysregulation
EBV-positive mucocutaneous ulcer	Lymphomas arising in immune deficiency/dysregulation
Inborn error of immunity-associated lymphoid proliferations and lymphomas	
Hodgkin lymphoma	
Classic Hodgkin lymphoma	Nodular lymphocyte predominant Hodgkin lymphoma
Plasma cell neoplasms and other diseases with paraproteins	
Monoclonal gammopathies	
Cold agglutinin disease	IgM monoclonal gammopathy of undetermined significance
Non-IgM monoclonal gammopathy of undetermined significance	Monoclonal gammopathy of renal significance

Diseases with monoclonal immunoglobulin deposition	
Immunoglobulin-related (AL) amyloidosis	
Monoclonal immunoglobulin deposition disease	
Heavy chain diseases	
Mu heavy chain disease	Gamma heavy chain disease
Alpha heavy chain disease	
Plasma cell neoplasms	
Plasmacytoma	Plasma cell myeloma
Plasma cell neoplasms with associated paraneoplastic syndrome -POEMS syndrome -TEMPI syndrome -AESOP syndrome	
T-CELL AND NK-CELL LYMPHOID PROLIFERATIONS AND LYMPHOMAS.	
Tumour like lesions with T cell predominance	
Kikuchi-Fujimoto disease	Indolent T-lymphoblastic proliferation
Autoimmune lymphoproliferative syndrome	
Precursor T-cell neoplasms	
T-lymphoblastic leukaemia /lymphoma	
T-lymphoblastic leukaemia /lymphoma, NOS	Early T-precursor lymphoblastic leukaemia / lymphoma
Mature T-cell and NK cell neoplasms	
Mature T-cell and NK cell leukaemia	
T-prolymphocytic leukaemia	T-large granular lymphocytic leukaemia
NK- large granular lymphocytic leukaemia	Adult T-cell leukaemia / lymphoma

Sezary syndrome	Aggressive NK-cell leukaemia
Primary cutaneous T-cell lymphomas	
Primary cutaneous CD4-positive small or medium T-cell lymphoproliferative disorder	Primary cutaneous acral CD8-positive lymphoproliferative disorder
Mycosis fungoides	Primary cutaneous CD30-positive T-cell lymphoproliferative disorder: Lymphomatoid papulosis
Primary cutaneous CD30-positive T-cell lymphoproliferative disorder: Primary cutaneous anaplastic large cell lymphoma	Subcutaneous panniculitis-like T-cell lymphoma
Primary cutaneous gamma/delta T-cell lymphoma	Primary cutaneous CD8-positive aggressive epidermotropic cytotoxic T-cell lymphoma
Primary cutaneous peripheral T-cell lymphoma, NOS	
Intestinal T-cell and NK-cell lymphoid proliferations and lymphomas	
Indolent T-cell lymphoma of the gastrointestinal tract	Indolent NK-cell lymphoproliferative disorder of the gastrointestinal tract
Enteropathy-associated T-cell lymphoma	Monomorphic epitheliotropic intestinal T-cell lymphoma
Intestinal T-cell lymphoma, NOS	
Hepatosplenic T-cell lymphoma	
Hepatosplenic T-cell lymphoma	
Anaplastic large cell lymphoma	
ALK-positive anaplastic large cell lymphoma	ALK-negative anaplastic large cell lymphoma
Breast implant-associated anaplastic large cell lymphoma	
Nodal T-follicular helper (TFH) cell lymphoma	
Nodal TFH cell lymphoma, angioimmunoblastic-type	Nodal TFH cell lymphoma, follicular-type
Nodal TFH cell lymphoma, NOS	
Other peripheral T-cell lymphomas	
Peripheral T-cell lymphoma, not otherwise specified	
EBV-positive NK/T-cell lymphomas	

EBV-positive nodal T- and NK-cell lymphoma	Extra nodal NK/T-cell lymphoma
EBV-positive T- and NK-cell lymphoid proliferations and lymphomas of childhood	
Severe mosquito bite allergy	Hydroa vacciniforme lymphoproliferative disorder
Systemic chronic active EBV disease	Systemic EBV-positive T-cell lymphoma of childhood
STROMA-DERIVED NEOPLASMS OF LYMPHOID TISSUES.	
Mesenchymal dendritic cell neoplasms	
Follicular dendritic cell sarcoma	EBV-positive inflammatory follicular dendritic cell sarcoma
Fibroblastic reticular cell tumour	
Myofibroblastic tumour	
Intranodal palisaded myofibroblastoma	
Spleen-specific vascular-stromal tumours	
Splenic vascular-stromal tumours	
Littoral cell angioma	Splenic hamartoma
Sclerosing angiomatoid nodular transformation of spleen	

IMAGING MODALITIES AND FINDINGS

Histological diagnosis is the primary method of final diagnosis. Ultrasound remains primary modalities of initial evaluation for superficial lymph node and testicular evaluation. Main value of ultrasonography in lymphoma is characterization of palpable lesions. Neck nodes are the common sites of lymphomatous involvement and an accurate diagnosis is essential as its treatment differs from other causes of neck lymphadenopathy. On ultrasound, grey scale sonography helps to evaluate nodal morphology, whilst power Doppler sonography is used to assess the vascular pattern (Fig 11). Greyscale sonographic features that help to identify metastatic and lymphomatous lymph nodes include size, shape and internal architecture (loss of hilar architecture, presence of intra-nodal necrosis and calcification)[32].
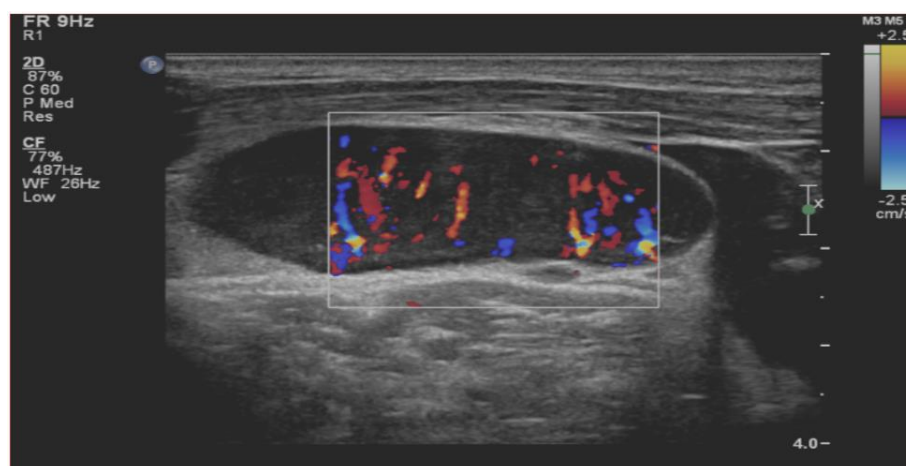
Figure 11: Ultrasound showing Hypoechoic lymphomatous node with increased vascularity

Chest radiography provides only a little information about mediastinal and lung involvement[33]. CT has been an important technology for lymphoma staging and evaluation and is helpful in the localization of lesions for image-guided biopsies[34]. Contrast-enhanced CT enlightens in-detail evaluation of the chest wall, mediastinum and pulmonary parenchyma, pleura or pericardium.
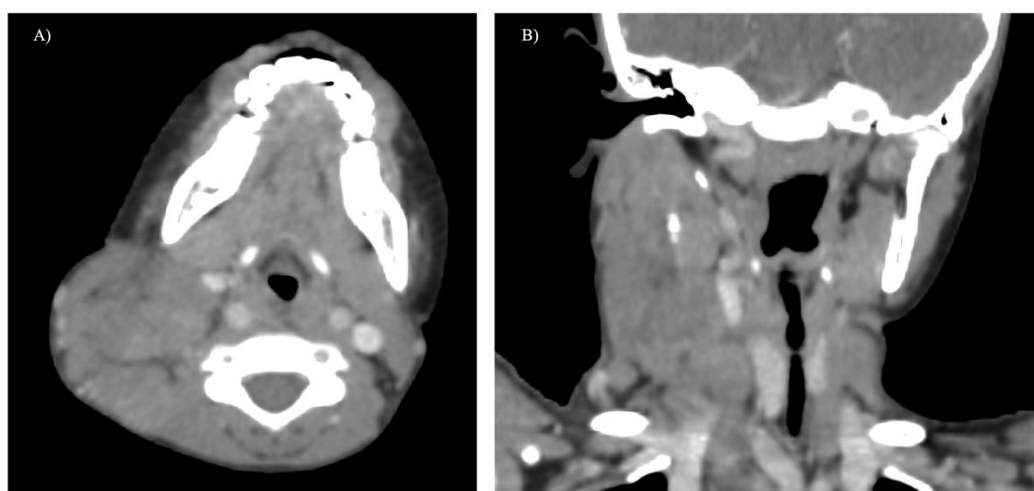
Figure 12: In a classical Hodgkin's lymphoma, contrast-enhanced CT shows multiple enlarged discrete nodal masses, surrounding the carotid vessels without obvious infiltration.

Neck CT is useful for the involvement of cervical lymph nodes, especially nodes inaccessible on ultrasound and for better evaluation of Waldeyer's ring. (Fig- 10) Abdominal CT helps in diagnosing abdominal and pelvic lymph nodes and extranodal

involvement such as liver, kidneys, spleen, peritoneum and mesentery. A paucity of fat in children evaluates abdominopelvic disease difficult[33].

MRI is more commonly used for the evaluation of lymphomas involving CNS[34]. DW imaging has emerged as a powerful clinical tool in the care of patients with cancer and can provide unique information related to tumour cellularity and integrity of the cellular membrane. In patients with lymphoma, whole-body DW imaging can be clinically useful for lesion characterization, disease detection, and assessment of treatment response. However, careful optimization of this technique is required to ensure high-quality images. Furthermore, hybrid PET/MR imaging could provide complementary functional and anatomic information and be a valuable aid in the treatment of patients with lymphoma[35].

NODAL LYMPHOMA

Lymph nodes are the most commonly affected sites in lymphoma–be it cervical, supraclavicular, axillary, mediastinal, abdominal, or inguinal. Extranodal lymphoma occurs in about 40% of patients with lymphoma. It is observed more frequently in NHL than with HL and is often intermediate to high grade. The incidence of extranodal lymphoma is higher in patients with AIDS and immunodeficient states. Lymphomatous nodes appear discretely enlarged or as soft-tissue masses, with variable FDG avidity depending on the histological type[36,37,38]. Enlarged lymph nodes in the cervical region are usually detected on neck ultrasonography done for neck swelling. On grey scale ultrasound, lymphoma appears as sharp-bordered, hypoechoic, pseudo cystic appearance with loss of fat, lack of calcification and tendency to aggregate into mass[36]. Exaggerated hilar flows with large and central branching vessels are usually seen on colour Doppler ultrasound[39]. Well-defined enlarged round nodes with homogenous internal echoes and increased flow centrally and peripherally may be seen[40].

Imaging features of mediastinal lymphadenopathy include widening of the right paratracheal stripe, aortopulmonary window bulge, displaced azygoesophageal line and lobular hilar shadows[41]. Mediastinal Hodgkin lymphoma may present as a mass extending more than one-third of the maximum intrathoracic diameter at the diaphragmatic dome level[42]. Mediastinal and hilar lymphadenopathy is the most

common thoracic manifestation of NHL. Mediastinal lymphoma causing extrinsic oesophageal compression results in the smooth indentation of the oesophagus and obtuse and gently sloping borders[43].

The most common retroperitoneal solid mass is lymphadenopathy and a few of the main causes are lymphoma and metastasis. The most common retroperitoneal malignant tumour is lymphoma and the common sonological appearance is hypoechoic lymph nodes[39]. A short axis diameter maximum of 10 mm may be taken as a criterion however jugulodigastric diameter, retro rural, pelvic and portogastric nodes may be suspicious at a size more than 13, 6, 8 and 8 respectively. Lymphomatous lymph nodes are usually homogeneous, soft tissue attenuating lesions with mild to moderate enhancement. Calcification is rarely seen. Necrotic components may be seen in aggressive masses or large nodal mass[37]. The lymphomatous node on MRI shows T1 hypo to iso intense signal, T2 and STIR high signal intensities[37].
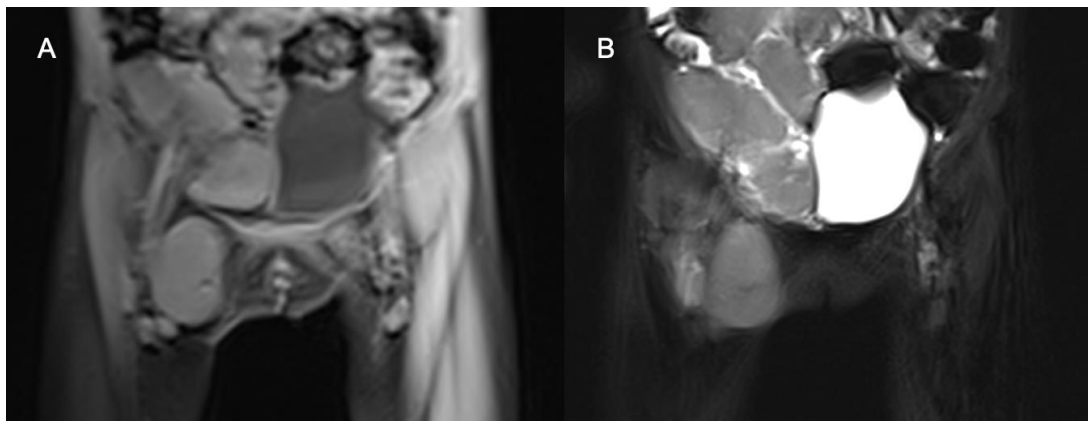
Figure 13: A & B. Coronal T1 and STIR images showing enlarged nodal masses in the right iliac and inguinal stations.
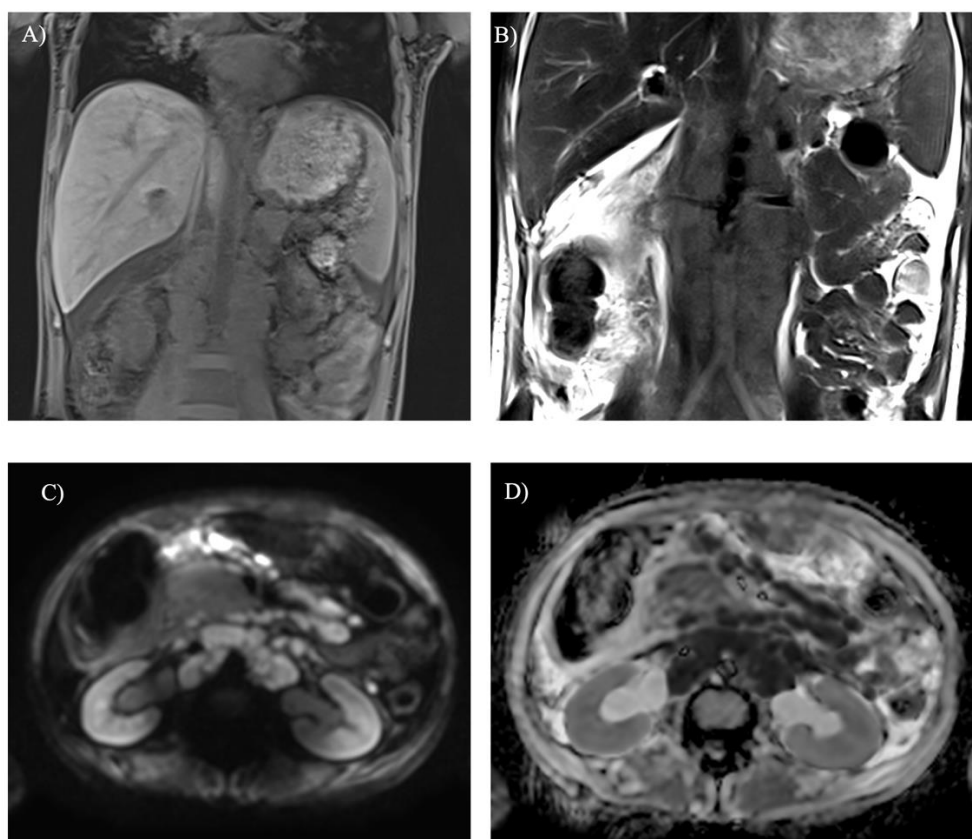
Figure 14: A) Coronal T1 vibe Dixon water-only image and B) STIR image showing iso-intense retroperitoneal lymph nodal mass in biopsy-proven case of DLBCL. Ascites and subcutaneous oedema are also seen. C) & D) DWI & ADC map images of enlarged retroperitoneal & mesenteric nodes showing diffusion restriction.
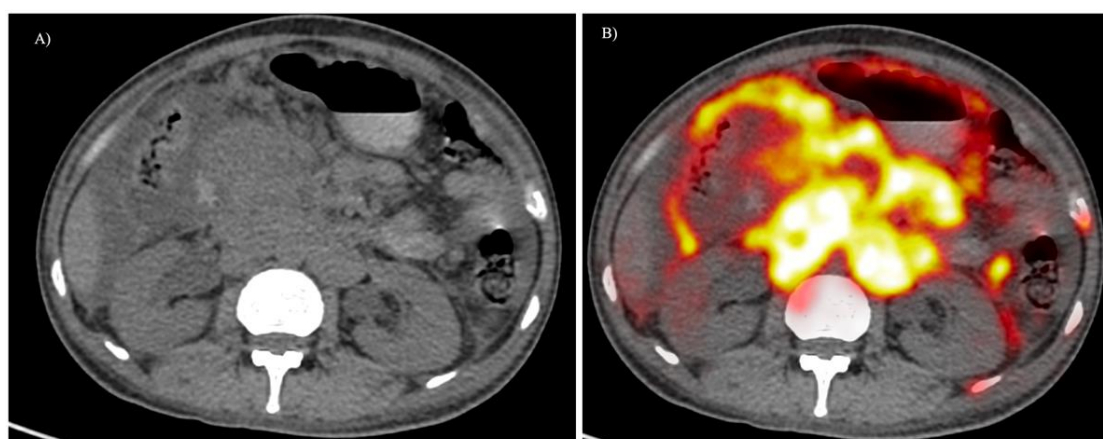
Figure 15: Non-contrast CT and PET/CT of the same patient in figure 14 showing retroperitoneal mass with FDG uptake.

EXTRANODAL LYMPHOMA

Extra-nodal involvement usually appears in the widespread extension of lymphoma. CT is helpful for various extra-nodal site evaluation and changes of staging to its respective extra-nodal counterpart.

Pulmonary lymphomas have a variable presentation that may include multiple ill-defined solid or ground-glass nodules or masses, atelectasis, consolidation with air bronchograms, reticulonodular shadows and interlobular septal thickening. Associated manifestations such as pleural effusion can be seen on the conventional thoracic radiograph. Differential diagnoses of mediastinal lymphoma such as teratoma, thymoma and retrosternal goitre need to be evaluated by further imaging[44,45,46].
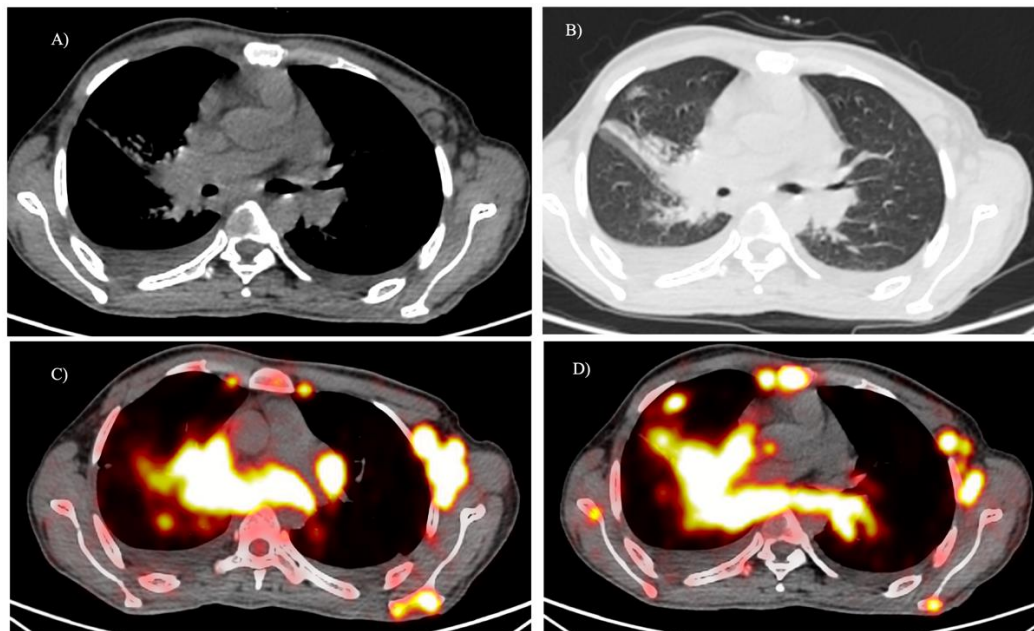
Figure 16: A) & B) Non-contrast CT chest, mediastinal & lung windows showing lymphomatous infiltration of the right lung with bilateral pleural effusion. C) & D) PET/CT images showing multiple FDG avid lesions in the mediastinum, lung and axilla and the sternum and scapula.

Liver involvement may occur in 15 % of adult NHL[37]. Lymphomatous involvement of the liver appears as hypoechoic masses or anechoic and septate masses. Diffuse organ involvement is possible in the liver and spleen with organomegaly and variable CT attenuation[47]. Most cases with splenic involvement in lymphoma represent

diffuse large B-cell lymphoma, Hodgkin lymphoma[48] or indolent B-cell lymphomas such as splenic marginal zone lymphoma, mantle cell lymphoma, chronic lymphocytic leukaemia, or hairy cell leukaemia.
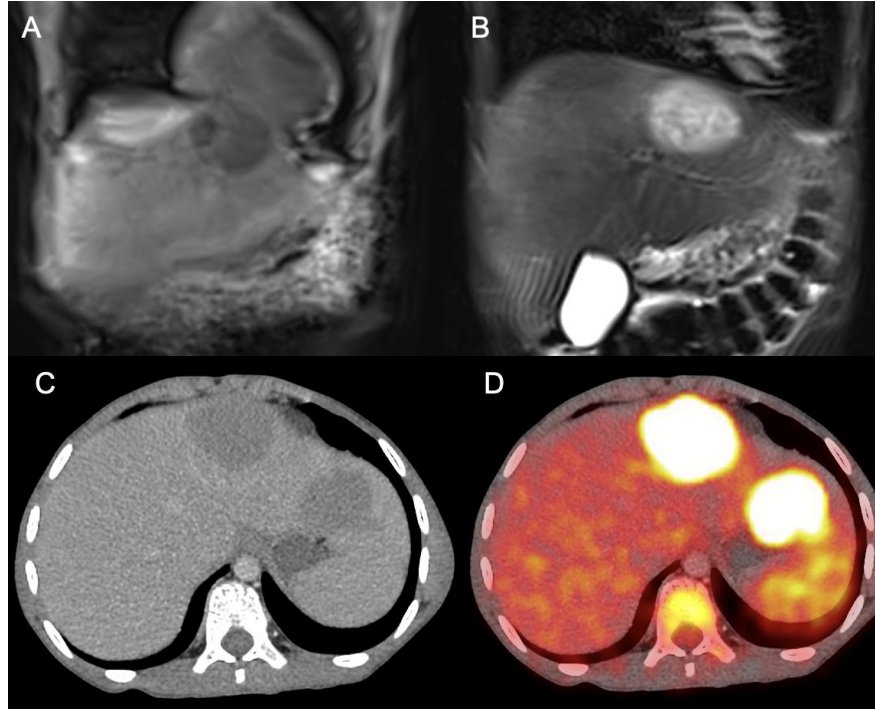
Figure 17: (A) Coronal T1WI, (B) STIR, (C) CECT and (D) PET images showing lymphomatous lesions in the liver.

Splenomegaly is the common presentation but it is neither sensitive nor specific for lymphomatous involvement; no size criterion has been widely accepted[49]. Lugano classification accepts splenic size > 13 cm as splenomegaly[50]. Splenic involvement may be seen as varying patterns on ultrasound that may be, diffuse enlarged, homogenous or inhomogeneous echotexture, focal small (< 3 cm) or large (> 3cm) hypoechoic hypovascular nodule, or bulky masses. Splenic involvement in NHL is characteristic of a few types like mantle cell and splenic marginal zone lymphoma. Splenic infarction may occur[37].

The most common extranodal site of NHL in GIT is the stomach followed by the small bowel followed by the colon[51]. Fluoroscopic barium procedures are helpful in the evaluation of lymphomatous masses compressing the gastrointestinal tract.

Almost all pharyngeal lymphomas arise from Waldeyer's ring (adenoids, palatine tonsils and lingual tonsils) and are of non-Hodgkin type.

Hodgkin lymphoma, although begins in cervical nodes, rarely involves Waldeyer's ring. The Nasopharynx and base of the tongue are other common sites. Radiographically, this appears as lobulated submucosal masses causing effacement of lymphoid follicular masses in double contrast barium swallow series.

Gastric lymphomas are the most common type of gastrointestinal lymphoma. Double-contrast studies may exhibit round and confluent nodules or diffuse segmental mural thickening in low-grade lymphomas. High-grade lymphoma may appear as small polypoid or ulcerated lesions or shallow, irregular ulcers with adjacent nodular mucosa, or distorted and enlarged rugal folds. Advanced gastric lymphoma may extend to a mean diameter of even more than 10 centimetres and may show infiltrative, polypoid, ulcerative or nodular lesions. Infiltrative pattern characterized by enlarged rugal folds, however, extensive involvement may show a linitis plastica-type pattern.
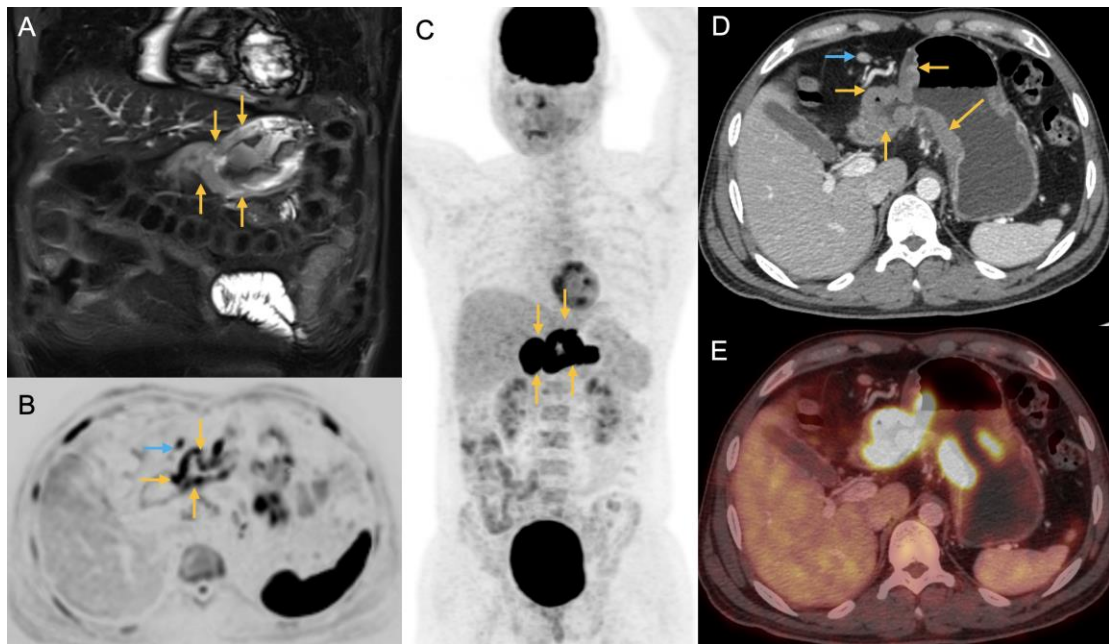
Figure 18: (A) Coronal STIR, (B) DWI, (C) PET MIP, (D) Axial CECT and PET-CT images showing lymphomatous involvement of the distal body and pylorus of the stomach in a case of DLBCL.

The ileum is the most common site of small bowel lymphoma. AIDS is associated with B cell lymphoma and celiac disease is associated with T cell lymphoma. Exocentric mass due to involvement of the myenteric plexus may lead to aneurysmal dilatation of the bowel. The colon is the third most common site of GI lymphoma. Systemic lymphoma involving the colon is more commonly B cell NHL and usually presents as long segmental bowel or entire colon involvement. The variable presentation can be localized form, infiltrating form, irregular haustral fold and smooth nodular surface lesion, diffuse multinodular form and conglomerate cecal masses[52].
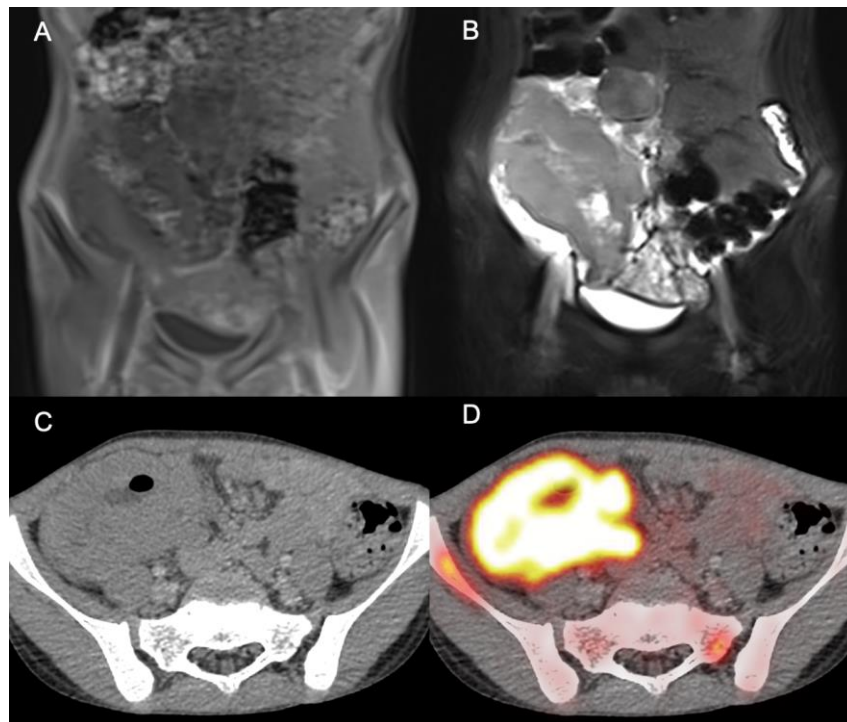
Figure 19: (A) Coronal T1, (B) STIR, (C) Axial CECT and (D) PET-CT images showing lymphomatous involvement of caecum and ascending colon.

Endoscopic features of lymphoma are variegated such as erosions or multifocal gastritis like benign entities or malignant lesions of adenocarcinoma of the stomach. Four imaging patterns have been described: superficial, diffuse–infiltrative, mass forming and mixed. Superficial involvement signifies the thickening of the second & third layers without involving the first & fourth layers.

However, early recognition, or the recognition of risk factors, of relapse of GI lymphoma has little value in a clinical scenario, repeated EUS follow-up assessments for MALT lymphomas are no more recommended[53]. CT better reveals the true extent of wall thickening and nodal involvement than barium studies.

Genitourinary lymphoma most commonly involves the test is followed by kidneys and perirenal spaces. Testicular involvement most commonly occurs in DLBCL or Burkitt lymphoma. Involvement is usually bilateral and painless. Renal involvement commonly presents as multiple masses that demonstrate a " density reversal sign" appearing as a reversal of pre-contrast hyperdense lesion and hypodense renal parenchyma into hypoenhancing lesion and enhanced renal parenchyma. Infiltrating lymphoma maintains a reniform shape but disrupts architecture. Contiguous involvement from large retroperitoneal mass may lead to adrenal gland involvement. Ureteric involvement in form of encasement, displacement or less commonly actual invasion may occur resulting in pelvicalyceal system dilatation. Bladder lymphoma appears as a submucosal mass, which arises from submucosal lymphoid follicles. Sonographic appearance consists of intramural mass with intact epithelium. A large mass may ulcerate. Adrenal lymphomatous involvement may be incidentally detected during routine staging workup. MRI may be more useful in gynaecological tract involvement in lymphoma. The usual subtypes involving the female genitourinary tract are DLBCL[37].
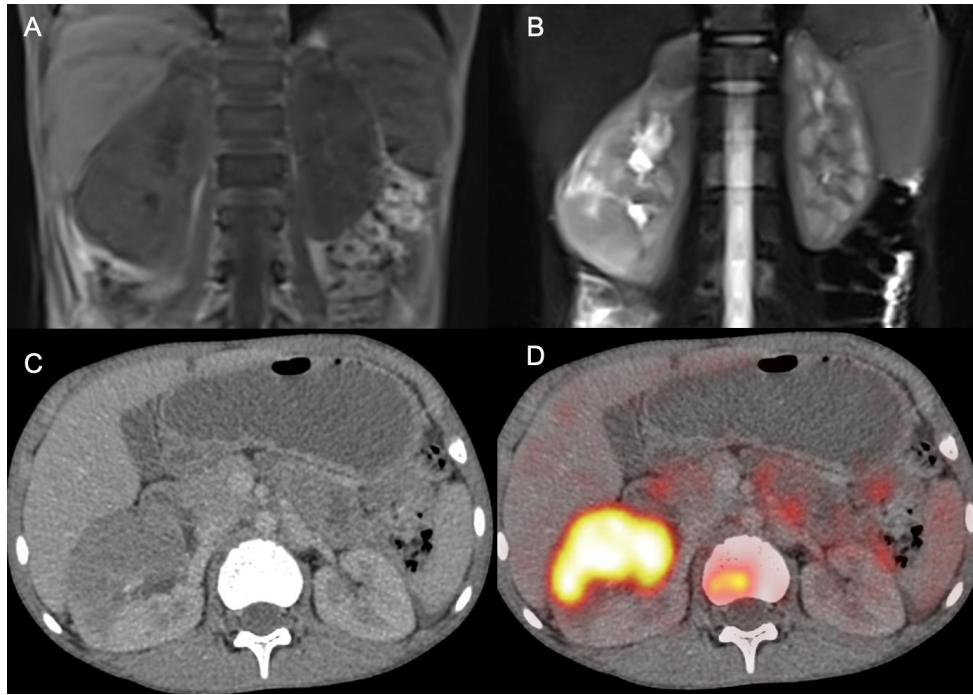
Figure 20: (A) Coronal T1, (B) STIR, (C) Axial CECT and (D) PET-CT images showing lymphomatous involvement of the right kidney, and lumbar vertebral bodies.

Involvement of bony cortex and marrow and skeletal muscle may be seen in both HL and NHL. Cortex involvement is usually included as an extranodal spread which may be characterized as IE, however, marrow involvement denotes distant spread and is labelled as stage IV and has a poorer prognosis than liver or spleen involvement. Marrow involvement in high-grade NHL is focal, whereas, in the Follicular type, it is seen as diffuse and para trabecular. T1 weighted MRI is the most sensitive for marrow infiltration. FDG PET/CT is moderately sensitive as diffuse and heterogeneous marrow uptake can be due to reactive marrow hyperplasia[37].

Primary lymphoma of bone (earlier described as "reticulum cell sarcoma") is uncommon and is usually either diffuse large B-cell lymphoma or follicular lymphoma[54]. CT appearance of osseous lymphoma may be variable that includes typically lytic focal lesions, sclerotic, may be seen with a classic "ivory vertebra," or may demonstrate a mixed pattern. Sclerosis may also develop post-treatment. Bone marrow involvement may occur in advanced stages. Bone marrow biopsy of posterior iliac crest or multifocal or diffuse FDG PET uptake on pre-treatment PET/CT may be diagnostic. MR imaging is also sensitive to focal bone lesions[55]. The most common

radiographic pattern is a permeative and osteolytic pattern. HL can commonly involve the skull, femora and spine and causes the classic appearance of a sclerotic ivory vertebra with anterior scalloping of vertebrae. CT will demonstrate the bony disease process and MRI is useful in assessing local staging[55].

Primary CNS lymphomas are usually restricted to neuraxis without systemic involvement[55]. Primary CNS lymphoma is rare, representing 1% of non-Hodgkin lymphoma cases[56]. The most common locations are cerebral white matter, or near the corpus callosum and usually abut ependyma. Butterfly distribution through corpus callosum spread is typical. On NCCT, primary CNS lymphoma deposits are classically hyperattenuating compared with white and grey matter[56]. Secondary involvement is seen in stage IV disease, lymphoblastic or immunoblastic histology, testicular or ovarian involvement or Burkitt lymphoma. This form commonly involves extra-axial spaces of the neuraxis. The subdural and leptomeningeal disease can be seen as enhancing plaque on contrast-enhanced MRI. Symptoms of cord compression, cauda equine syndrome and cranial nerve palsies can occur.
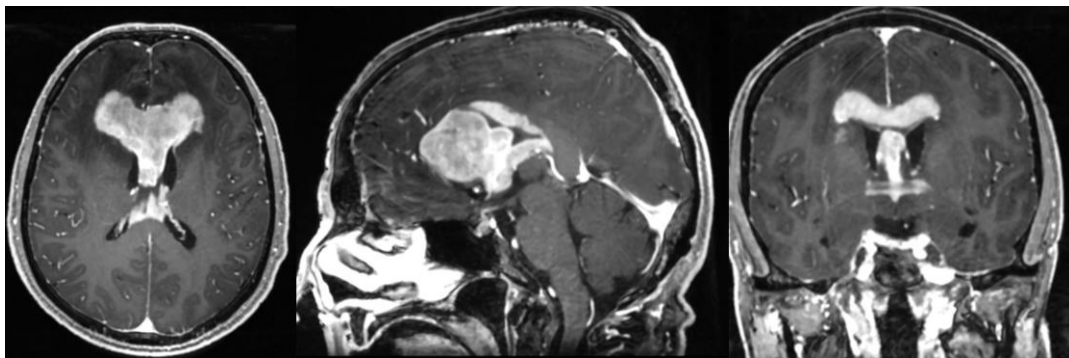
Figure 21: Post-contrast T1W images showing lymphomatous involvement of CNS. Leptomeningeal infiltration may manifest on MR images as a diffuse thickening or focal enhancing masses of the ependyma, meninges, or cranial or spinal nerves[57].

Orbital lymphoma can present in any manner depending on the site of involvement. These can involve any site. Retro-bulbar involvement can cause proptosis due to the involvement of extraocular muscle. MALT lymphoma of the lacrimal gland can present as periorbital swelling. Waldeyer's ring consisting of lymphoid tissue in the nasopharynx, oropharynx, faucial and palatine tonsil is the commonest side of the head and neck NHL, mostly MALT type, usually seen with synchronous

gastrointestinal involvement. Tonsils, a commonly affected structure, present as asymmetrical pharyngeal mucosal thickening. Circumferential involvement or multifocal involvement suggests NHL. Parotid NHL may appear as solitary to multiple uniform hypoechoic hypervascular intra-parotid masses[40]. These masses appear hyperdense on CT and intermediate signal on T1 and T2 weighted MRI[37].

Multiplanar fat-suppressed pre and post-contrast MRI is preferred for evaluating Head and Neck Lymphoma to know the extension of disease through skull-based foramina and infratemporal fossa[37].

DIAGNOSIS

An incisional or excisional biopsy, which may or may not be preceded by inadequate fine or core needle aspirate, is the mainstay of diagnosis. Morphological, immunohistochemical and flow cytometry and molecular data are needed to characterize the type of lymphoma. Paraffin block, frozen tissue or cell suspensions may be stored for future for research purposes[50].

Diagnosis of lymphoma is based on an integration of morphologic, immunophenotyping, and molecular and cytogenetic data. Few lymphomas have peculiar morphologic features. CT or PET/CT can help in the localization of the biopsy site in absence of clinically palpable lymphadenopathy. The advantage of PET/CT over CT in depicting sites of lymphoma to detect metabolically active disease is that, PET is more sensitive resulting in improved detection of true positive nodes[58]. Flow cytometry can help in expressing new characteristic antigenic expression of a few lymphoid neoplasms. Certain antigens, such as CD5, CD10, and CD23, may help in differentiating clonal B-cell lymphoma, such as follicular lymphoma (CD10+, CD5–, CD23+), from mantle cell lymphoma (CD10–, CD5+, CD23–). The immunophenotyping of T-cell neoplasms is less conclusive because of the lack of the equivalent of light-chain restriction. Chromosomal translocations in lymphoma often provide diagnostic and prognostic information. Translocations, such as t (11; 14) in mantle cell lymphoma and t (14;18) in follicular lymphoma may suggest prognostic information[59].

STAGING

The Ann Arbor staging system was first introduced in 1971[60] and then modified in 1989 to include the "Cotswolds modifications," which are applied to both non-Hodgkin lymphoma and Hodgkin lymphoma[61,62]. Staging with this system was based on the extent of involvement of nodal groups. There are some exceptions to the application of the Ann Arbor staging system: Primary central nervous system (CNS) and primary cutaneous lymphomas (such as mycosis fungoides and Sezary syndrome) are staged using the TNMB (tumour, lymph nodes, metastasis, blood) system, while Burkitt lymphoma is staged with St Jude staging criteria or a simpler risk stratification model, with the modifier "R" being used to refer to completely surgically resected disease[63].

Table 4: Cotswold's modification of Ann Arbor staging classification[61]

Stage I	Involvement of a single lymph node region or lymphoid structure (Spleen, thymus, Waldeyer's ring) or involvement of a single extra lymphatic site (IE)
Stage II	Involvement of two or more lymph node regions on the same side of diaphragm (II) or localized contiguous involvement of only one extra nodal organ or side and its regional lymph nodes with or without other lymph node regions on the same side of the diaphragm. Note: The number of anatomic regions involved may be indicated by a subscript (eg: II_3)
Stage III	Involvement of lymph node regions on both sides of the diaphragm (III), which may also be accompanied by involvement of the spleen (IIIS) or by localized contiguous involvement of only one extra nodal organ site (IIIE) or both (IIISE)
Stage IV	Disseminated (multifocal) involvement of one or more extranodal organs or tissues, with or without associated lymph node involvement or isolated extra lymphatic organ involvement with distant (non-regional) nodal involvement.

Few designations were described. Designation A represents no symptom. B represents associated clinical symptoms such as fever (temperature > 38 ^{0}C), drenching night sweats, and unexplained loss of more than 10% of body weight during the previous 6 months. X represents a bulky disease that is a thoracic ratio of maximum transverse mass diameter greater than or equal to one-third of the internal transverse thoracic diameter measured at the T5/6 inter-vertebral disk level on chest radiography. Other authors have designated a lymph node mass measuring 10 cm or more in the greatest dimension as the bulky disease.

The size of lymph nodes in normal individuals varies to a minor degree with the location of the node. Values varied by region from 8 to 11 mm, but with some normal pelvic nodes as large as 15 mm. Based on these data, at the time of diagnosis, a lymph node that was greater than 1 cm in its longest transverse diameter was considered compatible with involvement by NHL[64]. Revised response criteria for malignant lymphoma recommended a size of 1.5 cm on the long axis or a size of 1.1 cm on the long axis with ≥ 1cm on the short axis for lymphomatous disease. The revised Cheson 1999 criteria, more commonly known as the Cheson 2007 criteria, were developed to address limitations of the Cheson 1999 criteria and to incorporate bone marrow (BM) immunohistochemistry, flow cytometry, and the increased use of FDG PET imaging as a recognized and effective modality for visualizing the presence and distribution of lymphoma[65].

In 2007, International Harmonization Project defined criteria for response assessment based on PET/CT imaging of metabolic activity[51]. Pre-treatment PET was recommended as mandatory for variably FDG-avid lymphomas if PET has to be used to assess their response to treatment. If PET needs to be used for response assessment of patients, documentation of PET positivity needs to be at all disease sites of 1.5 cm in diameter by CT[66]. The Deauville criteria were subsequently proposed in 2009 for grading FDG avidity on PET[67].

The Lugano classification represents a major change from the Ann Arbor staging system and the IWG criteria for response assessment. Change in SUV (DSUV) between baseline and interim PET can serve to quantify metabolic response and also

has prognostic implications. These new criteria were the direct outgrowth of integrating the previously defined Deauville criteria with the input of investigators at follow-up International Workshop Conferences in 2011 and 2013[68]. The classification was developed following meetings in 2011 and 2013. The goal of the Lugano classification is the simplification and standardization of response assessment and reporting. The new classification also addresses the role of FDG PET/CT for staging and interim treatment response assessment. Given the expected rapid clinical application of the new staging criteria, radiologists and nuclear medicine specialists need to be aware of the associated implications for lymphoma imaging[63]. The Cotswold modifications have been updated in the recent Lugano classification. Evaluation of bulky disease and B symptoms has traditionally been inaccurate; removal of the associated modifiers "X" and "B" may help to standardize staging. Although the current definition of bulky disease in Hodgkin lymphoma is retained (namely a mass ≥10 cm or 1/3 of the transthoracic diameter), the associated "X" modifier is no longer applied in Hodgkin lymphoma or non-Hodgkin lymphoma. Instead, the longest diameter of a mass is simply recorded for staging purposes. The modifier "B" is only applied in patients with Hodgkin lymphoma as the presence of B symptoms only affects Hodgkin lymphoma treatment.

Lugano criteria recommend that tumour burden should be calculated at baseline staging by choosing up to six of the largest nodes, nodal complexes, or solid organ lymphoma deposits. Lesions chosen must be amenable to accurate measurement in two dimensions. Eligible lymph nodes with the longest diameter greater than 1.5 cm and extranodal lesions with the longest diameter greater than 1.0 cm should be multiplied by the shortest diameter of each lesion in the transverse plane. Add these products of diameters to give the "sum of the product of the diameters," or SPD. The SPD calculated at the time of staging will serve as the baseline for sequential quantification of tumour burden at interim and end-of-therapy FDG PET/CT[63].

The Lugano classification recommends modification of the Ann Arbor classification for the anatomic extent and categorizes patients as having "limited" (previously Ann Arbor stage I or II) or "advanced" (previously Ann Arbor stage III or IV) disease.

Table 5: Revised Staging systems for Primary Nodal Lymphoma

Stage	Nodal Characteristics	Extra-nodal characteristics
Limited		
I	One node or a group of adjacent nodes	Single extra nodal lesions without nodal involvement
II	Two or more nodal groups on the same side of the diaphragms	Stage I or II by nodal extent with limited contiguous extranodal involvement
II bulky	II as above with "bulky" disease	Not applicable
III	Nodes on both sides of the diaphragm; nodes above the diaphragm with spleen involvement	Not applicable
IV	Additional non-contiguous extra lymphatic involvement	Not applicable

Note: The extent of disease determined by Positron Emission Tomography /Computed Tomography for avid lymphomas and computed tomography for non-avid histologies. Tonsils, Waldeyer's ring, and spleen are considered nodal tissue. Whether stage II bulky disease is treated as a limited or advanced disease may be determined by histology and several prognostic factors[50].

Modification in Ann Arbor staging and discontinuation of routine bone marrow biopsies were salient updates in HL and FDG avid NHL. Other recommendations include an additional contrast-enhanced CT scan should be included at baseline for accurate measurement of lesion size, separation of bowel from lymphadenopathy, and differentiation of vascular structures from lymph nodes.

The baseline staging assessment workflow consists of CT assessment first and PET assessment later. CT assessment includes the selection of up to 6 sites labelled as index lesions and 10 sites labelled as non-index lesions. Index lesions are measurable lesions of ≥1.5cm in the nodal region and ≥1cm in the extranodal region. Other sites of disease or groups of lesions can be selected as non-index cases. Visual assessment of most metabolic lesions is done using 5PS criteria and the maximum SUV of the most metabolically active lesion is measured[69]. Lugano criteria recommended splenic size ≥ 13 cm for splenomegaly in lymphoma cases[50].

MANAGEMENT

Hodgkin lymphoma has been proven to be one of the curable human cancers. Current treatment aims to further improve treatment outcomes and try to reduce complications related to therapy. Up to the 1970s, radiotherapy was the major modality for treating HL, however, after the introduction of the MOPP and ABVD regimen, poly-chemotherapy has become increasingly important. Today ABVD combined with involved field radiotherapy is usually involved in early favourable or unfavourable conditions. In the era of high-quality imaging clinical staging methods have almost completely replaced pathological staging. Patients in clinical staging I or II without risk factors can be assigned as early-stage favourable. And risk factors assigned as unfavourable. Patients of stage III or IV are generally allocated to an advanced stage. Stage IIB with risk factors has been assigned to the advanced stage as an exception. Risk factors assigned to early stage unfavourable can be a) large mediastinal mass (> 1/3 of maximum thoracic diameter b) extranodal extension c) elevated ESR d) ≥ 3 involved areas. The treatment protocol accepted by most centres for the early favourable stages includes combined modality treatment consisting of 2-4 cycles of ABVD followed by 30Gy of involved field radiotherapy. The unfavourable treatment protocol currently consists of 4 to 6 cycles of chemotherapy with an ABVD regimen followed by 30Gy radiotherapy. The advanced stage group is treated with 6 to 8 cycles with BEACOPP escalated regimen that includes an increased dose of cyclophosphamide, adriamycin and etoposide[70].

ABVD treatment remains the standard first-line treatment regimen. Escalated BEACOPP may improve response rates but is associated with increased toxicity. Stage

I/II patients receive a combination of short-course chemotherapy with radiotherapy or full-course chemotherapy alone. Stage II bulky/III/IV patients with usually receive six cycles of ABVD for six cycles and the response is assessed by interim PET/CT[71].

Treatment in the majority of cases of DLBCL is combination chemotherapy immunotherapy or combined modality therapy. Patients with limited disease can be treated with a short course of R-CHOP with involved field radiotherapy. Advanced disease patients can be treated with 6 cycles of R-CHOP. Bulky disease at any stage is treated by 6 cycles of R-CHOP.

Other optional regimens may include R-CHOP with ICE combinations[72] or infusional chemotherapy with a dose-adjusted *R*-EPOCH regimen[73]. The intent of treatment usually aims to cure the disease, which is not usual in the case of low-grade lymphoma like follicular lymphoma[74].

Treatment of indolent lymphomas such as Follicular lymphoma, marginal zone lymphoma and small lymphocytic lymphoma depends on the disease stage. Patients with solitary or a couple of nodal involvement may be treated with localized irradiation. However, most patients have disseminated disease on presentation and are usually not curable. R-CVP or R-CHOP is considered to be the first-line treatment. Radioimmunoconjugates although infrequently used may produce a higher response rate. Stem cell transplantation can be considered in clinically aggressive indolent lymphoma[70].

Mantle cell lymphoma may require intensive initial immunochemotherapy, as it is not effectively treated with standard immunochemotherapy regimens. Intrathecal treatment with methotrexate is considered in central nervous system involvement. T cell lymphoma is usually treated with stem cell transplantation[70].

REVIEW OF LITERATURE

Luka Lambert et al (2022)[75],

A systemic review and metanalysis done by Luka Lambert et al (2022), which reviewed 15 studies with 519 patients, to evaluate the diagnostic performance of WB-MRI compared to PET/CT in the staging of lymphomas in adult patients, showed that in the assessment of nodal and extranodal involvement by lymphoma, the sensitivity of whole-body MRI was 0.93 and 0.89 respectively. The specificity of whole-body MRI was nearly 1.0. The whole-body MRI has high sensitivity and specificity in the evaluation of nodal and extra-nodal lymphoma involvement. The whole-body MRI has an almost perfect agreement with the reference standard.

Gil-Sun Hong, et al (2021)[76],

A study conducted by Gil-Sun Hong, et al (2021), on 30 patients, prospectively evaluated the diagnostic utility of WB-DWI with background signal suppression and STIR for the staging of indolent lymphoma, showed that WB-DWIBS/STIR had a very good agreement ($\kappa = 0.96$; confidence interval [CI], 0.88–1.00), high specificity (99.0–99.4%) and high sensitivity (93.4–95.1%), in the pretherapeutic staging for the whole-body regions. The WB-DWIBS/STIR results were similar to that of ^{18}F-FDG PET/CT, except for the sensitivity for extra-nodal lesions. As compared to ^{18}F-FDG PET/CT, the sensitivity of WB-DWIBS/STIR was higher (94.9– 96.8% vs. 79.6–86.3%, P = 0.058) for extranodal lesions. They have concluded that, when compared to 18F-FDG PET/CT, WB-DWIBS/STIR is a more advantageous modality for the pretherapeutic staging of indolent lymphoma and has advantages when assessing extra-nodal lesions.

Guisen Lin et al, (2021)[77]

A systemic review and meta-analysis, done by Guisen Lin et al, (2021) which included 14 studies & 457 patients with lymphoma, multiple myeloma and sarcoma, for evaluation of diagnostic accuracy of WB-MRI for assessment of "haematological malignancies" therapeutic response, showed that MRI-DWI had higher sensitivity compared to MRI without DWI (0.94 vs 0.55, p = 0.02). As compared to the reference standard, the WB-MRI pooled concordance rate, for assessing haematological malignancies treatment response, was 0.78 (95% Cl: 0.59 – 0.96). the diagnostic

performance of WB-MRI and PET/CT was similar. (specificity [0.87 vs, 0.76, p = 0.73] and sensitivity [0.83 vs 0.92, p = 0.11]). They concluded that, for assessing the treatment response of haematological malignancies, WB-MRI offers excellent diagnostic performance. Increased sensitivity of WB-MRI, is closely correlated with the addition of diffusion-weighted imaging.

Suzanne Spijkers et al (2021)[78]

Suzanne Spijkers et al (2021) conducted a study on fifty-one children to compare the whole-body MRI with an FDG PET/CT-based reference for early response assessment and restaging in children with Hodgkin's lymphoma. They observed that in 33/51 patients (65%, 95% CI 51–77%), WB-MRI-DWI agreed with the reference standard, while whole-body MRI without DWI agreed with the reference standard in only 15/51 patients (29%, 95% CI 19–43%) for early response assessment. For the evaluation of restaging, whole-body MRI / DWI agreed with the reference standard in 9/13 patients (69%, 95% CI 42–87%) while whole-body MRI without DWI agreed with the reference standard in only 5/13 patients (38%, 95% CI 18–64%). They have concluded that the WB-MRI protocol's early response assessment and restaging of paediatric HL were improved by the inclusion of DWI, which increased agreement with the [18F]FDG PET/CT-based reference standard. However, when compared to standard imaging for the detection of residual disease, WB-MRI was discrepant in 30% of the patients.

Siarhei, et al (2020)[79]

A study conducted by Siarhei, et al (2020). on 92 patients, compared diagnostic efficacy of Whole Body-MRI DWI and PET/CT for the staging of lymphoma, MRI-DWI showed 98.2% - Sensitivity, 99.9% - specificity, and 99.3% - accuracy while PET/CT showed 99.4%, - Sensitivity, 100.0%, - specificity, and 99.8%, - accuracy in the diagnosis of enlarged LN involvement. MRI-DWI had a sensitivity of 77.8% while PET/CT had a sensitivity of 88.1%, in the diagnosis of non-enlarged LN involvement. The study concluded that the efficacy of Whole Body-MRI DWI was comparable to PET/CT in the diagnosis of enlarged lymph node involvement while it was inferior to PET/CT in the diagnosis of non-enlarged lymph node and spleen involvement,

however, it was superior in diagnosing bone marrow involvement. MRI DWI and PET/CT determined the lymphoma stage in a similar number of patients.

Gali Shapira-Zaltsberg, et al. (2020)[80]

In a study by Gali Shapira-Zaltsberg, et al. (2020) relative to PET/CT, DW-MRI of nodal disease showed sensitivity and PPV of 0.651 and 1.0, respectively, at baseline, while the values were 0.697 and 0.885 at follow-up. Relative to PET/CT, DW-MRI of extra-nodal disease showed sensitivity and PPV of 0.545 and 0.6, respectively, at baseline, while the values were 0.167 and 0.333 at follow-up. The study concluded that in initial staging and assessment of treatment response WB-DWI MRI is inferior to PET/CT.

Gihan Hassan Gamal (2020)[81]

Gihan Hassan Gamal (2020), conducted a prospective study on thirty-two patients to evaluate the performance of whole-body MRI/DWI with background signal suppression (WB-MR/DWIBS) method, with that of 18F-FDG PET/CT, for the detection of lesions and initial staging of lymphoma patients using the histopathological diagnosis as a reference standard. He calculated the overall sensitivity, specificity and positive predictive value, negative predictive value accuracy of 18F-FDG PET/CT vs WB-MR/DWIBS. He observed that the sensitivity, specificity, PPV, NPV, and accuracy of WB-MR/DWIBS were 93%, 76%, 96%, 61%, and 91%, respectively. The overall sensitivity, specificity, PPV, NPV, and accuracy of 18F-FDG PET/CT were 96%, 100%, 100%, 80%, and 97% respectively. He concluded that, due to its greater sensitivity and specificity compared to WB-MR/DWIBS, 18F-FDG PET/CT remains the preferred imaging reference for the assessment of lymphoma. In the case of bone marrow involvement, WB-MRI/DWIBS plays a complementary role to PET/CT by avoiding unnecessary bone marrow biopsy.

Jose LDO Schiavon et al (2019)[82]

A study conducted by Jose LDO Schiavon et al (2019), on 33 patients, assessed the role of Whole-body MRI with DWI and FDG PET/CT, in the evaluation of Hodgkin's lymphoma patients. The WB-MRI with DWI showed concordance of 95.2%

to FDG PET/CT. The sensitivity and specificity are 96% and 95% respectively as demonstrated by the Kappa concordance correlation. The Kappa index was 0.8004 (p <0.001). They have concluded that with almost perfect Kappa agreement, and a very strong Pearson correlation, with the FDG PET/CT, WB-MRI / DWI can be used as an alternative, valuable & safe method in the evaluation of young adults, adolescents and children with Hodgkin's lymphoma.

Arash Latifoltojar et al (2018)[83]

A study conducted by Arash Latifoltojar et al (2018), on 50 patients to investigate the role of Whole Body-MRI compared to the standard investigation including [18]FDG PET/CT in staging and the interim response of Hodgkin's lymphoma patients, showed discordance for the full patient staging of 44% between Whole Body-MRI and a multiple modality reference. Compared to the enhanced reference standard, Whole Body-MRI had TPR of 91% and FPR of 1% for nodal disease and 79%, <1% respectively for non-nodal disease. The study concluded that the accuracy of Whole Body-MRI is reasonable for nodal and extra-nodal staging. They emphasised that the use of WB-MRI in place of routine tests, such as 18F- FDG PET/CT, is dubious because disease response may have been underestimated by this modality in extranodal locations.

Danyang Wang, et al (2018)[84]

According to a meta-analysis conducted by Danyang Wang, et al (2018), comprising 338 patients from 8 studies, the staging accuracy of Whole-Body MRI and PET/CT for lymphoma were 98% and 98% respectively. The pooled staging accuracy of [18]FDG PET/CT was 87% in patients with indolent lymphoma while it was 96% for Whole-Body MRI. The accuracy of [18]FDG PET/CT for the staging of less FDG avid indolent NHLs was 60% and that of Whole-Body MRI was 98%. The study concluded that Whole-Body MRI may serve as a viable alternative to [18]FDG PET/CT for the staging of FDG avid lymphoma. It may also be an imaging test of choice for staging indolent NHL with low FDG avidity.

Albano Domenico et al (2018)[85]

Albano Domenico et al (2018) did a study to evaluate the predictive role of whole-body DWI and PET/CT in Hodgkin's lymphoma, pre-treatment and post-two courses of ABVD. They reviewed WB-MRI and PET/CT of 41 Hodgkin's lymphoma patients before and after two courses of ABVD. Based on interim-ADC (1.83 0.34 103 mm2/s vs. 1.01 0.27 103 mm2/s; p .001), interim-size (3.1 cm2 vs. 9.4 cm2; p =.009), and bulky (8.2% vs. 66.7%; p =.002), there was a significant difference between responder and non-responder lesions. Based on baseline-SUV_{max} (p =.713), baseline-ADC (p =.253), ADC changes (p =.058), size changes (p =.085), site (p =.209), stage (p =.290), and baseline-size (p =.064), there was no statistically significant difference between responder and non-responder lesions. Size changes are ineffective, while interim-ADC is effective for identifying non-responder lesions. ADC and baseline-SUV_{max} are not predictive. The best imaging feature for predicting a subpar response to chemotherapy is a bulky disease. During ABVD treatment, DWI may be useful in separating responder from non-responder HL lesions on interim WB-MRI.

Albano Domenico et al (2016)[86]

Albano Domenico et al (2016) compared Whole-body MRI with diffusion-weighted imaging (DWI), FDG PET and bone marrow biopsy (BMB), to assess the involvement of bone marrow in patients with newly diagnosed lymphoma, in 104 patients. Using BMB and FDG PET/CT as the reference standard, the diagnostic efficacy of WB-MRI (1.5 Tesla MR scanner, with T1w, T2w-STIR, and DWI sequences) was assessed. To compare WB-MRI, FDG PET/CT, and BMB, they used Cohen's kappa coefficient to measure inter-observer agreement in WB-MRI interpretation. Excellent interobserver agreement was observed (k 5 - 0.937). With a k 5 of 0.935, the agreement between WB-MRI and FDG PET/CT was excellent. WB-MRI and BMB had a moderate (k 5 0.489) level of agreement, whereas FDG PET/CT and BMB had a medium level of agreement (k5 0.370). Four indolent non-Hodgkin lymphomas with bone marrow involvement of 30% of marrow cellularity had falsely negative WB-MRI and FDG PET/CT scans. On the other hand, all instances with a BMI > 30% of marrow cellularity were discovered by WB-MRI and FDG PET/CT. Patients with positive and negative BMB had similar mean ADC levels, which is not

statistically different (P 5 0.049). They concluded that WB-MRI and FDG PET/CT are useful techniques for determining bone marrow involvement.

Azzedine B, et al. (2015) [87]

Azzedine B, et al. (2015) did a study in which they compared 3T and 1.5T whole-body DWI MRI with FDG PET/CT as the reference standard, on twenty-three patients at initial diagnosis of lymphoma. They observed that there was an excellent concordance between 1.5T and 3T for nodal (Intra class Correlation Coefficient (CCI) = 0.995), extranodal / organ involvement (CCI =0.990) and Ann Arbor stages (k=0.967). They concluded that similar to 1.5T, a 3T WB-DW-MRI provides reliable lymphoma assessment and staging.

Rodrigo Regcini et al (2015)[88]

A systematic review is done by Rodrigo Regcini et al (2015), which reviewed six studies consisting of 116 patients, to evaluate the role of MRI-DWI vs FDG PET/CT for initial lymphoma staging, showed that in 90.5% ($\kappa = 0.871$; $P < 0.0001$) of the cases, WB-MRI and FDG PET/CT had a good agreement. MRI-DWI over-staged in relation to FDG PET/CT, whenever there was disagreement. As compared to clinical-radiological standards, the sensitivity of MRI-DWI ranged from 59 to 100% and that of FDG PET/CT ranged from 63-100%. They concluded that WB-MRI is a highly sensitive technique for the early staging of lymphoma. WB-MRI had a very good agreement with FDG PET/CT. Without ionizing radiation or an intravenous contrast agent, WB-MRI is a fantastic alternative for treating lymphoma patients.

Alessandro Stecco et al (2015)[89],

A study conducted by Alessandro Stecco et al (2015), on 17 newly diagnosed patients with primary abdominal gastrointestinal lymphoma, to evaluate the accuracy of whole-body MRI / DWI with that of FDG PET/CT in staging with histopathology or 6months clinical & radiological follow-up as the gold standard. They observed that the sensitivity, specificity, positive predictive value and negative predictive value of WB-MRI/DWI were 100%, 96.3%, 96.1% and 100% respectively. The study showed that there was no statistically significant difference between the two techniques (p = 0.05).

The kappa agreement statistics with a 95% confidence interval was 0.87 (0.82– 0.92) between the two methods. They concluded that in the staging of gastrointestinal lymphoma patients, the diagnostic value of WB-DWI-MRI is comparable to ^{18}F-FDG PET/CT.

Albano Domenico et al (2015)[90]

Albano Domenico et al (2015) conducted a comparative study on 68 patients to evaluate the role of whole-body – MRI with DWI and PET/CT in newly diagnosed FGD avid lymphomas. They observed that whole-body MRI had an excellent agreement with FDG PET/CT. In 62/68 patients (91.2%), the WB-MRI stage was equal to that of the FDG PET/CT. WB-MRI stage and the pathological stage had a high agreement (63/68 patients; 92.6%) as did FDG PET/CT stage and pathological stage (64/68 patients; 94.1%). WB-MRI under staged a patient with a lung lesion that was incorrectly identified as a peri-bronchial lymph node and over-staged one patient with HL because it assumed the patient had a peri-aortic lymph node without FDG uptake. The disparities between the stages were reported more frequently in patients with Mantle cell lymphoma. They concluded that for staging FDG avid lymphomas, WB-MRI can be viewed as a promising technique.

A Balbo-Mussetto et al (2015)[91],

A Balbo-Mussetto et al (2015), conducted a study on 41 patients to compare the accuracy of whole-body MRI with DWI to that of contrast-enhanced CT and FDG PET-CT in defining lymphoma staging. Of the 217 positive nodal sites (as determined by reference standard), CE-CT produced 11 false positives and 23 false negatives, whole body MRI-DWI made six false-positive errors and failed to recognise 17 localizations and FDG PET/CT detected all disease sites. Among 37 positives (according to the reference standard), four false-negative and two false-positive outcomes were produced by the FDG PET-CT. There were 17 false-negative results with CECT. There was only one false-negative result from the whole-body MRI-DWI. The most consistent imaging method for BM evaluation was whole-body MRI-DWI. Four patients with 18F-FDG PET-CT, twelve patients with CE-CT, and none with Wb-MRI-DWI would have had the final stage missed if each procedure were taken on its own. They concluded that the

current data support the use of whole-body MRI-DWI instead of CE-CT for staging, demonstrating its efficacy as a sensitive and specific imaging tool for lymphoma evaluation.

Marius E. Mayerhoefer (2014)[92]

Marius E. Mayerhoefer (2014) conducted a prospective study on 140 patients to evaluate the value of diffusion-weighted MRI (DWI-MRI) for pretreatment imaging of fluorodeoxyglucose (FDG)-avid lymphoma and lymphoma with variable FDG avidity. They observed that WB-MRI / DWI agreed with the reference standard in 94 of 100 patients (k – 0.92) with a sensitivity of 97%, in FDG avid lymphomas. In lymphomas with FDG variable avidity, WB-MRI / DWI agreed with the reference standard in 37 of 40 patients (k – 0.89) with a sensitivity of 97%. They concluded that WB-MRI / DWI is only slightly inferior to FDG PET/CT in therapeutic FDG-avid lymphoma staging evaluation. In lymphomas with FDG variable avidity, WB-MRI / DWI seems to be superior to both CECT and FDG PET/CT. For lymphoma staging, WB-MRI may be a useful alternative, particularly in younger patients or in locations without access to 18F-FDG PET/CT.

Annemieke S. Littooij (2014)[93]

Annemieke S. Littooij (2014) conducted a comparative study on 36 children to evaluate the role of whole-body MRI with DWI vs FDG PET/CT in newly diagnosed paediatric lymphoma. They observed that whole-body MRI with DWI had very good agreement with FDG PET/CT base reference standard for both nodal (k- 0.91) and extranodal (0.94) lymphoma staging. Consensus whole-body MRI-DWI had sensitivity and specificity of 93% and 98% for nodal staging and 89% and 100% for extranodal staging, respectively. In 28 out of 33 patients, the lymphoma stage determined by whole-body MRI-DWI coincided with the reference standard after MRI reader errors were corrected. They concluded that It is possible to stage paediatric lymphoma with whole-body MRI-DWI, which has the potential to be a good radiation-free substitute for FDG PET/CT.

Horger M et al (2014)[94],

Horger M et al (2014), in their study on 20 patients, evaluated the role of whole-body diffusion-weighted MRI for very early assessment of response to therapy in various lymphoma subtypes. They have shown a considerable increase in the ADC of responding lesions in successfully totally treated HL and NHL, but nonresponding lesions showed unchanged ADC values. Although less dramatically, size differences between responding and nonresponding lesions were also noted. They concluded that whole-body diffusion-weighted MRI can be a practical diagnostic technique for evaluating very early responses in lymphoma patients and predicting long-term responses.

Punwani S, et al (2013)[95]

Punwani S, et al (2013) conducted a study to evaluate the role of dynamic contrast-enhanced MRI for the evaluation of splenic involvement in Hodgkin's lymphoma. They recruited thirty-one children who underwent whole-body T2 MRI with supplementary dynamic contrast-enhanced splenic imaging, and whole-body PET CT pre and post-chemotherapy. They observed that the addition of dynamic contrast to T2-weighted MRI increased the sensitivity and specificity to 100%/100% compared to 57%/100% with T2-weighted MRI alone. They concluded that the evaluation of splenic involvement in Hodgkin's disease may be enhanced when T2-weighted imaging is combined with DCE-MRI imaging.

Hugo J. A. Adams (2013)[96]

Hugo J. A. Adams et al (2013), did a study on 116 patients to evaluate and compare the role of whole-body MRI with FDG PET for detecting bone marrow involvement in lymphoma. They observed that the sensitivity of whole-body MRI in all lymphomas, aggressive lymphomas and indolent lymphomas was 45.5%, 88.9% and 23.5% respectively. The sensitivity of FDG PET in aggressive lymphomas and indolent lymphoma was 83.3% and 12.5% respectively. Both modalities had higher sensitivity in aggressive lymphomas as compared to indolent lymphomas and there was no significant difference in sensitivity of the two modalities. They concluded that Whole-

body MRI's sensitivity to identify lymphomatous bone marrow involvement is too low to (completely) replace bone marrow biopsy (BMB).

Goran Abdulqadhr (2011)[97]

Goran Abdulqadhr (2011) conducted a study on 31 patients and compared whole-body diffusion-weighted imaging with FDG PET/CT in lymphoma staging. In 28 (90.3%) patients, the staging was the same for DWI and FDG PET/CT, while it was different in three (9.7%) patients. 11 patients out of the 28 patients that had the same staging on both modalities, had stage IV in both procedures, while 17 had stages 0 to III. There were no individuals with aggressive non-Hodgkin lymphoma or HL who had different staging. When compared to FDG PET/CT, the staging of three indolent small lymphocytic lymphoma/chronic lymphocytic leukaemia (SLL/CLL) lymphomas was higher with DWI. All other extranodal lesions were identified by both modalities, except one small subcutaneous breast lymphoma. They concluded that in both aggressive and indolent non-lymphoma Hodgkin's as well as HL, whole-body MRI / DWI is a promising staging method.

Short Punwani, et al (2010)[98]

In a study conducted by Shonit Punwani, et al (2010) Whole-body STIR half-Fourier RARE MR imaging showed sensitivity and specificity of 98% and 99%, respectively, for nodal disease while it was 91% and 99%, respectively, for extra-nodal disease. The study reported a very good agreement between MR imaging and enhanced PET/CT. The study concluded that MR imaging can be a radiation-free alternative for nodal and extra-nodal disease in paediatric and adolescent lymphoma at initial staging.

Henriëtte M. E. Quarles van Ufford et al (2010)[99],

A study was done by Henriëtte M. E. Quarles van Ufford et al (2010), which included 22 patients, to compare the whole-body MRI/DWI with FDG PET/CT in the staging of newly diagnosed lymphoma, showed, the whole-body MRI-DWI findings of Ann Arbor staging was concordant with that of FDG-PET/CT in 77% (17/22) of patients. In none of the patients under staging was done however, 23% of patients were over-staged relative to FDG PET/CT which had therapeutic consequences. They concluded that whole-body MRI / DWI had a moderate agreement with FDG PET/CT.

In a minority of patients, whole-body MRI / DWI leads to clinically important over-staging relative to FDG PET/CT. Until larger-scale studies demonstrate that the use of whole-body MRI-DWI yields proper staging in this minority of cases, FDG PET/CT remains the reference standard for lymphoma staging.

Lin C, et al (2009)[100]

Lin C, et al (2009) in their study on fifteen patients, to develop a whole-body MR protocol with exclusive diffusion-weighted imaging with respiratory gating and evaluated the technique's utility for lesion detection and staging in patients with diffuse large B-cell lymphoma (DLBCL) with integrated ^{18}F-FDG PET/CT as the gold standard. DWI had respective sensitivity and specificity of 90% and 94% for lymph nodal involvement. Size measurement and visual ADC analysis together raised DWI specificity to 100% with 81% sensitivity. DWI and ^{18}F-FDG PET/CT agreed in all 20 organs that were documented (100%) regarding organ involvement. Restricted diffusion was present in all implicated organ lesions. In 14 (93%) of the 15 patients, Ann Arbor stages were in agreement between WB-MRI and ^{18}F-FDG PET/CT. They concluded that in patients with DLBCL, whole-body DWI with ADC analysis may be used to identify and stage lesions.

Thomas C. Kwee, et al. (2013)[101]

In a study conducted by Thomas C. Kwee, et al. (2013) on 108 newly diagnosed lymphoma patients, MRI without DWI showed staging results equal to that of CT in 66.6%, higher in 24.1%, and lower in 9.3%, while MRI with DWI showed staging results equal to that of CT in 65.4%, higher in 27.9% and lower in 6.7% concluding Whole Body MRI equals CT staging in most of the patients and there is no added advantage of additional DWI. Thus Whole body MRI can be a radiation-free alternative to CT.

D. D. Brennan et al (2005)[102]

D. D. Brennan et al (2005) conducted a study on 23 patients to compare the role of whole-body MRI and computed tomography for lymphoma staging. The sensitivity of whole-body MRI in detecting lymph nodes varied significantly depending on their

size, yet it is an exceedingly specific diagnostic modality. The sensitivity of WB-MRI was 10.7%, 67.0% and 92% for lymph node sizes of 1-6mm, 6-12mm and >12mm respectively, however specificity for all three categories was >99%. They concluded that, with the ability to stage the disease, identify lymph nodes larger than 1.2 cm, and additionally assess for the presence or absence of disease dissemination to the bone marrow, whole-body MRI represents an alternative to CT in the staging of lymphoma. Compared to MRI, CT can identify more nodes (up to 1.2 cm), but this does not change the tumour stage.

HYPOTHESIS

Whole-body MRI with combined STIR and DWI has good diagnostic efficiency in detecting lymph nodal and extranodal site or organ involvement and staging of lymphoma.

AIMS AND OBJECTIVES

<u>Aim</u>:

- To evaluate the role of Whole-Body MRI for initial staging in cases of lymphoma.

<u>Objective:</u>

- To estimate the diagnostic accuracy of Whole-Body MRI and ^{18}F-FDG PET/CT using a composite reference standard.
- To evaluate the concordance between Whole-Body MRI and ^{18}F-FDG PET/CT in cases of lymphoma.

MATERIALS AND METHODS

STUDY DESIGN: Prospective observational study.

STUDY SITE: Department of Diagnostic and Interventional Radiology, All India Institute of Medical Sciences, Jodhpur.

STUDY GROUP: All patients with histologically proven lymphoma, referred from departments of Paediatrics and Medical Oncology, All India Institute of Medical Sciences (AIIMS), Jodhpur, who fulfil the following criteria, were enrolled in the study.

INCLUSION CRITERIA:
1. All newly diagnosed patients with histologically proven lymphoma.

EXCLUSION CRITERIA:
1. History of treatment (chemotherapy/radiotherapy) of lymphoma within the previous 2 years.
2. Patients with primary central nervous system lymphoma.
3. Non-consenting patients.
4. All pregnant and lactating women.
5. General MRI contra-indications (e.g.: Claustrophobia, Cochlear implants)

STUDY DURATION: From January 2021 To December 2022.

STUDY METHODOLOGY

  We conducted a prospective study among the patients who were referred from the departments of Paediatrics and Medical Oncology, at All India Institute of Medical Sciences (AIIMS), Jodhpur during the period between January 2021 and December 2022.

  Patients of either sex and all age groups who have pathologically confirmed cases of lymphoma were approached for participating in the study. Patients were primed about the study procedure, the possible benefits, and any adverse outcomes,

through a patient information sheet (in English/Hindi). They were enrolled after taking valid informed consent/Parental consent, permission and child Assent.

After taking written informed consent, all cases were subjected to the following MRI imaging protocol:

- T_1-weighted, short tau inversion recovery (STIR) and Diffusion-weighted imaging.

Lymphoma patients referred from departments of Paediatrics and Medical oncology, AIIMS, Jodhpur

Patients were explained about the study procedure, the benefits and any adverse

Informed consent/parental permission and childhood assent was taken

Cases were subjected to the following MRI imaging protocol – T1 weighted, Short Tau Inversion Recovery (STIR) & Diffusion Weighted Imaging (DWI)

Patients underwent ^{18}F-FDG PET/CT within 14days of WB-MRI or vice versa

A composite reference standard based on clinical evaluation, histology and standard imaging including ^{18}F-FDG PET/CT was established

Concordance between WB-MRI, PET/CT and a composite reference standard was evaluated

Imaging acquisition:

Whole-body MRI protocol

Patient preparation – Patients were advised to take a low-residue diet one night before. Patients were imaged on a 3T MRI system (SEIMENS MAGNETOM VIDA 3T / GE Discovery MR 750 w 3T SYSTEM USA) from the vertex to toe in the supine position, using the manufacturer's body and peripheral angiogram coils.

In brief, the coronal whole-body short tau inversion recovery (STIR) sequence was acquired in 3-5 stations depending on the patient's height. STIR sequence was complemented by the addition of axial free-breathing DWI (with three values b_{50}, b_{500}, b_{800}) acquired through the whole body in 3-5 stations. ADC maps were generated using the vendor's software. DWI images were reconstructed in coronal planes/whole-body composite images, whenever required.

An additional non-contrast T1-weighted sequence (3D LAVA Flex/Dixon) was also acquired however, it was not included in the whole-body MRI analysis for this study. The full WB-MRI scanning protocol was completed within 40-50 minutes. WB-MRI scanning parameters are summarized in Table 6.

Table 6: Whole-body MRI sequence parameter

	Coronal STIR	Axial DWI (b50,500,800)	3D LAVA Flex/DIXON
TR/TE (ms)	*800/60*	*4900/66*	*2.87/0.93*
Inversion time (ms)	*180*	*180*	*N/A*
Matrix	*128×96*	*128×96*	*256×176*
Slice Thickness (mm)	*4*	*4*	*2.5*
No. of slices	*27*	*27*	*80*
Averages	*8*	*8*	*1*
Echo train	*1*	*1*	*1*
PAT	*2*	*2*	*2*
Flip angle	*90*	*90*	*9*
Pixel spacing	*0.8×0.8*	*0.8×0.8*	*1.56×1.56*

SAMPLE SIZE CALCULATION

The sample size was calculated based on the study done by Latifoltojar et al[83]. Considering the sensitivity of a whole-body MRI of 91% in the detection of lymphoma with a relative precision of 10% at a 95% confidence interval, the sample size needed for the study was 31 subjects.

Sample Size (n) = $[Z (1-\alpha/2)]^2$ x p (1-p) /d^2]

P= sensitivity or specificity of the new test;

Z (1-α) = 1.96 as a significance level of 95%

N = 31 subjects for study.

DATA ANALYSIS AND INTERPRETATION

A radiologist (TY with 12 years of experience) and a nuclear medicine consultant (RK with 16 years of experience) independently read the whole-body MRI and PET/CT scans, respectively. Both of them did not have access to the findings of any other diagnostic imaging tests or information from bone marrow (BM) biopsy, but they were aware of the lymphoma's morphological subtype. Ten nodal groups (cervical, supra clavicular, axillary, mediastinal, hilar, mesenteric, hepatic hilar, para-aortic, iliac and inguinal groups) and 11 extranodal site/organ involvement (bone marrow, lungs, liver, spleen, stomach, bowel, pancreas, kidney, pleura, pericardium, and chest wall) and final modified Ann Arbor staging were assessed on a) whole body STIR, b) whole body DWI sequences separately followed by c) whole-body MRI (including both STIR and DWI) and d) PET/CT. All four of these were then compared with a composite reference standard (CRS - comprised of final diagnosis including information from initial PET/CT, Whole-body MRI, Bone marrow biopsy/focal bone lesion biopsy and HPE/ T1 weighted sequence for marrow infiltration/ follow up post-chemotherapy PET/CT if equivocal findings on initial PET/CT)

In the interpretation of the whole-body MRI examination, the following criteria were used. Lymph nodes were considered involved if they are enlarged with a short axis diameter >1cm, except those with prominent fatty hilum and minimal parenchyma[1]. Lymph nodes with prominent fatty hilum were considered reactive and not involved, if the short axis diameter was <1cm. In cases of round shape, absence of

hilum, local clustering, and localization in atypical locations, non-enlarged LN (1 cm in short-axis diameter) were believed to be involved. We did not separately analyse enlarged versus non-enlarged lymph nodes. The identification of foci or areas of abnormal signal intensity of a non-liquid or non-vascular character in the liver, spleen, and other organs and soft tissues, as well as the presence of foci or infiltrates in the lungs, were used to determine organ involvement[1]. More than a 13 cm increase in the vertical size of the spleen was considered to indicate diffuse involvement[2]. The indicators of BM involvement were taken as bone destruction, a pathologic soft tissue component, a signal increase/lytic lesion on short inversion time inversion recovery (STIR) images above the muscles, focal or diffusely reduced signal intensity on T1-weighted (T1w) images lower or equal to that of surrounding muscles (T1WI was only used in making composite reference standard, not during the evaluation of Whole body MRI diagnostic efficiency). The feature of a diffuse increase in spine signal intensity above the kidney parenchyma was considered to be the sign of diffuse BM involvement in NHL, while foci with signal intensity above the surrounding BM on DWI b800 images were considered to be the sign of focal BM involvement. In Hodgkin's lymphoma diffuse increase in bone, marrow signal was not considered as a sign of involvement[4].

Regardless of their size, LN was considered implicated when FDG uptake rose above the background or the mediastinal blood pool during PET/CT interpretation. Focal FDG uptake above the surrounding background or the mediastinal blood pool was considered a sign of organ involvement. Spleen was considered involved if there was diffuse FDG uptake above the liver in both HL and NHL. Bone marrow was considered involved if there was diffuse FDG uptake above the liver only in NHL. Bone marrow was also considered positive, with SUV of more than 100% or 150% of the liver SUV.

Table 7: Predefined criteria for nodal assessment.

	Cross-sectional imaging (Anatomical MRI sequences, CT component of PET/CT)	**PET/CT***	**WB-MR imaging.**
Positive	Nodes >2 cm**	N/A	Nodes >2 cm**
	Nodes 1-2 cm	FDG PET positive	Nodes 1-2 cm with ADC $\leq$ 1.2 and morphological criteria
	Nodes < 1 cm	FDG PET positive	Nodes <1 cm with ADC $\leq$ 0.8 and morphological criteria
Negative	Nodes 1-2 cm	FDG PET negative	Nodes 1-2cm with ADC $\geq$ 1.8 and morphological criteria
	Nodes <1cm	FDG PET negative	Nodes < 1cm with ADC $\geq$ 0.8 and morphological criteria

* Involvement defined as uptake above surrounding background in a location incompatible with normal physiological activity

** Long axis diameter.

Table 8: Pre-defined criteria for extra-nodal assessment

Site	PET-CT	WB-MRI
Pleura	Involvement of the pleura is assumed if • the lymphoma is contiguous with the pleura without fat lamella or • the lymphoma invades the chest wall or • a pleural effusion occurs which cannot be explained by venous congestion. Extension: Abnormal nodular tissue within the pleura	Extension: Abnormal nodular moderate- high signal of equal intensity to nodal tissue within the pleura contiguous with the main nodal mass. Separate: Abnormal high signal of fluid intensity anatomically in keeping with a pleural effusion which cannot be explained by associated pulmonary oedema; or, pleural nodules discrete to the main lymph node mass.

	contiguous with the main nodal mass.	
Pericardium	Pericardial involvement is assumed if • the lymphoma has a broad area of close contact towards the heart surface beyond the valve level (ventriculus area) or • a pericardial effusion occurs/ nodules without associated mediastinal lymph node mass. Extension: Extensive contact between mediastinal lymph node mass and pericardium to the level of the ventricles in the presence of pericardial effusion and/or pericardial nodules.	Extension: Extensive contact between mediastinal lymph node mass and pericardium to the level of the ventricles in the presence of pericardial effusion and/or pericardial nodules. Separate: Pericardial effusion/nodules without associated mediastinal lymph node mass.
Chest wall	Chest wall infiltration is defined as an extension of a mediastinal mass on CT and/or PET-positive focal chest wall lesion.	Extension: Moderate-high signal infiltration of the chest wall in continuum with a lymphatic mass/or positive focal chest wall lesion on T2-STIR, DWI and/or post-contrast.
Lungs	A disseminated lung involvement (implying stage IV) is assumed if • there are more than three foci or • an intrapulmonary focus has a diameter of more than 10 mm. Extension: Abnormal infiltration of the lung in continuum with a lymphatic mass.	Extension: Abnormal moderate-high signal infiltration of the lung in continuum with a lymphatic mass. Separate: Abnormal moderate-high signal focus (>1cm diameter) within the lung discrete to lymphatic tissue or more than three foci.
Bone marrow	Bone involvement is assumed if a bone biopsy is positive **or** CT bony window is positive with or without further confirmation by other imaging methods in the same region **or** by either FDG PET.	Homogenous moderate-high signal foci within bone on T2-STIR, DWI and/or post- contrast at a site discrete to the bone marrow biopsy.

Liver	The liver is considered involved if FDG PET is positive. Extension: Moderate-high signal infiltration of the liver in continuum with an adjacent lymphatic mass	Extension: Moderate-high signal infiltration of the liver in continuum with an adjacent lymphatic mass on T2-STIR, DWI and/or post-contrast. Separate: Low signal (relative to surrounding liver) discrete foci within the liver not in continuation with an adjacent lymphatic mass.
Spleen	Spleen is considered involved if FDG PET signal is more than liver or Moderate-high signal infiltration of the spleen in continuum with an adjacent lymphatic mass.	Extension: Moderate-high signal infiltration of the spleen in continuum with an adjacent lymphatic mass. Separate: Low signal (relative to surrounding spleen) discrete foci within the spleen on T2-STIR, DWI and/or DCE not in continuation with an adjacent lymphatic mass.
Kidney	Diffuse enlargement with distortion of the renal parenchyma or focal lesion on PET/CT with positive disease.	Global or focal renal enlargement and / or discrete renal mass.
Stomach	Focal thickening that demonstrates PET/CT positivity.	Marked wall thickening in a distended stomach with moderate-high signal.
Pancreas	Diffuse enlargement with distortion of the pancreatic parenchyma or focal lesion with PET/CT positive disease.	Focal signal change within the pancreas or global pancreatic enlargement.
Bowel	Focal thickening that demonstrates PET/CT positivity	Focal bowel wall thickening and elevated STIR-HASTE signal intensity.

Tables 7 & 8 are adopted and modified from a study by Arash Latifoltojar et al[83].

The mediastinal blood pool or focused FDG uptake above the background were indicators of organ involvement. Diffuse FDG uptake above the liver was a marker of

diffuse spleen involvement in HL and NHL, as well as diffuse BM involvement in NHL solely[4].

STATISTICAL ANALYSIS

A binary classification of each disease status as either negative or positive was made as part of the composite reference standard including both nodal and extra-nodal sites. Results were calculated as frequency and percentage of patients who will have a concordance below 100% for all disease sites combined, and separately for nodal and extra-nodal sites. Sensitivity, specificity, and diagnostic accuracy parameters of WB-MRI (STIR, DWI separately for each of these two sequences, whole-body MRI including both STIR and DWI combined) and PET/CT separately were calculated for nodal and extra-nodal disease sites. The analysis of ROC curves with AUC comparison was used for integrated assessment of the diagnostic efficiency. The AUC value of 0.5–0.6 corresponds to insufficient diagnostic efficiency, while 0.6–0.7 to low, 0.7–0.8 to medium, 0.8–0.9 to good, and 0.9–1.0 to high. Cohen's kappa was calculated for WB-MRI and PET/CT separately for nodal, and extra-nodal sites and combined for including both nodal and extra-nodal sites. The kappa (k) value of 0.00–0.20 indicates low agreement, 0.21–0.40 medium, 0.41–0.60 Moderate, 0.61–0.80 good, and 0.81–1.00 high. Agreement for Ann Arbor staging between WB-MRI and PET/CT were summarised in terms of frequency, and percentages. The differences were considered statistically significant at $p < 0.05$. Statistical analysis was performed using the SPSS (Version 29), and MedCalc (version 20.211).

OBSERVATIONS AND RESULTS

In our study, a total of 42 patients with histopathologically proven lymphoma, underwent whole-body MRI. Out of the 42 patients, 5 patients were excluded due to lack of PET/CT and 2 patients were excluded due to a discrepancy in the histopathological report (found to be benign). We included a total of 36 patients, out of which, 15 patients were of Hodgkin's lymphoma and 21 patients were of non-Hodgkin's lymphoma. The most common lymphoma in the group was classical Hodgkin's lymphoma.
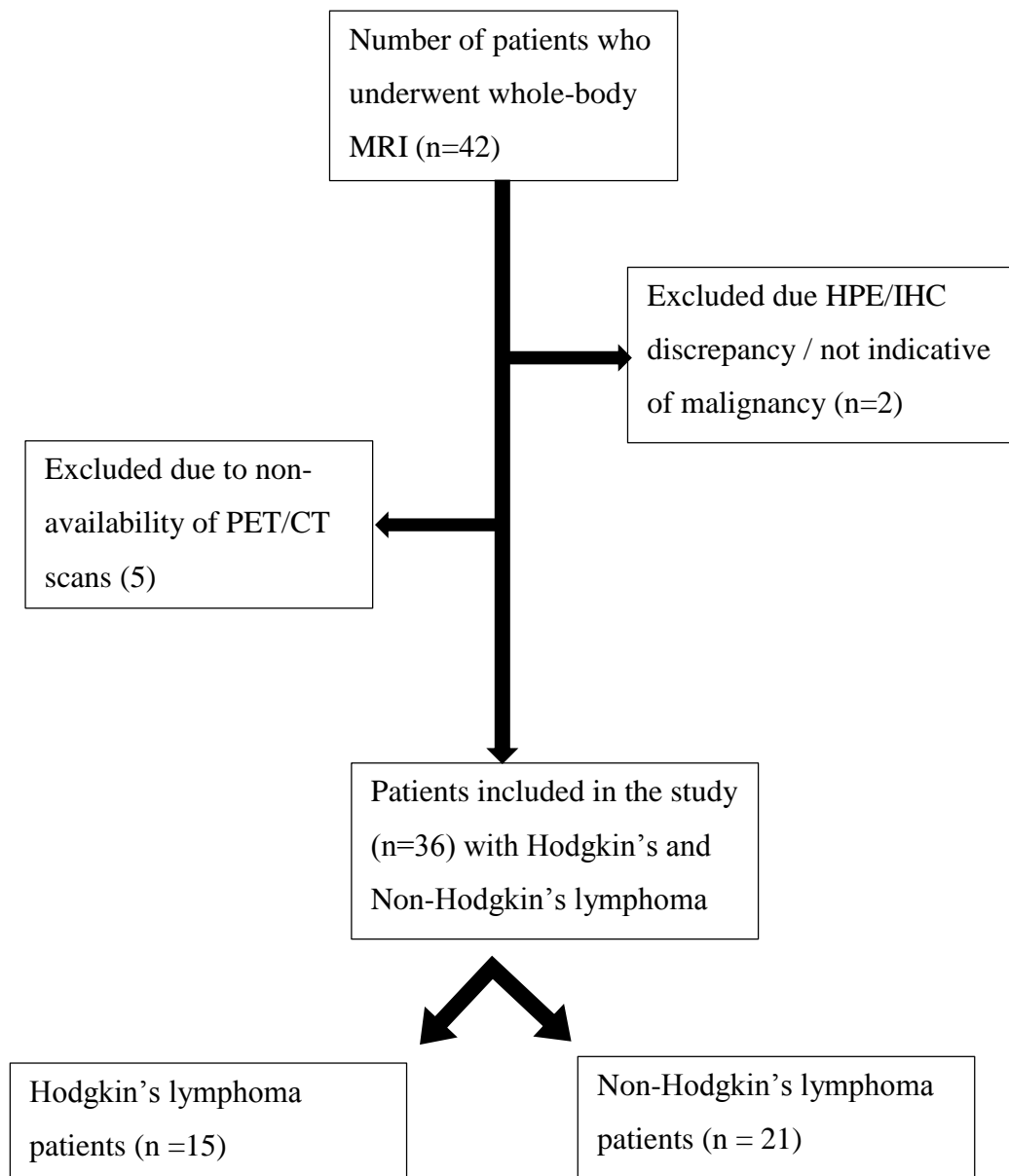
Figure 22: Flowchart of the patients in the study.

Patient-wise data:

Gender distribution:

The total number of patients included in the study was 36. Out of the 36 patients, 23 patients (~64%) were males and 13 patients (~36%) were females, suggesting male predominance of the disease in our study group (Figure - 23).
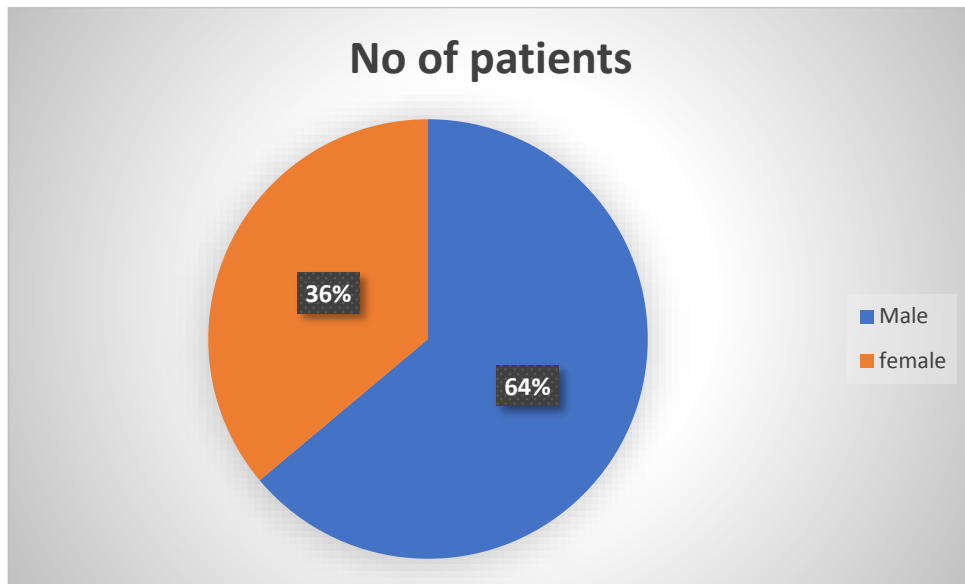
Figure 23: Pie chart denoting gender distribution among patients of lymphoma (n = 36)

Age distribution:

The age of the patients ranged from 7 years to 70 years with the mean age being 37.5 years (standard deviation of 20.1 years) and the median age of the population was 39 years.

Out of the 36 patients, 10 patients were in the 1-18 years age group, 9 patients were in the 18-40 years age group, 12 patients were in the 40-60 years age group and 6 patients were in the 60 -80 years age group. The predominant age group was 40-60 years having 12 patients. There were 10 pediatric patients with a mean age of 12 years and the median age of 11.5 years. Of the 36 patients, 23 patients were males and 13 patients were females, with a mean age of males and females 37 years and 38 years respectively. The mean age among the Hodgkin's lymphoma age group was 29 years, while that of the non-Hodgkin's lymphoma group was 44 years (Figure 24).
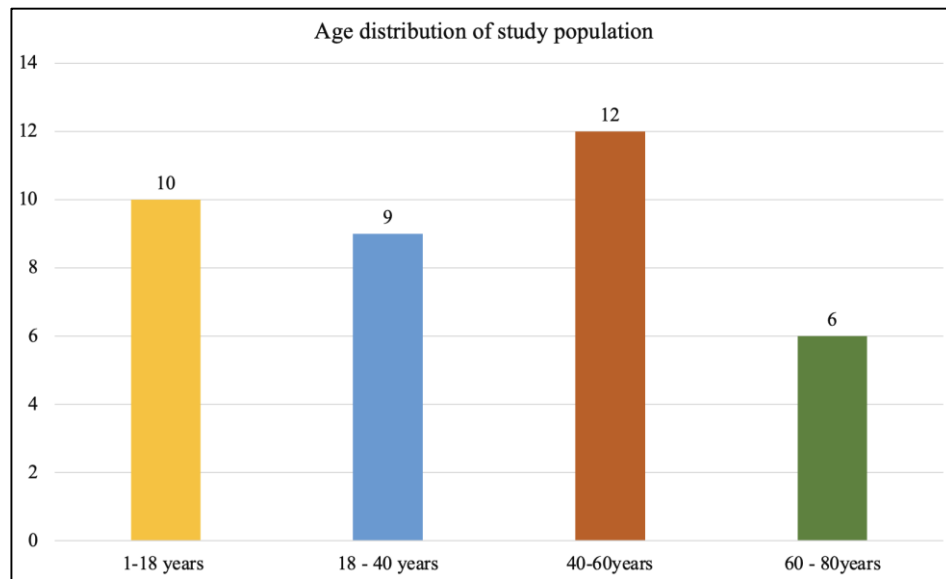
Figure 24: Bar chart showing age group distribution among lymphoma patients (n = 36)

<u>Lymphoma type and subtype distribution:</u>

Of the 36 patients with lymphoma, 15 patients were of Hodgkin's lymphoma and non-Hodgkin's lymphoma (figure 25).
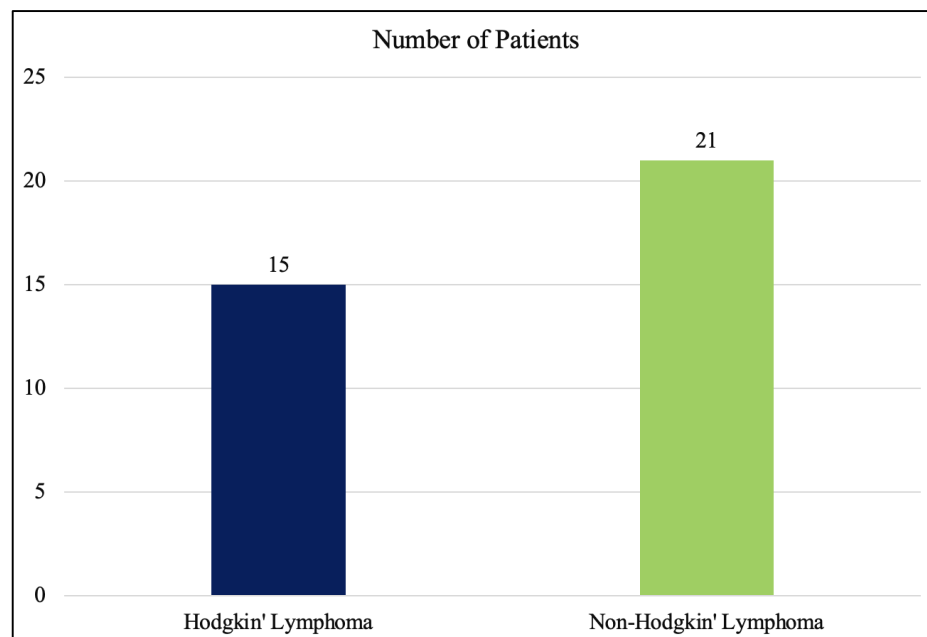
Figure 25: Bar chart showing type of lymphoma distribution.

Hodgkin's lymphoma patients were predominantly consisting of the classical subtype of Hodgkin's lymphoma (13 patients) with a minor contribution from nodular lymphocyte predominant Hodgkin's lymphoma (2 patients) (figure 26).
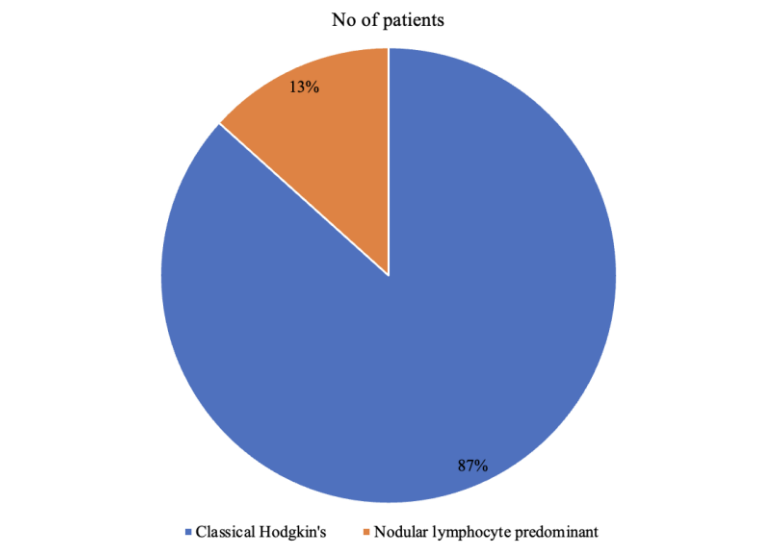
Figure 26: Pie chart showing HL subtype distribution

NHL patients' group was consisting of further subtypes. DLBCL and primary mediastinal large B cell lymphoma included >50% (12 patients) of NHL patients. Other contributory subtypes were chronic lymphocytic leukaemia (***CLL***) / small lymphocytic lymphoma (***SLL***), Burkitt's lymphoma, follicular lymphoma, mantle cell lymphoma, anaplastic large cell lymphoma (figure 27).
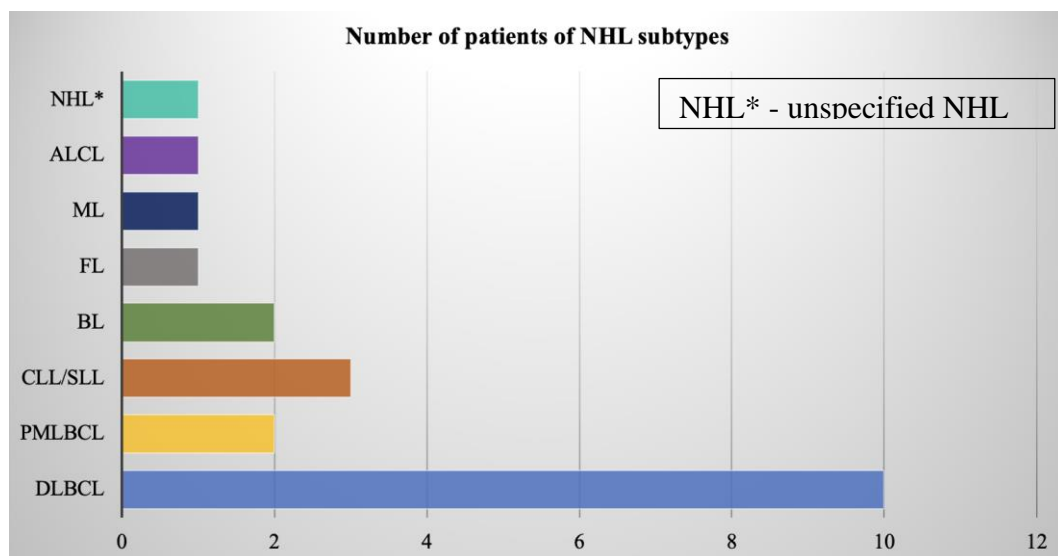
Figure 27: Bar chart showing NHL subtypes.

Comparison of the number of nodes detected by each modality

In our study, of the 193 nodal sites involved by lymphoma, whole-body STIR detected approximately 153 nodal stations, whole-body DWI detected 169 nodal stations, whole-body MRI detected 171 stations and PET-CT detected all 193 nodal stations (figure 28).
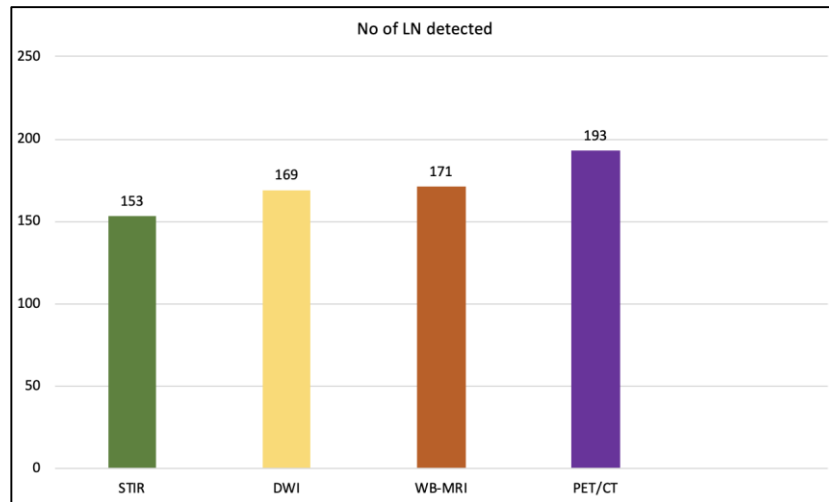
Figure 28: Bar chart showing the total number of nodal sites detected by each modality.

Comparison of the number of extranodal sites detected by each modality

In our study, of the 80 extranodal sites involved by lymphoma, whole-body STIR detected approximately 64 extranodal stations, whole-body DWI detected 74 nodal stations, whole-body MRI detected 75 stations and PET-CT detected 78 nodal stations.
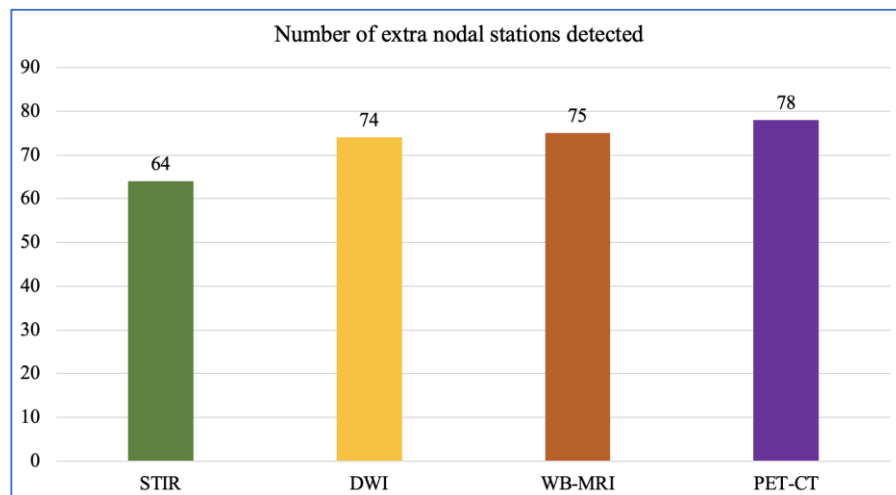
Figure 29: Bar chart showing the total number of extranodal sites detected by each modality.

Comparison of STIR, DWI, WB-MRI and PET/CT in lymph node involvement

According to the composite reference standard, 360 groups of lymph nodes, the involvement of 194 groups of nodes were established. The comparison results of STIR, DWI, WB-MRI and PET/CT are shown in Table 9 and figure 30, and 31. The sensitivity, specificity, and accuracy in the diagnosis of both lymph node involvement were 78.8%, 95.7% and 86.6% for STIR, 87.1%, 92.7%, and 89.7% for DWI, 88.1%, 96.7% and 92.2% for WB-MRI and 99.4%, 99.4% and 99.4% for PET/CT. The measure of agreement (kappa) between WB-MRI and PET/CT for lymph nodal involvement was 0.834.

STIR, DWI, WB-MRI and PET/CT efficiency in the diagnosis of LN involvement in 36 patients with lymphoma											
Method	Number of LN groups					Diagnostic efficiency characteristics					
	TP	FP	TN	FN	Total	Sensitivity (%)	Specificity (%)	Accuracy(%)	PPV (%)	NPV(%)	AUC
STIR	153	7	159	41	360	78.9	95.8	86.7	95.6	79.5	0.873
DWI	169	12	154	25	360	87.1	92.8	89.7	93.4	86.0	0.899
WB-MRI	171	5	161	23	360	88.1	96.7	92.2	97.2	87.5	0.926
PET/CT	193	01	165	01	360	99.5	99.4	99.4	99.5	99.4	0.994

Table 9: Showing the diagnostic efficiency of STIR, DWI, WB-MRI and PET/CT in the evaluation of lymph node involvement
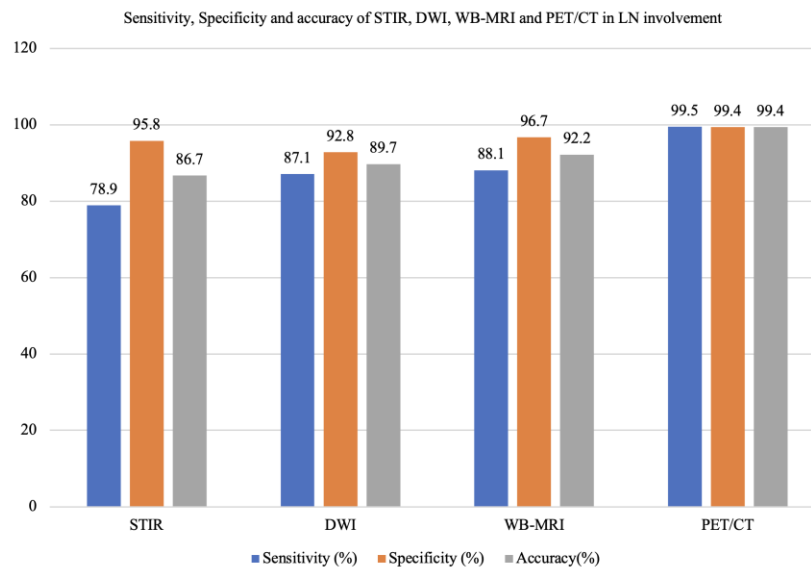
Figure 30: Bar chart showing the diagnostic efficiency of STIR, DWI, WB-MRI and PET/CT in the evaluation of lymph node involvement
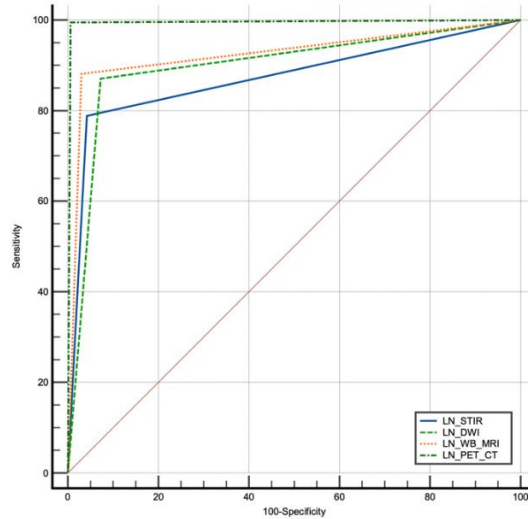
Figure 31: Showing comparison of the ROC curve of various modalities for LN detection.

Comparison of STIR, DWI, WB-MRI and PET/CT in extranodal site/organ involvement

According to the composite reference standard, lung involvement was established in 7 (19%) patients, liver involvement in 10 (27%), spleen involvement in 17 (47%), BM involvement in 19 (52%), pancreas involvement in 7 (19%), pleural involvement in 6 (16%), bowel involvement in 5 (13%) and other organ involvement in 18 (20%). The kidney was involved in 3 patients, the stomach was involved in 2 patients, the pericardium was involved in one patient and the chest wall was involved in 3 patients. The measure of agreement (kappa) between WB-MRI and PET/CT for extranodal site/organ involvement was 0.920. The comparison results of STIR, DWI, WB-MRI and PET/CT for extranodal site/organ involvement are shown in Table 10 and figure 32, and 33.

STIR, DWI, WB-MRI and PET/CT efficiency in the diagnosis of extra nodal organ involvement in 36 patients with lymphoma										
Method	Number of extra nodal groups					Diagnostic efficiency characteristics				
	TP	FP	TN	FN	Total	Sensitivity (%)	Specificity (%)	Accuracy (%)	PPV (%)	NPV(%)	AUC
STIR	64	02	314	16	396	80.0	99.4	95.5	97.0	92.0	0.897
DWI	74	04	312	06	396	92.5	98.7	97.5	94.9	98.1	0.956
WB-MRI	75	02	314	05	396	93.8	99.4	98.2	97.4	98.4	0.966
PET/CT	78	01	315	02	396	97.5	99.7	99.2	98.7	99.4	0.986

Table 10: Showing the diagnostic efficiency of STIR, DWI, WB-MRI and PET/CT in the evaluation of extranodal site/organ involvement

Figure 32: Bar chart showing the diagnostic efficiency of STIR, DWI, WB-MRI and PET/CT in the evaluation of extranodal site/organ involvement

The sensitivity, specificity, and accuracy in the diagnosis of extranodal site/organ involvement were 80.0%, 99.4% and 95.5% for STIR, 92.5%, 98.7%, and 97.5% for DWI, 93.8%, 99.4% and 98.2% for WB-MRI and 97.5%, 99.7% and 99.2% for PET/CT.
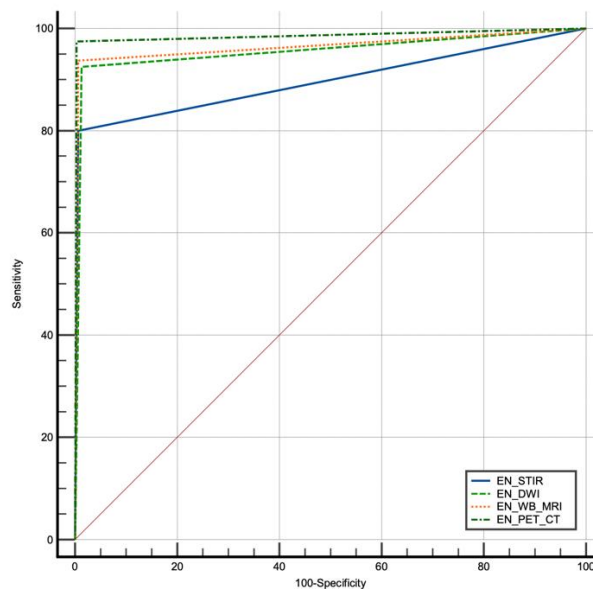
Figure 33: Showing comparison of the ROC curve of various modalities for extranodal site detection.

Comparison of STIR, DWI, WB-MRI and PET/CT in both lymph node and extranodal site/organ involvement

The sensitivity, specificity, and accuracy in the diagnosis of both nodal and extranodal site/organ involvement were 79.2%, 98.1% and 91.3% for STIR, 88.7%, 96.7%, and 93.8% for DWI, 89.8%, 98.6% and 95.4% for WB-MRI and 98.9%, 99.6% and 99.3% for PET/CT.

The measure of agreement (kappa) between WB-MRI and PET/CT for both nodal and extranodal site/organ involvement was 0.883. The comparison results of STIR, DWI, WB-MRI and PET/CT in both lymph nodes and extranodal site/organ involvement are shown in Table 11 and figure 34, and 35.

STIR, DWI, WB-MRI and PET/CT efficiency in the diagnosis of both nodal and extra nodal organ involvement in 36 patients with lymphoma											
Method	Number of LN and extra nodal groups					Diagnostic efficiency characteristics					
	TP	FP	TN	FN	Total	Sensitivity (%)	Specificity (%)	Accuracy (%)	PPV (%)	NPV(%)	AUC
STIR	217	09	473	57	756	79.2	98.1	91.3	96.0	89.3	0.887
DWI	243	16	466	31	756	88.7	96.7	93.8	93.8	93.8	0.927
WB-MRI	246	07	475	28	756	89.8	98.6	95.4	97.2	94.4	0.942
PET/CT	271	02	480	03	756	98.9	99.6	99.3	99.3	99.4	0.992

Table 11: Showing the diagnostic efficiency of STIR, DWI, WB-MRI and PET/CT in the evaluation of lymph nodal and extranodal site/organ involvement

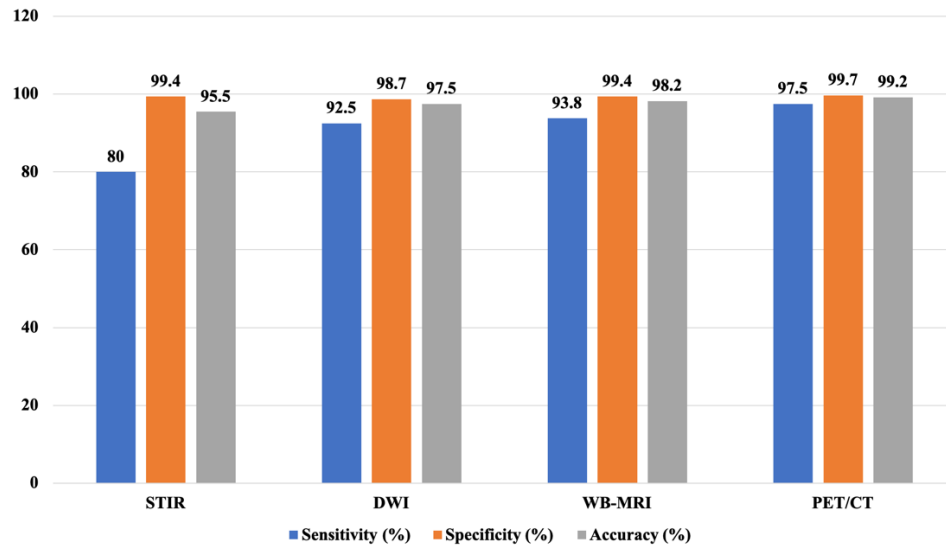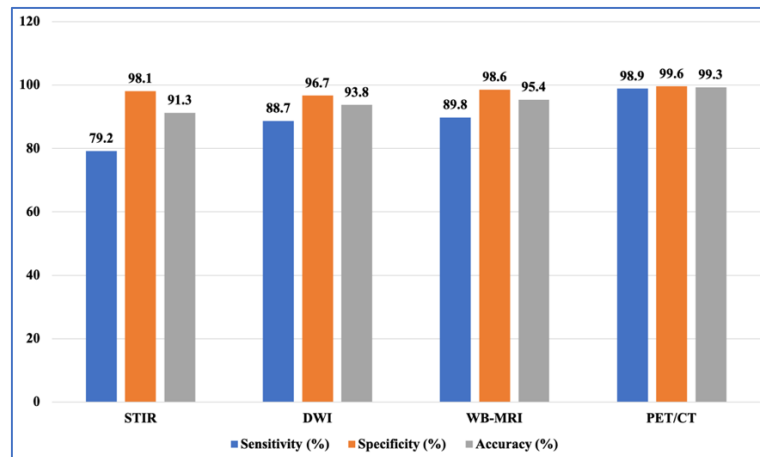**Figure 34**: Bar chart showing the diagnostic efficiency of STIR, DWI, WB-MRI and PET/CT in the evaluation of lymph nodal and extranodal site/organ involvement.
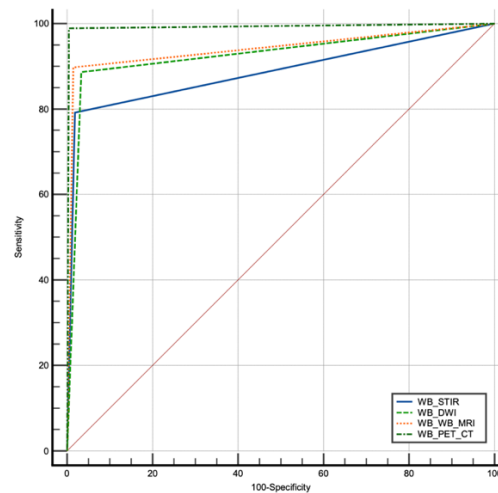
Figure 35: Showing comparison of the ROC curve of various modalities for both LN and extranodal station detection.

Comparison of STIR, DWI, WB-MRI and PET/CT in bone marrow involvement

The sensitivity, specificity, and accuracy in the diagnosis of bone marrow involvement were 73.7%, 100% and 86.1% for STIR, 94.7%, 94.1%, and 94.4% for DWI, 94.7%, 100% and 97.2% for WB-MRI and 94.7%, 94.1% and 94.4% for PET/CT.

The comparison results of STIR, DWI, WB-MRI and PET/CT in bone marrow involvement are shown in Table 12 and figure 36, and 37.

STIR, DWI, WB-MRI and PET/CT efficiency in the diagnosis of bone marrow involvement in 36 patients with lymphoma										
Method	Number of LN and extra nodal groups					Diagnostic efficiency characteristics				
	TP	FP	TN	FN	Total	Sensitivity (%)	Specificity (%)	Accuracy (%)	PPV (%)	NPV(%)	AUC
STIR	14	00	17	05	36	73.7	100	86.1	100	77.3	0.868
DWI	18	01	16	01	36	94.7	94.1	94.4	94.7	94.1	0.944
WB-MRI	18	00	17	01	36	94.7	100	97.2	100	94.4	0.974
PET/CT	18	01	16	01	36	94.7	94.1	94.4	94.7	94.1	0.944

Table 12: Showing the diagnostic efficiency of STIR, DWI, WB-MRI and PET/CT in the evaluation of bone marrow involvement

Figure 36: Bar chart showing the diagnostic efficiency of STIR, DWI, WB-MRI and PET/CT in the evaluation of bone marrow involvement.
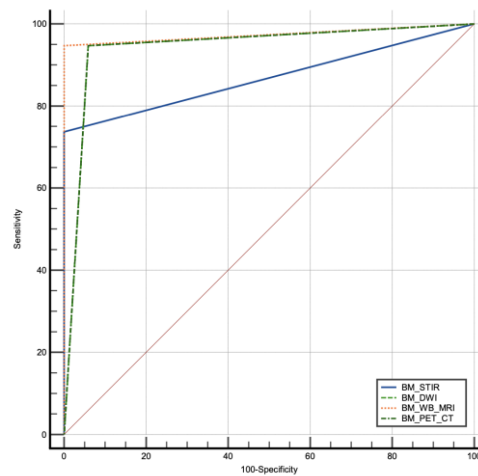
Figure 37: Showing comparison of ROC curve of various modalities for bone marrow involvement.

Comparison of STIR, DWI, WB-MRI and PET/CT in lung involvement

The sensitivity, specificity, and accuracy in the diagnosis of lung involvement were 85.7%, 100%, and 97.2 for STIR, 85.7%, 100% and 97.2% for DWI, 85.7%, 100% and 97.2% for WB-MRI and 100%, 100%, 100% for PET/CT (table 13).

STIR, DWI, WB-MRI and PET/CT efficiency in the diagnosis of LUNG involvement in 36 patients with lymphoma											
Method	Number of LUNG involvement groups					Diagnostic efficiency characteristics					
	TP	FP	TN	FN	Total	Sensitivity (%)	Specificity (%)	Accuracy (%)	PPV (%)	NPV(%)	AUC
STIR	06	00	29	01	36	85.7	100	97.2	100	96.7	0.929
DWI	06	00	29	01	36	85.7	100	97.2	100	96.7	0.929
WB-MRI	06	00	29	01	36	85.7	100	97.2	100	96.7	0.929
PET/CT	07	00	29	00	36	100	100	100	100	100	1

Table 13: Showing the diagnostic efficiency of STIR, DWI, WB-MRI and PET/CT in the evaluation of lung involvement

Comparison of STIR, DWI, WB-MRI and PET/CT in spleen involvement

The sensitivity, specificity, and accuracy in the diagnosis of spleen involvement were 94.1%, 89.5% and 91.7% for STIR, 94.1%, 84.2% and 88.9% for DWI, 100%, 89.4% and 94.4% for WB-MRI and 94.1%, 100% and 97.2% for PET/CT (table 14).
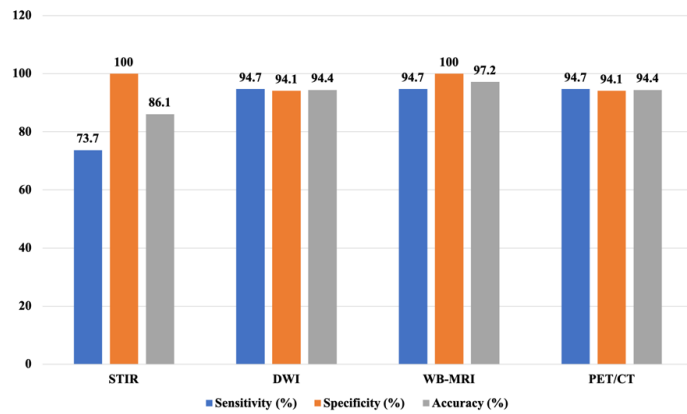
STIR, DWI, WB-MRI and PET/CT efficiency in the diagnosis of spleen involvement in 36 patients with lymphoma											
Method	Number of spleen involvement groups					Diagnostic efficiency characteristics					
	TP	FP	TN	FN	Total	Sensitivity (%)	Specificity (%)	Accuracy (%)	PPV (%)	NPV(%)	AUC
STIR	16	02	17	01	36	94.1	89.5	91.7	88.9	94.4	0.918
DWI	16	03	16	01	36	94.1	84.2	88.9	84.2	94.1	0.892
WB-MRI	17	02	17	00	36	100	89.4	94.4	89.4	100	0.947
PET/CT	16	00	19	01	36	94.1	100	97.2	100	95.0	0.971

Table 14: Showing the diagnostic efficiency of STIR, DWI, WB-MRI and PET/CT in the evaluation of spleen involvement

Comparison of Ann Arbor stages established in STIR, DWI, WB-MRI and PET/CT.

The lymphoma Ann Arbor stage characterization is presented in Table 15. PET/CT could establish the correct stage in all 36 patients (100%), while WB-MRI correctly establish the stage in 35 patients (97.2%). WB-MRI underdiagnosed a stage IV patient as stage IIIS due to non-detection of the bone marrow involvement. So, the stages were matching in 35 patients (97.2%) and the agreement between PET/CT and WB-MRI was high.

Table 15: Modified Ann Arbor stages in 36 patients of lymphoma

Method	Stage					When compared with the reference standard		
	I	II	III	IV	Total	Established correctly	Overdiagn-osed	Underdiagno-sed
Composite Reference standard	1	5	5	25	36	-	-	-
STIR	2	5	6	23	36	33	-	3
DWI	1	5	6	24	36	35	-	1
WB-MRI	1	5	6	24	36	35	-	1
PET/CT	1	5	5	25	36	36	-	-

STIR had underdiagnosed a patient due to the presence of non-enlarged peri-gastric lymph nodes in one patient. STIR also under diagnosed a patient due to its inability to detect diffuse bone marrow involvement. Both STIR and DWI had underdiagnosed a patient due to their inability to detect two subcentimetric focal marrow lesions in a pediatric patient.

Representative Cases

Case 1:

- A 16-year-old female presented with left-side cervical swelling for 1.5 years.
- HPE - Classical Hodgkin's lymphoma - Lymphocyte predominant type.
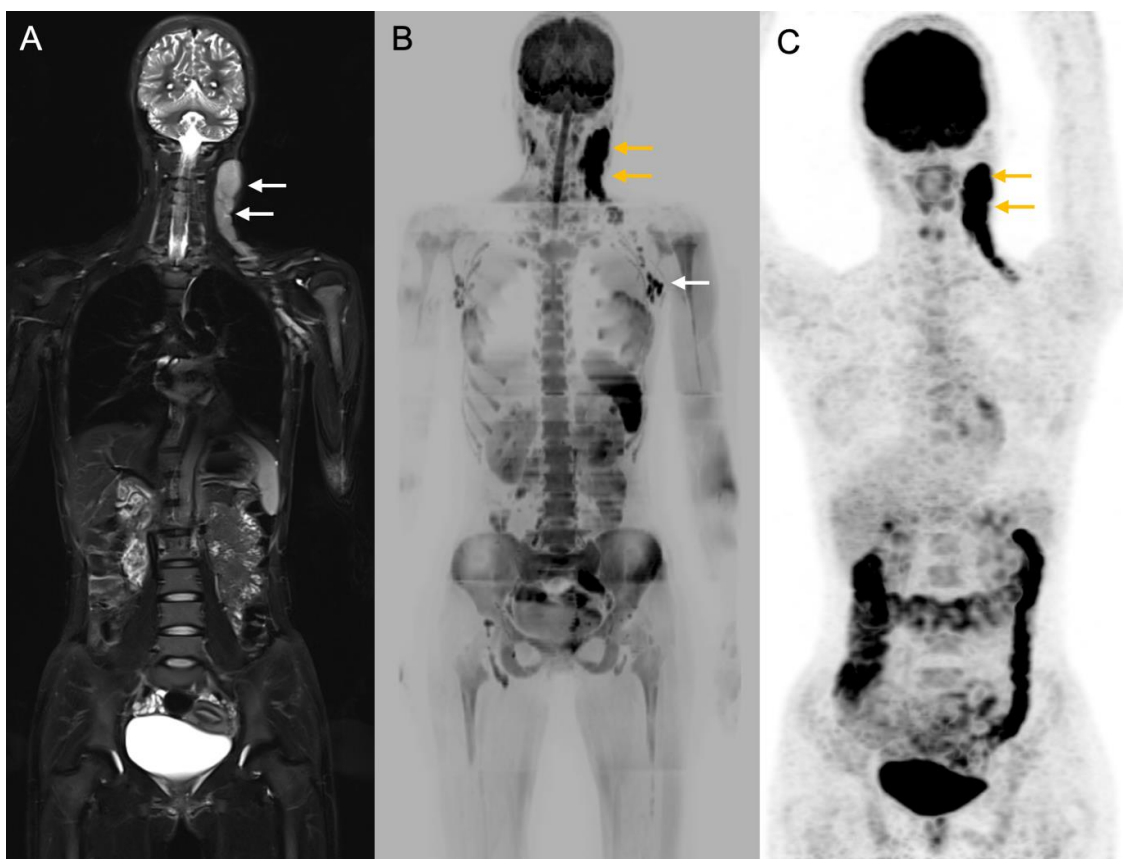
Figure 38: Stage I on both WB-MRI and PET-CT. A. Coronal STIR image showing hyperintense, enlarged lymph nodes in the left cervical level II-V region (white arrows). B. Coronal MIP DWI image showing, enlarged lymph nodes in the left cervical level II-V region which are showing diffusion restriction (yellow arrows). A few reactive left axillary lymph nodes are also seen. C. Coronal MIP PET image showing enlarged lymph nodes in the left cervical level II-V region which are showing FDG uptake (yellow arrows).

Case 2:

- A 45-year-old male, presented with swelling in the right cervical region.

- HPE: Classical Hodgkin's lymphoma – Nodular sclerosis variant.

-
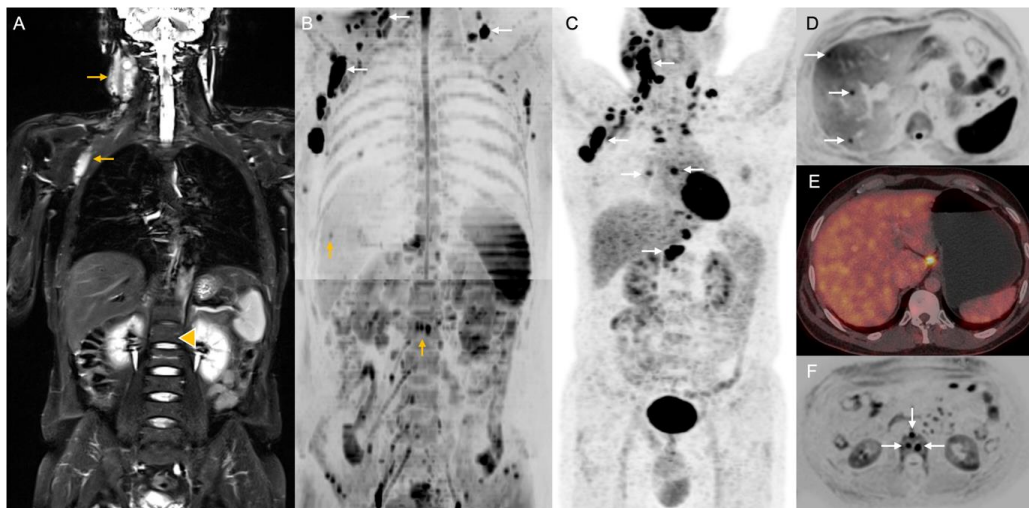
Figure 39: Stage IV on both WB-MRI and PET-CT. A. Coronal STIR image showing STIR hyperintense enlarged cervical and axillary lymph nodes (yellow arrows). B. Coronal MIP DWI images showing multiple enlarged diffusion-restricting lymph nodes in the cervical and axillary regions (white arrows). Multiple small diffusion-restricting lesions are also seen in the L1 vertebra and Liver (yellow arrows). The vertebral lesions are not detectable on the STIR (yellow arrowhead on A). C. Coronal PET MIP image showing multiple FDG avid lesions in the cervical, axillary, mediastinal, hilar and periportal nodes (yellow). However, the vertebral lesions and liver lesions which were better seen on DWI images are not seen. D. Axial DWI image showing multiple small diffusion-restricting lesions (white arrows) in the right lobe of the liver. E. Axial PET-CT image at the corresponding level does not show any FDG avid lesions. F. Axial DWI image showing multiple vertebral lesions (white arrows) involving the L1 vertebral body.

Case 3:

- An 11-year-old male, presented with swelling over the right side of the neck associated with fever, anorexia and involuntary weight loss x 1 month. Large mediastinal mass on chest radiograph.

- HPE - Classical Hodgkin's lymphoma - mixed cellularity variant.
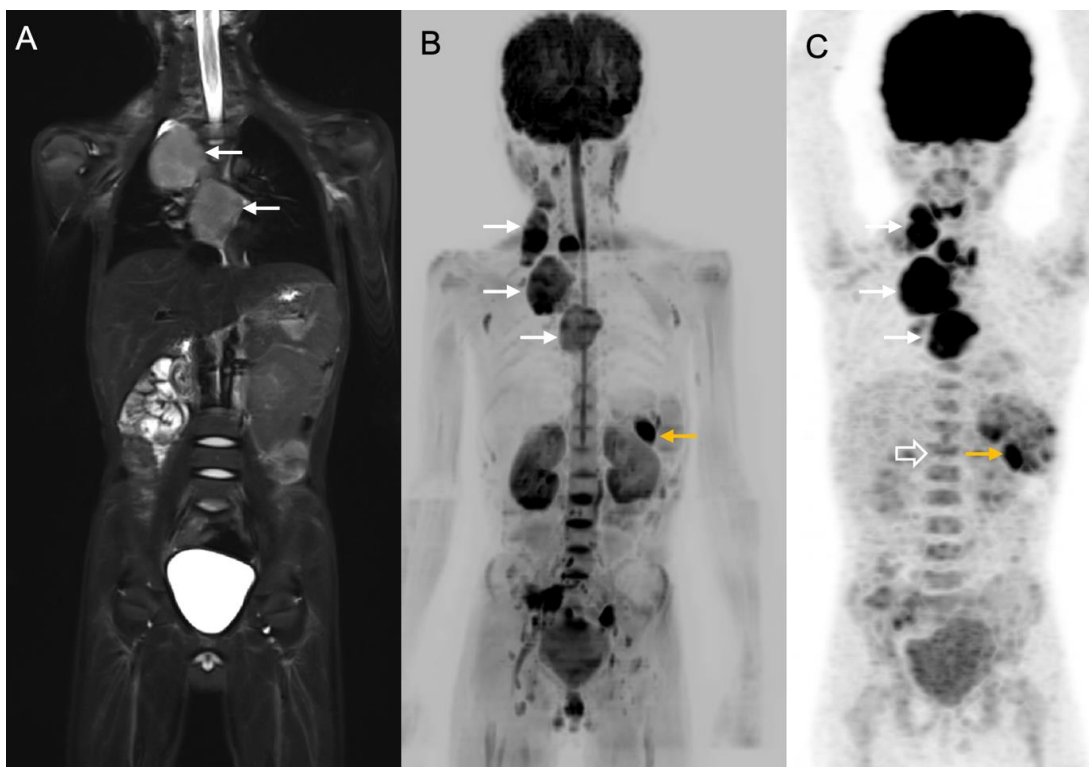
Figure 40: Stage IIIS on both WB-MRI and PET-CT. A. Coronal STIR image showing STIR hyperintense enlarged mediastinal nodal masses. B. Coronal MIP DWI image showing diffusion restricting nodal masses in the right cervical, supra clavicular, mediastinal regions (white arrows) and spleen (yellow arrow). C. Coronal MIP PET-CT image showing FDG avid lesions in the right cervical, supra clavicular, mediastinal nodal masses (white arrow) and splenic lesion (yellow arrow). Mild diffuse FDG uptake is noted in the marrow of visualized axial and appendicular skeleton (open arrow), so PET-CT was false positive for marrow involvement. Bone marrow biopsy revealed normocellular marrow with all hematopoietic components. Also, follow-up PET-CT after 2 cycles of chemotherapy showed an absence of FDG uptake in the axial and appendicular skeleton. So, in composite reference, standard bone marrow involvement was taken as negative.

Case 4:

- A 9-year-old female, presented with swelling in the right inguinal region x 2 years.

- HPE - Classical Hodgkin's lymphoma - mixed cellularity variant.
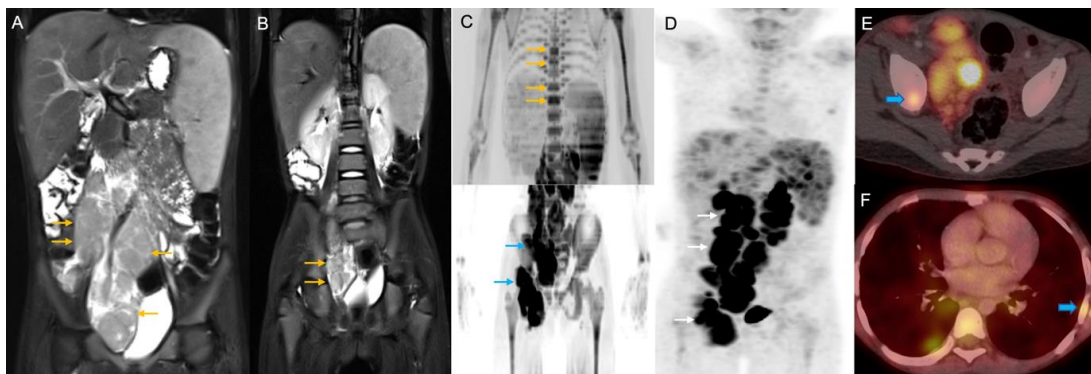
Figure 41: Stage IV on both WB-MRI and PET-CT. A & B. Coronal STIR images showing bulky STIR hyperintense nodal mass in the para-aortic, right iliac and inguinal region (yellow arrows). The nodal mass is encasing the iliac vessels. C. Coronal MIP DWI image showing diffusion restricting para-aortic, iliac and inguinal nodal mass. Diffusion-restricting lesions are also seen involving the multiple thoracic vertebral bodies. D. Coronal MIP PET image showing FDG avid para-aortic, iliac and inguinal nodal mass. No obvious lesions are seen involving the vertebral bodies, which are seen on DWI. E. Axial PET-CT image showing focal FDG avid lesion involving the roof of right acetabulum. F. Axial PET-CT image showing focal FDG avid lesion involving the lateral part of the left 5th rib. MRI had detected multifocal and diffuse marrow involvement unlike PET-CT, which detected focal lesions only.

Figure 42: G & H. Coronal in-phase and out-of-phase T1 vibe Dixon images showing suppression of the normal red marrow on the out-of-phase image (white arrows). However, the vertebral marrow involved in the lymphoma does not show suppression (yellow arrows)
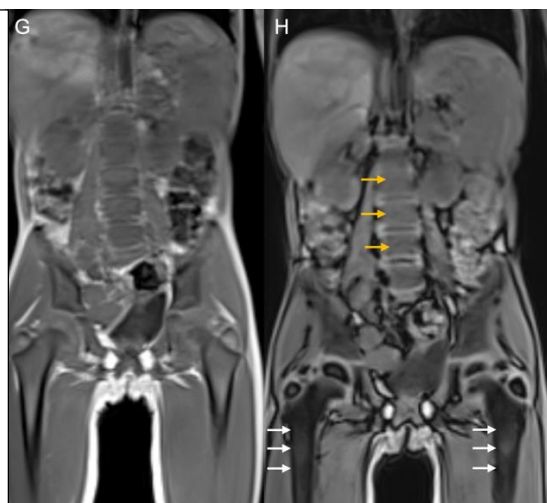
Case 5:

- A 38-year-old male, presented with bilateral cervical neck swelling.

- HPE- Chronic lymphocytic leukaemia/Small lymphocytic lymphoma–variable FDG-avid lymphoma.
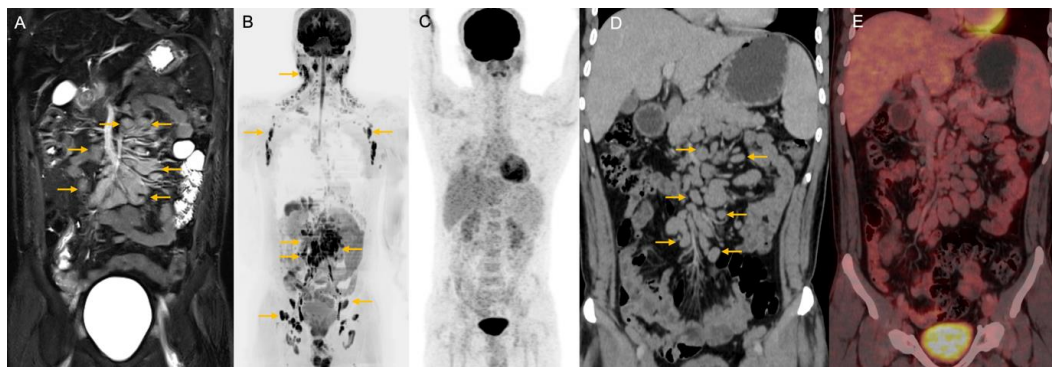
Figure 43: Stage IV on both WB-MRI and PET-CT. A. Coronal STIR image showing multiple enlarged STIR hyperintense para-aortic and mesenteric nodes (yellow arrows). B. Coronal MIP DWI image showing multiple diffusion-restricting enlarged nodes in the cervical, axillary, liver hilar, para-aortic, mesenteric, iliac and inguinal stations. C. Coronal MIP PET image does not show significant lymphadenopathy. D. Coronal CECT image showing multiple enlarged, homogeneously enhancing periportal and mesenteric lymph nodes (yellow arrow). E. Corresponding PET-CT fused images do not show significant FDG uptake in the enlarged lymph nodes.

Case 6:

- A 14-year-old male presented with pain abdomen and non-projectile vomiting for 2 months.
- HPE - Burkitt's lymphoma.
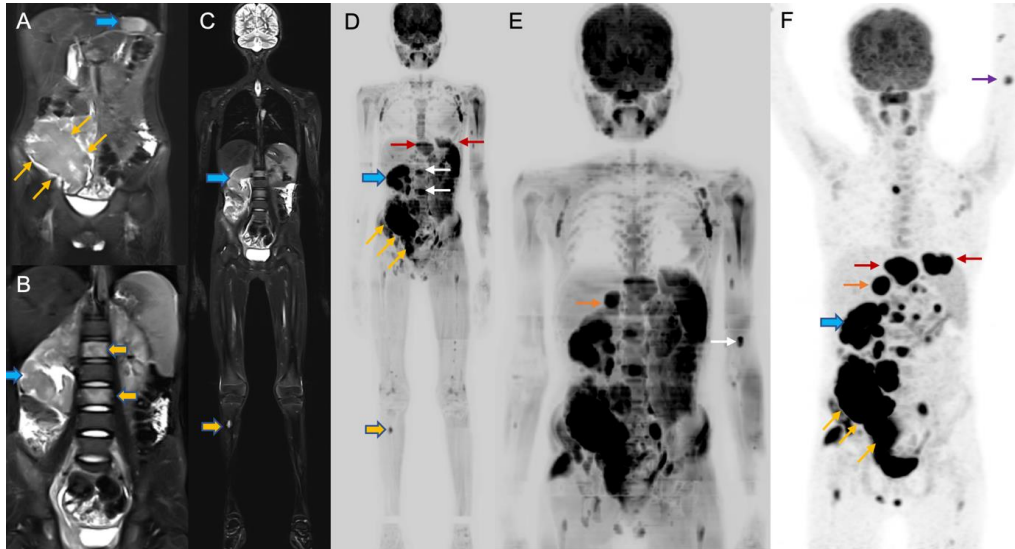
Figure 44: Stage IV on both WB-MRI and PET-CT. A. Coronal STIR image showing hyperintense thickening involving the terminal ileum, caecum and ascending colon (yellow arrows). A focal STIR hyperintense lesion is also seen in the left lobe of the liver (blue solid arrow). B. Coronal STIR image showing hyperintense lesion involving the right kidney (blue solid arrow) with mild hydronephrosis. STIR hyperintense lesions are also seen involving the L1 and L3 vertebrae (yellow solid arrows). C. Coronal STIR hyperintense focal lesion is seen involving the proximal shaft of the right tibia (yellow solid arrow). The image also shows a lesion in the right kidney (blue solid arrow). D & E. Coronal MIP DWI images showing diffusion-restricting lesions involving the terminal ileum, caecum, ascending colon (yellow arrows), right kidney (blue solid arrow), liver (red arrows) vertebral lesions (white arrows), right proximal tibia lesion (solid yellow arrow) right adrenal lesion (orange arrow in E) and left humerus lesion (white arrow in E). F. Coronal MIP PET image showing FDG avid lesions involving the terminal ileum, caecum, ascending colon (yellow arrows), right kidney (blue solid arrow), liver (red arrows), right adrenal lesion (orange arrow) and left humerus lesion (purple arrow). An additional lesion was seen in the right tibia on WB-MRI which was not covered in PET-CT, however, it did not change the stage of lymphoma.

Case 7:

- A 44-year-old male, presented with swelling over the right side of the neck, USG s/o Multiple enlarged lymph nodes along a right jugular chain and supraclavicular region.

- HPE - classical Hodgkin's lymphoma – Nodular sclerosis variant.
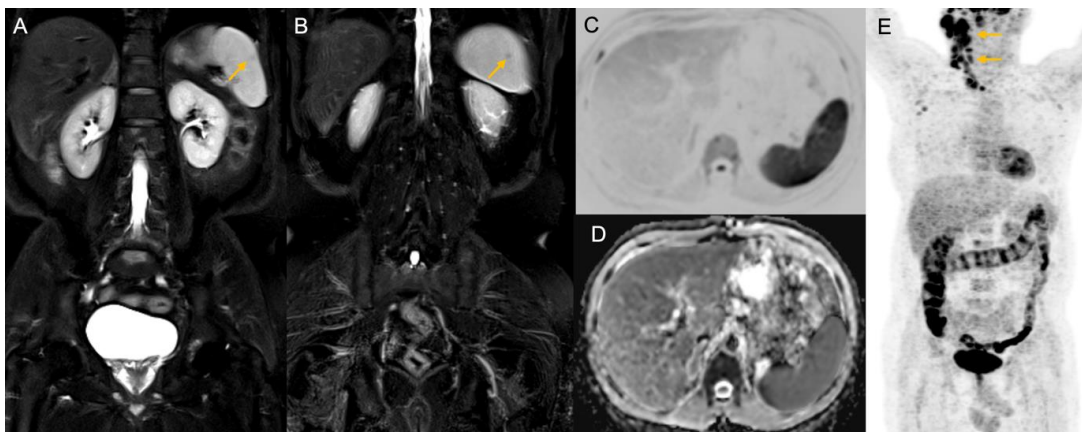
Figure 45: Stage IV on both WB-MRI and PET-CT. A & B. Coronal STIR images showing focal hypointense lesions in the normal-sized spleen (yellow arrows). C & D. Axial DWI image and ADC map do not reveal any focal lesion in the spleen. STIR sequence is better in the detection of small splenic nodules than DWI as the spleen shows physiological diffusion restriction which decreases the DWI sensitivity in lesion detection. E. Coronal MIP PET image showing multiple enlarged FDG avid right cervical lymph nodes. No obvious FDG avid focal lesion was seen in the spleen.

Case 8:

- A 29-year-old female, presented with cough and chest pain x 3-4 months
- HPE – primary mediastinal large B cell lymphoma.
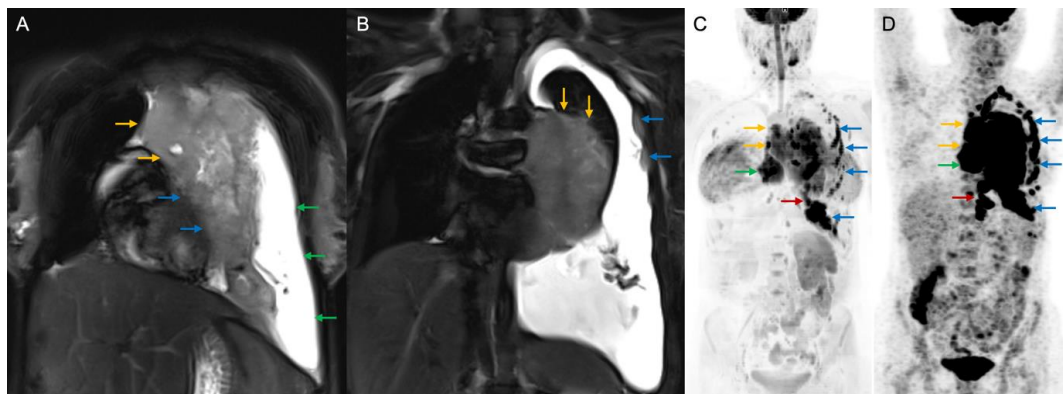
Figure 46: Stage IV on both WB-MRI and PET-CT. A. Coronal STIR image showing large heterogeneously hyperintense mediastinal mass (yellow arrows) with few cystic components within. The mass can be seen infiltrating into the pericardium inferiorly (blue arrow). Associated pleural effusion (green arrows) is also seen. B. The mass is seen infiltrating into the left lung (yellow arrows). A few hyperintense pleural deposits (blue arrows) are also seen along the left lateral chest wall. C. Coronal MIP DIW image showing diffusion restricting large mediastinal mass. Multiple diffusion-restricting pleural deposits are seen along the left lateral chest wall and diaphragmatic pleura (blue arrows). Diffusion-restricting lymph nodes are also seen in the para-cardiac region (green arrow) and para-oesophagal (red arrow). D. Coronal MIP PET image showing FDG avid large mediastinal mass. Multiple FDG avid pleural deposits are seen along the left lateral chest wall and diaphragmatic pleura (blue arrows). FDG avid lymph nodes are also seen in the para-cardiac region (green arrow) and para-oesophagal (red arrow).
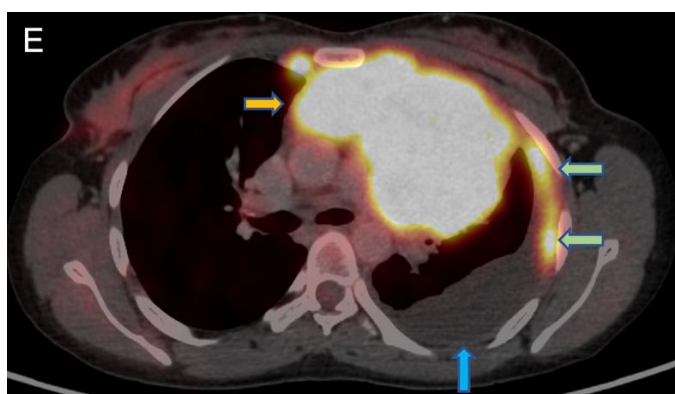
Figure 47: Axial PET-CT image showing large mediastinal mass (yellow arrow) with diffuse FDG uptake. FDG avid pleural deposits (green arrow) are seen along the left lateral chest wall. Left pleural effusion (blue arrow) also seen.

Case 9:

- A 64-year-old female presented with multiple swellings in the neck left axilla and right inguinal regions for 2 months.
- HPE – Diffuse large B cell lymphoma.
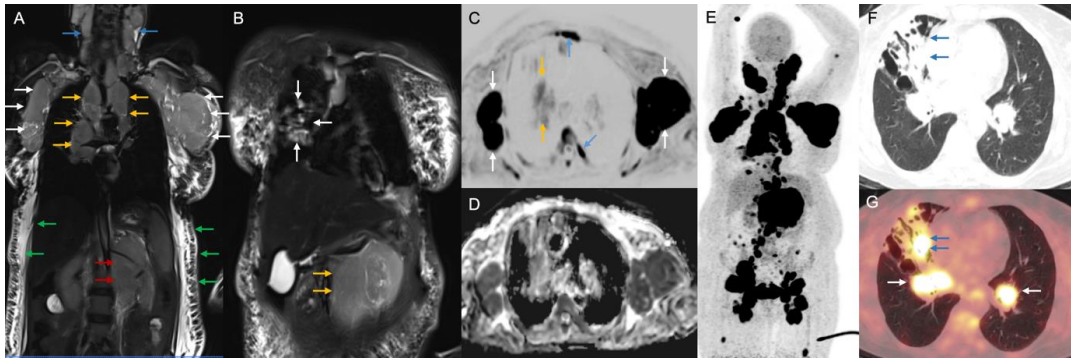
Figure 48: Stage IV on both WB-MRI and PET-CT. A. Coronal STIR image showing multiple large nodal masses in the bilateral cervical (blue arrows), mediastinal (yellow arrows) axillary (white arrows) para-aortic (red arrows) stations. Diffuse subcutaneous oedema (green arrows) is seen as likely due to lymphatic and venous obstruction due to disease involvement. B. Coronal STIR image showing bronchiectasis and lung nodules in the right lung (white arrows). The image also shows a large mesenteric nodal mass. C & D. Axial DWI image and ADC maps showing diffusion restricting axillary masses (white arrow), sternal & rib lesions (blue arrows). The right lung changes (yellow arrow) are not as prominent as seen in STIR images. E. Coronal MIP PET-CT image showing extensive FDG avid lesions involving the bilateral cervical, axillary, mediastinal, hilar, right lung, mesenteric, para-aortic, iliac and inguinal stations. F. Axial lung window image showing patchy areas of consolidation with cavitation in the right middle lobe (blue arrows) with associated bronchiectasis – likely due to infective aetiology. G. Axial PET-CT showing FDG uptake in the infective lesions (blue arrows). Enlarged bilateral hilar nodes are also seen (white arrows).

Case 10:

- A 39-year-old male, presented with pain abdomen x 2-3 months

- HPE: Diffuse large B cell lymphoma – germinal centre type
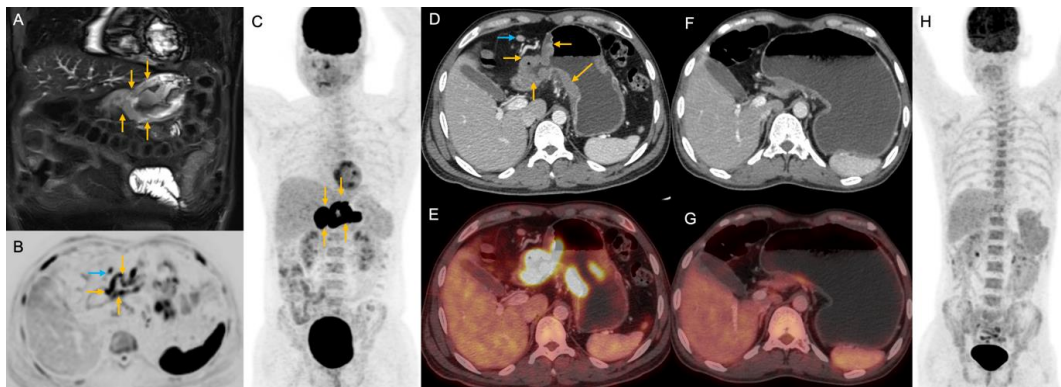
Figure 49: Stage IIE on both WB-MRI and PET-CT. A. Coronal STIR image showing hyperintense diffuse asymmetric wall thickening (yellow arrows) involving the lesser and greater curvatures of the distal body and pyloric regions of the stomach. B. Axial DWI image showing diffusion restricting asymmetric wall thickening (yellow arrows) involving the lesser and greater curvatures of the distal body and pyloric regions of the stomach. Diffusion restricting the peri-gastric lymph node (blue arrow) is also seen. C. Coronal MIP DWI image showing diffusion restricting asymmetric wall thickening (yellow arrows) involving the lesser and greater curvatures of the distal body and pyloric regions of the stomach. D & E. Axial CECT and PET-CT images showing FDG avid asymmetric wall thickening (yellow arrows) involving the lesser and greater curvatures of the distal body and pyloric regions of the stomach. A round, homogeneously enhancing peri-gastric lymph node (blue arrow on D) is seen, which is likely involved in the disease. However, it does not show FDG uptake. F, G & H. Axial CECT, PET-CT and MIP PET-CT images of the scan done after 3 months, show total resolution of the disease. There is a mild increase in FDG uptake in the axial and appendicular skeleton – likely due to marrow reactivation.

DISCUSSION

In our study, we prospectively assessed the diagnostic efficiency of whole-body MRI with STIR and DWI and PET/CT in lymphoma staging in 36 patients of histopathologically proven lymphoma. The study included both pediatric and adult patients.

A. Lymph nodal involvement

Whole body STIR had sensitivity, specificity and diagnostic accuracy of 78.8%, 95.7% and 86.6% respectively, in evaluating the lymph nodal involvement. The diagnostic efficiency of the STIR in detecting the lymph nodal involvement was comparable with that of whole-body DWI (p=0.16), however, it showed a statistical difference when compared to WB-MRI (p = 0.002) and whole-body PET-CT (p < 0.0001). The low sensitivity of the whole-body STIR in detecting lymph node involvement can be attributed to its low sensitivity in detecting hilar and mediastinal lymph nodal involvement. The sensitivity of the STIR in detecting the hilar and mediastinal lymph node involvement was 56.5% and 82.1% respectively.

Whole body DWI had sensitivity, specificity and diagnostic accuracy of 87.1%, 92.7%, and 89.7% respectively, in evaluating the lymph node involvement. The diagnostic efficiency of the whole body DWI in detecting the lymph nodal involvement was statistically lower than that of WB-MRI (p = 0.0428) and PET-CT (p < 0.0001). Similar to whole-body STIR, the low sensitivity of the whole-body DWI in detecting lymph node involvement can be attributed to its low sensitivity in detecting hilar and mediastinal lymph nodal involvement. The sensitivity of the DWI in detecting the hilar and mediastinal lymph node involvement was 60.87%% and 85.7% % respectively.

Whole-body MRI (including both STIR and DWI) had sensitivity, specificity and diagnostic accuracy of 88.1%, 96.7% and 92.2% respectively, in evaluating the lymph node involvement. The diagnostic efficiency of the whole-body MRI in detecting the lymph nodal involvement was statistically lower than that of PET-CT (p < 0.0001). Similar to whole-body STIR & DWI the low sensitivity of the whole-body DWI in detecting the lymph node involvement can be attributed to its low sensitivity in

detecting the hilar and mediastinal lymph nodal involvement. The sensitivity of the whole body MRI in detecting the hilar and mediastinal lymph node involvement was 65.2%% and 85.7% % respectively.

For the evaluation of lymph nodal involvement, whole-body STIR, whole-body DWI and WB-MRI had an area under the curve (AUC) of 0.873, 0.899, and 0.962 respectively, suggesting good diagnostic efficiency of STIR and DWI and high diagnostic efficiency of WB-MRI in detecting the lymph nodal involvement. PET-CT showed sensitivity, specificity and diagnostic accuracy of 99.5%, 99.4% and 99.4% respectively (AUC – 0.994). So, WB-MRI when compared to PET-CT showed a statistically significant difference (p<0.05) in detecting lymph nodal involvement. However, this lowered diagnostic efficiency for lymph nodal involvement alone did not change the stage of WB-MRI in any of the patients.

Our results are in concordance with the previously published literature. In the study by Mayerhoefer et al[92], DWI-MRI showed overall sensitivity and specificity of 97% and 99.7% for the detection of lymph node involvement in FDG-avid lymphomas, and sensitivity and specificity of 93.8% and 99.8% for nodal regions and 98.6% and 99.8% for extranodal regions, in FDG avid lymphoma group. In the variable FDG avid lymphoma group, DWI-MRI showed overall sensitivity and specificity of 94.4% and 100%, sensitivity and specificity of 94.9% and 100% for nodal regions and sensitivity and specificity of 93.9% and 100% for extranodal regions. In a study by Siarhei et at[79] (2020), MRI-DWI had sensitivity, and specificity of 98.2% and 99.9% respectively, in the evaluation of enlarged lymph nodes, while it had relatively low sensitivity, specificity of 77.8% and 88.1% respectively in the evaluation of non-enlarged lymph nodes. The study conducted by Latifoltojar[83] (2018) showed TPR, FPR of 91% and 100% respectively for nodal disease and TPR, FPR of 79% and <1% for extranodal disease. In the study by Gali Shapira et al[80], sensitivity and PPV of DW-MRI were 0.651 and 1 respectively.

In an adult patient of gastric diffuse large B cell lymphoma, STIR failed to detect non-enlarged peri-gastric lymph nodes resulting in the downstaging of the patient from stage IIE to stage IE. This can be explained by the fact that the STIR sequence was acquired in the Coronal plane in our study so lymph nodes located in the axial plane

with smaller craniocaudal dimensions can be missed when interpreted in a single plane. The peri-gastric nodes were showing diffusion restriction despite being small in size on DWI images resulting in correct staging on WB-MRI. The lymph nodes were not showing FDG uptake on PET due to the tumour sink effect. The Tumour sink effect can happen when radiotracer is sequestered in the highly active tumour component with the absence of accumulation of radiotracer in less metabolically active tissues. However, based on the location, morphology and enhancement pattern on the CT component of the PET-CT, the nodes were considered positive on PET-CT thus resulting in the accurate stage II. These perigastric lymph nodes disappeared completely on follow-up PET-CT after chemotherapy confirming their involvement with the disease.

B. Extranodal site or organ involvement

Whole body STIR had sensitivity, specificity and diagnostic accuracy of 80.0%, 99.4% and 95.5% respectively, in evaluating the extranodal site or organ involvement. The diagnostic efficiency of the STIR in detecting the extranodal site or organ involvement was statistically lower when compared to DWI ($p = 0.0146$), WB-MRI ($p = 0.0007$) and PET-CT ($p = 0.0017$). The low sensitivity of the whole body STIR in detecting the extranodal site or organ involvement can be attributed to its low sensitivity in detecting bone marrow involvement. The sensitivity of the STIR in detecting bone marrow involvement was 73.7%.

Whole body DWI had sensitivity, specificity and diagnostic accuracy of 92.5%, 98.7%, and 97.5% respectively, in evaluating the extranodal site or organ involvement. The diagnostic efficiency of the whole body DWI in detecting the extranodal site or organ involvement was comparable to both WB-MRI ($p = 0.4743$) and PET-CT ($p = 0.1331$).

Whole-body MRI had sensitivity, specificity and diagnostic accuracy of 93.8%, 99.4% and 98.2% respectively, in evaluating the extranodal site or organ involvement. The diagnostic efficiency of the whole-body MRI in detecting the extranodal site or organ involvement was comparable to that of PET-CT ($p = 0.2837$).

For the evaluation of extranodal site or organ involvement, whole-body STIR, whole-body DWI and WB-MRI had an area under the curve (AUC) of 0.897, 0.956, and 0.966 respectively, suggesting good diagnostic efficiency of STIR and high diagnostic efficiency of DWI and WB-MRI in detecting the extranodal site or organ involvement. However, when compared to PET-CT, whole-body STIR showed a statistically significant difference in detecting the extranodal site or organ involvement, while whole-body DWI and WB-MRI showed no statistically significant difference in detecting the extranodal site or organ involvement, with PET-CT having sensitivity, specificity and diagnostic accuracy of 97.5%, 99.7% and 99.2% respectively (AUC – 0.986).

Our results are more promising and better than a few of the previously published literature. In a study by Gali Shapira et al[80], DW-MRI had sensitivity and PPV of 0.545 and 0.6 in extranodal disease involvement. In a study by Siarhei et al[79], MRI-DWI showed sensitivity, specificity, and accuracy of 72.9%, 98.1% and 92.2%. respectively, for extranodal organ involvement. As per the study by Gil-Sun Hong et al[76], the sensitivity of WB-DWIBS/STIR was higher (94.9– 96.8% vs. 79.6–86.3%, P = 0.058) for extranodal lesions when compared with ^{18}F-FDG PET/CT. As per the study by Mayerhoefer et al[92], the sensitivity of WB-MRI with DWI was almost the same as that of PET-CT.

C. Both lymph nodal and extranodal site or organ involvement

Whole body STIR had sensitivity, specificity and diagnostic accuracy of 79.2%, 98.1% and 91.3% respectively, in evaluating both lymph nodal and extranodal site/ organ involvement. The diagnostic efficiency of the STIR in detecting both lymph nodal and extranodal site or organ involvement was statistically lower when compared to DWI (p = 0.0040), WB-MRI (p < 0.0001) and PET-CT (p < 0.0001). The low sensitivity of the whole body STIR in detecting both the lymph nodal and extranodal site/organ involvement can be attributed to its low sensitivity in detecting the mediastinal, hilar lymph nodes and bone marrow involvement.

Whole body DWI had sensitivity, specificity and diagnostic accuracy of 88.7%, 96.7%, and 93.8% respectively, in evaluating both lymph nodal and extranodal site /

organ involvement. The diagnostic efficiency of the whole body DWI in detecting both the lymph nodal and extranodal site / organ involvement was comparable to WB-MRI (p=0.0958), however, it was statistically lower when compared to PET-CT (p < 0.0001). Similar to whole-body STIR, the low sensitivity of the whole-body DWI in assessing the involvement of both the lymph nodal and extranodal site or organ involvement can be attributed to its low sensitivity in detecting the mediastinal and hilar nodal stations.

Whole body MRI had sensitivity, specificity and diagnostic accuracy of 89.8%, 98.6% and 95.4% respectively, in evaluating both the lymph nodal and the extranodal site or organ involvement. The overall diagnostic efficiency of the whole-body MRI in detecting both the lymph nodal and the extranodal site or organ involvement was statistically lower than that of PET-CT (p < 0.0001) due to its lower diagnostic efficiency in lymph nodal involvement.

For the evaluation of both the lymph nodal and extranodal site or organ involvement, whole-body STIR, whole-body DWI and WB-MRI had an area under the curve (AUC) of 0.887, 0.927, and 0.942 respectively, suggesting good diagnostic efficiency of STIR and high diagnostic efficiency of DWI and WB-MRI in detecting both the lymph nodal and the extranodal site or organ involvement. However, when compared to PET-CT, whole body STIR, whole body DWI and WB-MRI had shown statistically significant weakness in the evaluation of both the lymph nodal and the extranodal site or organ involvement, with PET-CT having sensitivity, specificity and diagnostic accuracy of 98.9%, 99.6% and 99.3% respectively (AUC – 0.992). The low sensitivity of whole-body STIR, whole-body DWI and WB-MRI in the assessment of both nodal and extranodal organ involvement can be contributed mainly to the inherent weakness in detecting mediastinal & hilar nodal involvement for both STIR and DWI.

D. Bone marrow involvement

Whole body STIR had sensitivity, specificity and diagnostic accuracy of 73.7%, 100% and 86.1% respectively, in evaluating bone marrow involvement. The diagnostic efficiency of the STIR in detecting bone marrow involvement was comparable to that of DWI (p = 0.2993), WB-MRI (p = 0.1184) and PET-CT (p = 0.2993).

Whole body DWI had sensitivity, specificity and diagnostic accuracy of 94.7%, 94.1%, and 94.4% respectively, in evaluating bone marrow involvement. The diagnostic efficiency of the whole body DWI in detecting bone marrow involvement was comparable to that of WB-MRI (p = 0.5086), and PET-CT (p = 1.0000).

Whole-body MRI had sensitivity, specificity and diagnostic accuracy of 94.7%, 100% and 97.2% respectively, in evaluating bone marrow involvement. The diagnostic efficiency of the whole-body MRI in detecting the bone marrow was comparable to that of PET-CT (p = 0.5852).

For the evaluation of bone marrow involvement, whole-body STIR, whole-body DWI and WB-MRI had areas under the curve (AUC) of 0.868, 0.944, and 0.974 respectively, suggesting good diagnostic efficiency of STIR and high diagnostic efficiency of DWI and WB-MRI in detecting the bone marrow involvement. The sensitivity, specificity and diagnostic accuracy of PET-CT in evaluating bone marrow involvement are 94.7%, 94.1% and 94.4% respectively (AUC – 0.944). The AUC of WB-MRI was more than that of PET-CT, suggesting that WB-MRI was more efficacious in diagnosing bone marrow involvement however, it was not statistically significant.

In one paediatric patient of classical Hodgkin's lymphoma, STIR, DWI and WB-MRI all failed to detect the two subcentimetric focal marrow lesions which resulted in the downstaging from stage IV to stage IIIS.

In one adult patient of classical Hodgkin's lymphoma, STIR failed to detect the multifocal marrow lesions, which were picked up by DWI, resulting in the downstaging of the patient on STIR from stage IV. PET-CT also failed to detect the focal marrow lesions in this patient making PET-CT false negative for marrow involvement, however, that did not change the stage, due to the presence of focal FDG-avid liver lesions in this patient.

Our study results are better than previously published literature on bone marrow involvement. In a study by Siarhei et al[79], MRI-DWI had sensitivity, specificity, and accuracy of 71.4%, 88.2% and 80.6%. In the study by Hugo et al[96], WB-MRI had a sensitivity of 45.5% in bone marrow involvement for both aggressive and indolent

lymphomas. They observed that WB-MRI had higher sensitivity in aggressive lymphoma than in indolent lymphoma in detecting bone marrow involvement. There was no significant difference in the sensitivity of WB-MRI and PET-CT in detecting bone marrow involvement.

E. Spleen Involvement

Spleen was considered involved if the vertical length of the spleen was more than 13cm or focal lesions are seen on STIR /DWI. STIR had sensitivity, specificity, and accuracy of 94.1%, 89.5% and 91.7%, DWI had sensitivity, specificity, and accuracy of 94.1%, 84.2% and 88.9% and WB-MRI had sensitivity, specificity, and accuracy of 100%, 89.4% and 94.4% respectively. The DWI-MRI was less sensitive in detecting the splenic involvement due to inherent physiological diffusion restriction shown by the spleen leading to decreased conspicuity of smaller splenic lesions. In a patient, STIR had detected focal subcentimetric splenic lesions, which were missed on both the DWI and PET-CT.

F. Lung Involvement

In the assessment of lung involvement STIR had sensitivity, specificity, and accuracy in the 85.7%, 100%, and 97.2, DWI had sensitivity, specificity, and accuracy of 85.7%, 100% and 97.2%, and WB-MRI had sensitivity, specificity, and accuracy of 85.7%, 100% and 97.2% respectively. Although STIR and DWI had similar sensitivity and specificity, lung parenchymal changes were subjectively more obvious in STIR sequence. PET/CT was more sensitive in detecting lung involvement with sensitivity, specificity, and accuracy of 100%, 100%, and 100% respectively due to excellent spatial resolution on CT.

Staging agreement

In our study PET/CT stage was in complete agreement with the composite reference standard in all 36 (100%) patients. Whole body-MRI and whole-body DWI stage correlated with the reference standard in 35 patients (97.2%). Both DWI alone and WB-MRI had under-staged a pediatric patient, as two subcentimetric focal bone marrow lesions were not detectable in this patient. Whole body STIR alone made the

correct staging with the composite reference standard in 33 patients (91.7%). STIR had under-staged one patient as it failed to detect non-enlarged involved peri-gastric lymph nodes. It also under-staged two patients, in which it was not able to detect focal marrow lesions.

In a study conducted by Siarhei et al[2], whole-body MRI with DWI and PET/CT had a good agreement in lymphoma staging, matching of stage in 72 (78%) patients and both correctly established staging in 79 (86%) patients. Similar to our study, they also observed that wrong staging was mainly due to incorrect assessment of BM involvement in 4 patients, while other reasons being an incorrect assessment of non-enlarged LN in 4 patients, spleen in 2 patients, lung& liver in 1 patient each and bone marrow & stomach in 1 patient. However, PET/CT under staged in a significantly higher number of patients (n = 10) due to incorrect assessment of the bone marrow involvement. In a study conducted by Mayerhoefer et al[92], DWI-MRI agreed with the reference standard in 94 of 100 (94%) patients with FDG-avid lymphomas and it agreed with the reference standard in 37 of 40 (92%) patients with variable-FDG avidity. In a study conducted by Latifoltojar et al[83], WB-MRI agreed with enhanced reference standard in 96% (48 of 50) patients. In a study by Gali Shapira et al[80], MRI-DWI determined correct staging in 72% (8 of 11 patients) patients. As per the study by Gil-Sun Hong et al[76], WB-DWIBS/STIR had a very good agreement ($\kappa = 0.96$; confidence interval [CI], 0.88–1.00), high specificity (99.0–99.4%) and high sensitivity (93.4–95.1%), in the pretherapeutic staging for the whole-body regions.

Whole body MRI scan with coronal STIR, axial DWI and coronal T1 LAVA/vibe Dixon was completed in an average time of approximately 45min to 50min and acquired in 3 to 5 stations depending on the patient's height. We acquired imaging from vertex to toes and found additional lesions below the thigh region in 4 patients (11%). However, in none of these patients, findings of additional lesions below the thigh as compared to PET-CT led to a change in the staging. Thus, advocating that omitting the additional two stations, below the thigh region, can reduce the scanning time further by at least 15min.

As per the study by Gil sun Hong, et al[76], WB-MRI DWI with BS/STIR had higher sensitivity and specificity than PET-CT in evaluating indolent lymphomas. In

our study, we didn't separately evaluate WB-MRI for the evaluation of aggressive (n=16, NHL) vs indolent lymphomas (n=5) due to a smaller number of indolent lymphomas.

Similarly, we didn't perform a study on the efficiency of WB-MRI in FDG-avid (n = 31) vs variable FDG-avidity lymphomas (n = 5) due to a smaller number of variable FDG-avidity lymphomas. As per the study by Mayerhoefer et al[92], WB-MRI was only slightly inferior to FDG PET-CT in pretherapeutic evaluation and staging of FDG-avid lymphoma patients. WB-MRI was superior to FDG PET-CT in pretherapeutic evaluation and staging of variable FDG-avid lymphoma patients.

LIMITATIONS OF STUDY

1. Our study is a single institute study with a small sample size so for better validation of the diagnostic efficiency of whole-body MRI, a larger study would be preferable. The sample population for a few lymphoma subtypes was too small to be representative of the general population.

2. The COVID-19 pandemic had a role to play in reducing the sample size of the study.

3. Diagnostic efficiency of WB-MRI may vary in adult versus paediatric patients, we did not evaluate adult and paediatric patients separately.

4. We did not study the diagnostic efficiency of WB-MRI separately in terms of enlarged versus non-enlarged nodal masses.

5. Comparison of WB-MRI with PET/CT may give different results in aggressive versus indolent lymphomas and the analysis was not done separately.

6. Comparison of WB-MRI with PET/CT may give different results in FDG-avid versus variable FDG-avid lymphomas and the analysis was not done separately.

7. Due to the absence of a histological evaluation of all sites and bone marrow in all patients, there is a chance of error in the composite reference standard leading to minor variations in the diagnostic accuracy of WB-MRI.

CONCLUSION

1. WB-MRI is highly accurate and had a high agreement with PET-CT in the initial staging of lymphoma.

2. WB-STIR and WB-DWI alone had good sensitivity, specificity and accuracy in assessing the involvement of both lymph nodal and extra-nodal site involvement. However,

   WB-MRI (combination of both WB-STIR and WB-DWI) had high diagnostic efficiency in assessing the involvement of both lymph nodal and extra-nodal site/organ involvement.

3. WB-MRI showed statistically lower diagnostic efficiency in assessing the lymph nodal involvement as compared to PET/CT. However, this lowered diagnostic efficiency for lymph nodal involvement did not change the stage. No significant difference was seen between WB-MRI and PET-CT for the assessment of extra-nodal site/organ involvement.

4. WB-MRI had higher diagnostic efficiency in assessing the involvement of bone marrow than PET/CT.

5. Detection of additional lesions below the thigh in WB-MRI did not change the stage in any patient. So, a WB-MRI protocol should consist of a combination of both WB-STIR and WB-DWI from the superior orbital margin till mid-thighs.

6. WB-MRI can be used as an alternative tool in the staging of lymphoma in variable FDG-avid lymphomas or pediatric/pregnant patients as a radiation-free imaging modality.

BIBLIOGRAPHY

1. Kumar, V., Abbas, A. K., & Aster, J. C. (Eds.). (2018). *Robbins basic pathology* (10th ed.). Elsevier.

2. Mugnaini EN, Ghosh N. Lymphoma. *Primary Care: Clinics in Office Practice*. 2016 Dec 1;43(4):661-75.

3. Siegel R. Naishadham D and Jemal A: Cancer statistics for Hispanics/Latinos, 2012. *CA Cancer J Clin*. 2012;62(5):10-29.

4. Siegel DA, King J, Tai E, Buchanan N, Ajani UA, Li J. Cancer incidence rates and trends among children and adolescents in the United States, 2001–2009. *Paediatrics*. 2014 Oct 1;134(4):e945-55.

5. Sung H, Ferlay J, Siegel RL, Laversanne M, Soerjomataram I, Jemal A, et al. Global cancer statistics 2020: GLOBOCAN estimates of incidence and mortality worldwide for 36 cancers in 185 countries. *CA: a cancer journal for clinicians*. 2021 May;71(3):209-49.

6. Huang J, Pang WS, Lok V, Zhang L, Lucero-Prisno DE, Xu W, et al. Incidence, mortality, risk factors, and trends for Hodgkin lymphoma: a global data analysis. *Journal of haematology & oncology*. 2022 Dec;15(1):1-1.

7. Mathur P, Sathishkumar K, Chaturvedi M, Das P, Sudarshan KL, Santhappan S, et al, ICMR-NCDIR-NCRP Investigator Group. Cancer statistics, 2020: report from national cancer registry programme, India. *JCO Global oncology*. 2020 Jul;6:1063-75.

8. Adam A, Dixon AK, Gillard JH, Schaefer-Prokop C, Grainger RG, Allison DJ. *Grainger & Allison's Diagnostic Radiology E-Book*. Elsevier Health Sciences; 2014 Jun 16.

9. Cheson BD, Fisher RI, Barrington SF, Cavalli F, Schwartz LH, Zucca E, et al. Recommendations for initial evaluation, staging, and response assessment of Hodgkin and non-Hodgkin lymphoma: the Lugano classification. *Journal of clinical oncology*. 2014 Sep 20;32(27):3059

10. Paquin AR, Oyogoa E, McMurry HS, Kartika T, West M, Shatzel JJ. The diagnosis and management of suspected lymphoma in general practice. *Eur J Haematol*. 2023;110(1):3-13. doi:10.1111/ejh.13863

11. Matasar MJ, Zelenetz AD. Overview of lymphoma diagnosis and management. *Radiologic Clinics of North America*. 2008 Mar 1;46(2):175-98.

12. Johnson SA, Kumar A, Matasar MJ, Schöder H, Rademaker J. Imaging for staging and response assessment in lymphoma. *Radiology*. 2015 Aug;276(2):323-38.

13. Maher MM, McDermott SR, Fenlon HM, Conroy D, O'Keane JC, Carney DN, et al. Imaging of primary non-Hodgkin's lymphoma of the liver. Clinical radiology. 2001 Apr 1;56(4):295-301

14. Albano D, Bruno A, Patti C, Micci G, Midiri M, Tarella C, et al. Whole- body magnetic resonance imaging (WB- MRI) in lymphoma: State of the art. *Hematological Oncology*. 2020 Feb;38(1):12-21

15. Kwee TC, Basu S, Torigian DA, Nievelstein RA, Alavi A. Evolving importance of diffusion-weighted magnetic resonance imaging in lymphoma. *PET clinics*. 2012 Jan 1;7(1):73-82.

16. El- Galaly TC, Villa D, Gormsen LC, Baech J, Lo A, Cheah CY. FDG- PET/CT in the management of lymphomas: current status and future directions. *Journal of internal medicine*. 2018 Oct;284(4):358-76.

17. Huang B, Law MW, Khong PL. Whole-body PET/CT scanning: estimation of radiation dose and cancer risk. *Radiology*. 2009;251(1):166-174.

18. Chien SH, Liu CJ, Hu YW, et al. Frequency of surveillance computed tomography in non-Hodgkin lymphoma and the risk of secondary primary malignancies: A nationwide population-based study. *Int J Cancer*. 2015;137(3):658-665. doi:10.1002/ijc.29433

19. Singh I. Human embryology. JP Medical Ltd; 2014 Sep 30.

20. Eisenmenger LB, Wiggins RH. Imaging of head and neck lymph nodes. *Radiologic Clinics*. 2015 Jan 1;53(1):115-32.

21. Rusch VW, Asamura H, Watanabe H, Giroux DJ, Rami-Porta R, Goldstraw P. The IASLC lung cancer staging project: a proposal for a new international lymph node map in the forthcoming seventh edition of the TNM classification for lung cancer. *Journal of thoracic oncology*. 2009 May 1;4(5):568-77.

22. Haaga JR, Boll D. Computed Tomography & Magnetic Resonance Imaging of The Whole Body E-Book. Elsevier Health Sciences; 2016 Jun 6.

23. El-Sherief AH, Lau CT, Wu CC, Drake RL, Abbott GF, Rice TW. International association for the study of lung cancer (IASLC) lymph node map: a radiologic review with CT illustration. *Radiographics*. 2014 Oct 13;34(6):1680-91.

24. Morón FE, Szklaruk J. Learning the nodal stations in the abdomen. *The British journal of radiology*. 2007 Oct;80(958):841-8.

25. Kumar I, Sharma S, Prakash A, Aggarwal P, Shukla RC, Verma A. CT-Based Definition and Structured Reporting of Abdominal Lymph Node Stations. *Indian J Radiol Imaging*. 2022;32(1):62-70. Published 2022 Apr 6. doi:10.1055/s-0041-1741089

26. Author. In: Mescher AL. eds. *Junqueira's Basic Histology: Text and Atlas, 15e*. McGraw Hill; 2018. Accessed January 01, 2023. https://accessmedicine.mhmedical.com/content.aspx?bookied=2430 & sectioned = 190220001

27. Kumar V, Abbas AK, Fausto N, Aster JC. Robbins and Cotran pathologic basis of disease, professional edition e-book. Elsevier health sciences; 2014 Aug 27.

28. Harris NL, Jaffe ES, Stein H, Banks PM, Chan JK, Cleary ML, et al. A revised European-American classification of lymphoid neoplasms: a proposal from the International Lymphoma Study Group. *Blood*. 1994 Sep 1;84(5):1361-92

29. Harris NL, Jaffe ES, Diebold J, Flandrin G, Muller-Hermelink HK, Vardiman J, et al. The World Health Organization classification of neoplastic diseases of the haematopoietic and lymphoid tissues: report of the Clinical Advisory Committee Meeting, Airlie House, Virginia, November 1997. *Histopathology*. 2000 Jan 1;36(1):69-86.

30. Campo E, Swerdlow SH, Harris NL, Pileri S, Stein H, Jaffe ES. The 2008 WHO classification of lymphoid neoplasms and beyond: evolving concepts and practical applications. *Blood*. 2011 May 12;117(19):5019-32.

31. Alaggio R, Amador C, Anagnostopoulos I, et al. The 5th edition of the World Health Organization Classification of Haematolymphoid Tumours: Lymphoid Neoplasms. *Leukaemia*. 2022;36(7):1720-1748. doi:10.1038/s41375-022-01620-2

32. Ahuja AT, Ying M, Ho SY, Antonio G, Lee YP, King AD, et al. Ultrasound of malignant cervical lymph nodes. *Cancer Imaging*. 2008;8(1):48.

33. Weber AL, Rahemtullah A, Ferry JA. Hodgkin and non-Hodgkin lymphoma of the head and neck: clinical, pathologic, and imaging evaluation. *Neuroimaging Clinics*. 2003 Aug 1;13(3):371-92.

34. Lister TA, Crowther D, Sutcliffe SB, Glatstein E, Canellos GP, Young RC, et al. Report of a committee convened to discuss the evaluation and staging of patients with Hodgkin's disease: Cotswolds meeting. *Journal of Clinical Oncology*. 1989 Nov;7(11):1630-6

35. Toledano-Massiah S, Luciani A, Itti E, Zerbib P, Vignaud A, Belhadj K, et al. Whole-body diffusion-weighted imaging in Hodgkin lymphoma and diffuse large B-cell lymphoma. *Radiographics*. 2015 Mar 27;35(3):747- 64.

36. Toma P, Granata C, Rossi A, Garaventa A. Multimodality imaging of Hodgkin disease and non-Hodgkin lymphomas in children. *Radiographics*. 2007 Sep;27(5):1335-54.

37. Adam A, Dixon AK, Gillard JH, Schaefer-Prokop C, Grainger RG, Allison DJ. Grainger & Allison's Diagnostic Radiology E-Book. Elsevier Health Sciences; 2014 Jun 16.

38. D'souza MM, Jaimini A, Bansal A, Tripathi M, Sharma R, Mondal A, Tripathi RP. FDG-PET/CT in lymphoma. *The Indian journal of radiology & imaging*. 2013 Oct;23(4):354.

39. Rumack CM, Levine D. Diagnostic Ultrasound E-Book. Elsevier Health Sciences; 2017 Aug 8

40. Koch BL, Hamilton BE, Hudgins PA, Harnsberger HR. Diagnostic Imaging: Head and Neck E-Book. Elsevier Health Sciences; 2016 Nov 22.

41. David S. Textbook of radiology and imaging. David Sutton (ed.). 2003

42. White KS. Thoracic imaging of pediatric lymphomas. *Journal of thoracic imaging*. 2001 Oct 1;16(4):224-37.

43. Brisse H, Pacquement H, Burdairon E, Plancher C, Neuenschwander S. Outcome of residual mediastinal masses of thoracic lymphomas in children: impact on management and radiological follow-up strategy. *Pediatric radiology*. 1998 Jun 1;28(6):444-50.

44. Rosado-de-Christenson ML, Abbott GF. Diagnostic Imaging: Chest. 2012

45. Hare SS, Souza CA, Bain G, Seely JM, Frcpc, Gomes MM, Quigley M. The radiological spectrum of the pulmonary lymphoproliferative disease. *The British journal of radiology.* 2012 Jul;85(1015):848-64.

46. Paes FM, Kalkanis DG, Sideras PA, Serafini AN. FDG PET/CT of extranodal involvement in non-Hodgkin lymphoma and Hodgkin disease. *Radiographics.* 2010 Jan;30(1):269-91.

47. Fishman EK, Kuhlman J, Jones RJ. CT of lymphoma: spectrum of disease. *Radiographics.* 1991:Jul;11(4):647-69.

48. Saboo SS, Krajewski KM, O'regan KN, Giardino A, Brown JR, Ramaiya N, et al. Spleen in haematological malignancies: spectrum of imaging findings. *The British journal of radiology.* 2012 Jan;85(1009):81-92.,

49. Kaneko J, Sugawara Y, Matsui Y, Ohkubo T, Makuuchi M. Normal splenic volume in adults by computed tomography. *Hepato-gastroenterology.* 2002;49(48):1726-7.

50. Cheson BD, Fisher RI, Barrington SF, Cavalli F, Schwartz LH, Zucca E, Lister TA. Recommendations for initial evaluation, staging, and response assessment of Hodgkin and non-Hodgkin lymphoma: the Lugano classification. *Journal of clinical oncology.* 2014 Sep 20;32(27):3059.

51. Federle MP , Raman SP . Diagnostic Imaging: Gastrointestinal E-Book. Elsevier Health Sciences; 2015 Jul 29.

52. Gore RM, Levine MS. Textbook of Gastrointestinal Radiology E-Book. Elsevier Health Sciences; 2014 Dec 1.

53. Vetro C, Romano A, Amico I, Conticello C, Motta G, Figuera A, et al. Endoscopic features of gastro-intestinal lymphomas: From diagnosis to follow-up. *World Journal of Gastroenterology*: WJG. 2014 Sep 28;20(36):12993.

54. Chua SC, Rozalli FI, O'Connor SR. Imaging features of primary extranodal lymphomas. *Clinical radiology.* 2009 Jun 1;64(6):574-88

55. Hwang S. Imaging of lymphoma of the musculoskeletal system. *Radiologic Clinics.* 2008 Mar 1;46(2):379-96.

56. Slone HW, Blake JJ, Shah R, Guttikonda S, Bourekas EC. CT and MRI findings of intracranial lymphoma. *American Journal of Roentgenology.* 2005 May;184(5):1679- 85.

57. Haldorsen IS, Espeland A, Larsson EM. Central nervous system lymphoma: characteristic findings on traditional and advanced imaging. *American Journal of Neuroradiology*. 2011 Jun 1;32(6):984-92.

58. Bruzzi JF, Macapinlac H, Tsimberidou AM, Truong MT. Detection of Richter's transformation of chronic lymphocytic leukaemia by PET/CT. *The Journal of Nuclear Medicine*. 2006 Aug 1;47(8):1267.

59. Higgins RA, Blankenship JE, Kinney MC. Application of immunohistochemistry in the diagnosis of non-Hodgkin and Hodgkin lymphoma. *Archives of pathology & laboratory medicine.* 2008 Mar;132(3):441-61

60. Carbone PP, Kaplan HS, Musshoff K, Smithers DW, Tubiana M. Report of the committee on Hodgkin's disease staging classification. *Cancer research*. 1971 Nov 1;31(11):1860-1

61. Matasar MJ, Zelenetz AD. Overview of lymphoma diagnosis and management. *Radiologic Clinics.* 2008 Mar 1;46(2):175-98.

62. Townsend W, Linch D. Hodgkin's lymphoma in adults. *The Lancet*. 2012 Sep 1;380(9844):836-47.

63. Johnson SA, Kumar A, Matasar MJ, Schöder H, Rademaker J. Imaging for staging and response assessment in lymphoma. *Radiology*. 2015 Jul 23;276(2):323-38

64. Cheson BD, Horning SJ, Coiffier B, Shipp MA, Fisher RI, Connors JM, et al. Report of an international workshop to standardize response criteria for non-Hodgkin's lymphomas. *Journal of clinical oncology*. 1999 Apr;17(4):1244-.

65. Cheson BD, Pfistner B, Juweid ME, Gascoyne RD, Specht L, Horning SJ, et al. Revised response criteria for malignant lymphoma. *Journal of clinical oncology*. 2007 Feb 10;25(5):579.

66. Juweid ME, Stroobants S, Hoekstra OS, Mottaghy FM, Dietlein M, Guermazi A, et al. Use of positron emission tomography for response assessment of lymphoma: consensus of the Imaging Subcommittee of International Harmonization Project in Lymphoma. *Journal of Clinical Oncology*. 2007 Feb 10;25(5):571-8.

67. Meignan M, Gallamini A, Meignan M, Gallamini A, Haioun C. Report on the first international workshop on interim-PET scan in lymphoma. *Leukaemia & lymphoma*. 2009 Jan 1;50(8):1257-60.

68. Meignan M, Barrington S, Itti E, Gallamini A, Haioun C, Polliack A. Report on the 4th international workshop on positron emission tomography in lymphoma held in

Menton, France, 3–5 October 2012. *Leukaemia & lymphoma*. 2014 Jan 1;55(1):31-7.

69. Van Heertum RL, Scarimbolo R, Wolodzko JG, Klencke B, Messmann R, Tunc F, et al. Lugano 2014 criteria for assessing FDG- PET/CT in lymphoma: an operational approach for clinical trials. *Drug design, development and therapy*. 2017;11:1719.

70. Klimm B, Diehl V, Pfistner B, Engert A. Current treatment strategies of the German Hodgkin Study Group (GHSG). *European Journal of Haematology*. 2005 Jul 1;75(s66):125-34.

71. Papadakis M, McPhee SJ, Rabow MW. CURRENT Medical Diagnosis and Treatment 2016.

72. Moskowitz CH, Schöder H, Teruya-Feldstein J, Sima C, Iasonos A, Portlock CS, et al. Risk-adapted dose-dense immunochemotherapy determined by interim FDG-PET in advanced-stage diffuse large B-cell lymphoma. *Journal of Clinical Oncology*. 2010 Apr 10;28(11):1896

73. Wilson WH, Dunleavy K, Pittaluga S, Hegde U, Grant N, Steinberg SM, et al. Phase II study of dose-adjusted EPOCH- rituximab in untreated diffuse large B-cell lymphoma with analysis of germinal centre and post-germinal center biomarkers. *Journal of clinical oncology: official journal of the American Society of Clinical Oncology*. 2008 Jun 1;26(16):2717.

74. Barrington SF, Mikhaeel NG. PET scans for staging and restaging in diffuse large B- cell and follicular lymphomas. Current hematologic malignancy reports. 2016 Jun 1;11(3):185-95.

75. Lambert L, Burgetova A, Trneny M, et al. The diagnostic performance of whole-body MRI in the staging of lymphomas in adult patients compared to PET/CT and enhanced reference standard-systematic review and meta-analysis. *Quant Imaging Med Surg*. 2022;12(2):1558-1570.

76. Hong, GS., Chae, E.J., Ryu, JS. *et al.* Assessment of naive indolent lymphoma using whole-body diffusion-weighted imaging and T2-weighted MRI: results of a prospective study in 30 patients. *Cancer Imaging* 21, 5 (2021).

77. Lin G, Zong X, Li Y, et al. Whole-Body MRI Is an Effective Imaging Modality for Hematological Malignancy Treatment Response Assessment: A Systematic Review and Meta-Analysis. *Front Oncol*. 2022;12:827777. Published 2022 Feb 18.

78. Spijkers S, Littooij AS, Kwee TC, et al. Whole-body MRI versus an [18F]FDG-PET/CT-based reference standard for early response assessment and restaging of paediatric Hodgkin's lymphoma: a prospective multicentre study. *Eur Radiol*. 2021;31(12):8925-8936.

79. Kharuzhyk S, Zhavrid E, Dziuban A, Sukolinskaja E, Kalenik O. Comparison of whole-body MRI with diffusion-weighted imaging and PET/CT in lymphoma staging. *European Radiology*. 2020 Feb 27:1-9.

80. Shapira-Zaltsberg G, Wilson N, Trejo Perez E, Abbott L, Dinning S, Kapoor C, et al. Whole-Body Diffusion-Weighted MRI Compared to 18 FFDG PET/CT in Initial Staging and Therapy Response Assessment of Hodgkin Lymphoma in Pediatric Patients. *Canadian Association of Radiologists Journal*. 2020 May;71(2):217-25.

81. Gamal, G.H. Whole-body magnetic resonance/diffusion-weighted sequence with background signal suppression (WB-MR/DWIBS) vs. 18F-FDG PET/CT in the diagnosis of lymphoma. *Egypt J Radiol Nucl Med* 51, 210 (2020).

82. Schiavon JL, Regacini R, Luisi FAV, Lederman HM (2019) Whole-body MRI with diffusion sequence Versus FDG-PET/CT: Correlation study on children, adolescents and young adults with Hodgkin lymphoma. Oncol Res Rev 2.

83. Latifoltojar A, Punwani S, Lopes A, et al. Whole-body MRI for staging and interim response monitoring in paediatric and adolescent Hodgkin's lymphoma: a comparison with multi-modality reference standard including (18)F-FDG-PET-CT. *Eur Radiol*. 2019;29(1):202- 212.

84. Wang D, Huo Y, Chen S, et al. Whole-body MRI versus (18)F-FDG PET/CT for pretherapeutic assessment and staging of lymphoma: a meta-analysis. *Onco Targets Ther*. 2018;11:3597-3608.

85. Albano D, Patti C, Matranga D, Lagalla R, Midiri M, Galia M. Whole-body diffusion-weighted MR and FDG-PET/CT in Hodgkin Lymphoma: Predictive role before treatment and early assessment after two courses of ABVD. *Eur J Radiol*. 2018;103:90-98.

86. Albano D, Patti C, Lagalla R, Midiri M, Galia M. Whole-body MRI, FDG-PET/CT, and bone marrow biopsy, for the assessment of bone marrow involvement in patients with newly diagnosed lymphoma. *J Magn Reson Imaging*. 2017;45(4):1082-1089.

87. Azzedine B, Kahina MB, Dimitri P, Christophe P, Alain D, Claude M. Whole-body diffusion-weighted MRI for staging lymphoma at 3.0 T: a comparative study with MR imaging at 1.5 T. *Clin Imaging*. 2015;39 (1):104-109

88. Regacini R, Puchnick A, Shigueoka DC, Iared W, Lederman HM. Whole-body diffusion-weighted magnetic resonance imaging versus FDG-PET/CT for initial lymphoma staging: a systematic review on diagnostic test accuracy studies. *Sao Paulo Med J*. 2015;133(2):141-150.

89. Stecco A, Buemi F, Quagliozzi M, et al. Staging of Primary Abdominal Lymphomas: Comparison of Whole-Body MRI with Diffusion-Weighted Imaging and (18)F-FDG-PET/CT. *Gastroenterol Res Pract*. 2015;2015:104794.

90. Albano Domenico, Patti Caterina, La Grutta Ludovico, Agnello Francesco, Grassedonio Emanuele, Mulgravee Antonino, et al. Comparison between whole-body MRI with diffusion-weighted imaging and PET/CT in staging newly diagnosed FDG-avid lymphomas. *European Journal of Radiology*.

91. Balbo-Mussetto A, Cirillo S, Bruna R, et al. Whole-body MRI with diffusion-weighted imaging: a valuable alternative to contrast-enhanced CT for initial staging of aggressive lymphoma. *Clin Radiol*. 2016;71(3):271-279.

92. Mayerhoefer ME, Karanikas G, Kletter K, et al. Evaluation of diffusion-weighted MRI for pretherapeutic assessment and staging of lymphoma: results of a prospective study in 140 patients. *Clin Cancer Res*. 2014;20(11):2984-2993.

93. Littooij AS, Kwee TC, Barber I, et al. Whole-body MRI for initial staging of paediatric lymphoma: prospective comparison to an FDG-PET/CT-based reference standard. *Eur Radiol*. 2014;24(5):1153-1165.

94. Horger M, Claussen C, Kramer U, Fenchel M, Lichy M, Kaufmann S. Very early indicators of response to systemic therapy in lymphoma patients based on alterations in water diffusivity—a preliminary experience in 20 patients undergoing whole-body diffusion-weighted imaging. *Eur J Radiol*. 2014;83(9):1655-1664.

95. Punwani S, Cheung KK, Skipper N, et al. Dynamic contrast-enhanced MRI improves accuracy for detecting focal splenic involvement in children and adolescents with Hodgkin disease. *Pediatr Radiol*. 2013; 43(8):941-949

96. Adams HJA, Kwee TC, Vermoolen MA, et al. Whole-body MRI for the detection of bone marrow involvement in lymphoma: prospective study in 116 patients and comparison with FDG-PET. *Eur Radiol*. 2013;23(8):2271-2278.

97. Abdulqadhr G, Molin D, Aström G, et al. Whole-body diffusion-weighted imaging compared with FDG-PET/CT in the staging of lymphoma patients. *Acta Radiol*. 2011;52(2):173-180.

98. Punwani S, Taylor SA, Bainbridge A, et al (2010) Pediatric and adolescent lymphoma: comparison of whole-body STIR half-Fourier RARE MR imaging with an enhanced PET/CT reference for initial staging. *Radiology* 255:182-190.

99. Van Ufford HM, Kwee TC, Beek FJ, et al. Newly diagnosed lymphoma: initial results with whole-body T1-weighted, STIR, and diffusion-weighted MRI compared with 18F-FDG PET/CT. *AJR Am J Roentgenol*. 2011;196(3):662-669.

100. Lin C, Luciani A, Itti E, et al. Whole-body diffusion-weighted magnetic resonance imaging with apparent diffusion coefficient mapping for staging patients with diffuse large B-cell lymphoma. *Eur Radiol*. 2010;20(8):2027-2038.

101. Kwee TC, Vermoolen MA, Akkerman EA, et al. Whole-body MRI, including diffusion-weighted imaging, for staging lymphoma: comparison with CT in a prospective multicenter study. *J Magn Reson Imaging*. 2014;40(1):26-36.

102. Brennan DD, Gleeson T, Coate LE, Cronin C, Carney D, Eustace SJ. A comparison of whole-body MRI and CT for the staging of lymphoma. *AJR Am J Roentgenol*. 2005;185(3):711-716.

103. Albano D, Bruno A, Patti C, et al. Whole-body magnetic resonance imaging (WB-MRI) in lymphoma: State of the art. *Hematol Oncol*. 2020;38(1):12-21.

ANNEXURE I
ETHICAL CLEARANCE CERTIFICATE

अखिल भारतीय आयुर्विज्ञान संस्थान, जोधपुर
All India Institute of Medical Sciences, Jodhpur
संस्थागत नैतिकता समिति
Institutional Ethics Committee

No. AIIMS/IEC/2021/ 3558

Date: 12/03/2021

ETHICAL CLEARANCE CERTIFICATE

Certificate Reference Number: **AIIMS/IEC/2021/3393**

Project title: **"Role of Whole-Body MRI in lymphoma staging: A Comparison with composite reference standard including ^{18}F-FDG-PET/CT"**

Nature of Project:	**Research Project Submitted for Expedited Review**
Submitted as:	**M.D. Dissertation**
Student Name:	**Dr. Lunavath Veeranna**
Guide:	**Dr. Taruna Yadav**
Co-Guide:	**Dr. Pushpinder Singh Khera, Dr. Rajesh Kumar, Dr. Puneet Pareek, Dr. Siyaram Didel, Dr. Binit Sureka, Dr. Arun Prashanth & Dr. Poonam Elhence**

Institutional Ethics Committee after thorough consideration accorded its approval on above project.

The investigator may therefore commence the research from the date of this certificate, using the reference number indicated above.

Please note that the AIIMS IEC must be informed immediately of:
- Any material change in the conditions or undertakings mentioned in the document.
- Any material breaches of ethical undertakings or events that impact upon the ethical conduct of the research.

The Principal Investigator must report to the AIIMS IEC in the prescribed format, where applicable, bi-annually, and at the end of the project, in respect of ethical compliance.

AIIMS IEC retains the right to withdraw or amend this if:

- Any unethical principle or practices are revealed or suspected
- Relevant information has been withheld or misrepresented

AIIMS IEC shall have an access to any information or data at any time during the course or after completion of the project.

Please Note that this approval will be rectified whenever it is possible to hold a meeting in person of the Institutional Ethics Committee. It is possible that the PI may be asked to give more clarifications or the Institutional Ethics Committee may withhold the project. The Institutional Ethics Committee is adopting this procedure due to COVID-19 (Corona Virus) situation.

If the Institutional Ethics Committee does not get back to you, this means your project has been cleared by the IEC.

On behalf of Ethics Committee, I wish you success in your research.

Dr. Praveen Sharma
Member Secretary
Member secretary
Institutional Ethics Committee
AIIMS,Jodhpur

Basni Phase-2, Jodhpur, Rajasthan-342005; **Website:** www.aiimsjodhpur.edu.in; **Phone:** 0291-2740741 Extn. 3109
E-mail : ethicscommittee@aiimsjodhpur.edu.in; ethicscommitteeaiimsjdh@gmail.com

Annexure II

PATIENT INFORMATION SHEET

Title of study: **Role of Whole-Body MRI in lymphoma staging: A Comparison with composite reference standard including ^{18}F-FDG-PET/CT.**

1. Aim of the study: To evaluate the role of Whole-Body MRI for staging in cases of lymphoma.
2. Expected duration of the subject participation: 2 years
3. Benefits from the Study:
    The study, if successful, will help in establishing Whole-Body Diffusion-Weighted MRI as the diagnostic modality of choice in staging and interim response assessment as a radiation-free and cost-effective alternative to ^{18}F-FDG-PET/CT which will improve patient management.
4. Risks to the patients: No risks.
5. Confidentiality: Your participation will be kept confidential. Your medical records will be treated with confidentiality and will be revealed only to doctors/ scientists involved in this study. The results of this study may be published in a scientific journal, but you will not be identified by name.
6. Provision of free treatment for research-related injury.
7. Compensation of subjects for disability or death resulting from such injury.
8. Freedom of the individual to participate and to withdraw from the research at any time without penalty or loss of benefits to which the subject would otherwise be entitled - You have complete freedom to participate and to withdraw from the research at any time without penalty or loss of benefits to which you would otherwise be entitled. Your participation in the study is optional and voluntary. A copy of the results of the investigations performed will be provided to you for your record. You can withdraw from the project at any time, and this will not affect your subsequent medical treatment or relationship with the treating physician. Any additional expense for the project, other than your regular expenses, will not be charged to you.
9. Costs and source of investigations, disposables, and drugs
    Institute charges for ^{18}F-FDG-PET/CT and Whole-Body Diffusion-Weighted MRI- Exempted.
10. For further information and to report any side effects/complications, kindly contact:

    Dr. Lunavath Veeranna

    Junior resident

    Department of Diagnostic and Interventional radiology

    AIIMS, Jodhpur

    Mobile no: 9493293808

Annexure III

रोगी सूचना पत्र

अध्ययन का शीर्षक: लिम्फोमा मंचन में पूरे शरीर एमआरआई की भूमिका: 18-एफ एफडीजी-पीईटी / सीटी सहित समग्र संदर्भ मानक के साथ तुलना ।

1. अध्ययन का उद्देश्य: लिम्फोमा के मामलों में मंचन के लिए होल-बॉडी एमआरआई की भूमिका का मूल्यांकन   करना।

2. विषय भागीदारी की अपेक्षित अवधि: 2 वर्ष

3. अध्ययन से लाभ: अध्ययन सफल होने पर, यह लिंफोमा के स्टेजिंग और अंतरिम प्रतिक्रिया के आकलन में होल-बॉडी डिफ्यूजन एमआरआई को 18-एफ एफडीजी-पीईटी / सीटी के विकल्प के रूप में एक पूर्ण रूप से विकिरण मुक्त, लागत प्रभावी और जो रोगी प्रबंधन को बेहतर बनाता है, यह स्थापित करने में मदद करेगा।

4. मरीजों को जोखिम: कुछ नहीं

5. गोपनीयता: आपकी भागीदारी को गोपनीय रखा जाएगा। आपके मेडिकल रिकॉर्ड को गोपनीयता के साथ माना जाएगा और इस अध्ययन में शामिल डॉक्टरों / वैज्ञानिकों के लिए ही पता चलेगा। इस अध्ययन के परिणाम एक वैज्ञानिक पत्रिका में प्रकाशित हो सकते हैं, लेकिन आपको नाम से नहीं पहचाना जाएगा।

6. अनुसंधान से संबंधित चोट के लिए मुफ्त उपचार का प्रावधान।

7. इस तरह की चोट के परिणामस्वरूप विकलांगता या मृत्यु के लिए विषयों का मुआवजा।

8. भाग लेने या लाभ के नुकसान के बिना किसी भी समय अनुसंधान से पीछे हटने की स्वतंत्रता, जिस पर विषय अन्यथा हकदार होगा - आपको दंड या लाभ के नुकसान के बिना किसी भी समय अनुसंधान से भाग लेने और वापस लेने की पूरी स्वतंत्रता है। जिसके लिए आप अन्यथा हकदार होंगे। अध्ययन में आपकी भागीदारी वैकल्पिक और स्वैच्छिक है। आपके द्वारा रिकॉर्ड की गई जांच के परिणामों की प्रति आपको प्रदान की जाएगी। आप किसी भी समय परियोजना से हट सकते हैं, और यह आपके बाद के चिकित्सा उपचार या उपचार चिकित्सक के साथ संबंध को प्रभावित नहीं करेगा। परियोजना के लिए कोई अतिरिक्त खर्च, आपके नियमित खर्च के अलावा, आपसे कोई शुल्क नहीं लिया जाएगा।

9. जांच, डिस्पोजल और ड्रग्स की लागत और स्रोत: 18-एफ एफडीजी-पीईटी / सीटी और संपूर्ण बॉडी एमआरआई के लिए संस्थान शुल्क की छूट ।

10. अधिक जानकारी के लिए और किसी भी दुष्प्रभाव / जटिलताओं की रिपोर्ट करने के लिए, कृपया संपर्क करें:

डॉ। लूणावत वीरन्ना

जूनियर निवासी

डायग्नोस्टिक और इंटरवेंशनल रेडियोलॉजी विभाग

एम्स, जोधपुर

मोबाइल नंबर: 9493293808

Annexure IV
PARTICIPANT INFORMED CONSENT FORM

Participant identification number for this trial: _____

Title of project: **Role of Whole-Body MRI in lymphoma staging: A Comparison with composite reference standard including ^{18}F-FDG PET/CT**.

Name of Principal Investigator: Dr. Lunavath Veeranna.

Contact no 9493293808

The Contents of the information sheet dated ………………. that was provided have been read carefully by me / explained in detail to me, in a language that I comprehend, and I have fully understood the contents. I confirm that I have had the opportunity to ask questions. The nature and purpose of the study and its potential risks/benefits and expected duration of the study and other relevant details of the study have been explained to me in detail. I understand that my participation is voluntary and that I am free to withdraw at any time, without giving any reason, without my medical care or legal right being affected.

I understand that the information collected about me from my participation in this research and sections of any of my medical notes may be looked at by responsible individuals from AIIMS. I permit these individuals to have access to my records.

I agree to take part in the above study.

Date: _ _ _ _ _ _ _ _   Place: _ _ _ _ _ _ _ _

(Signatures / Left Thumb Impression):

Name of the Participant: _____

Son / Daughter / Spouse of: _____

Complete postal address:

_____

This is to certify that the above consent has been obtained in my presence:
_____

Signature of the Principal Investigator:

Date: Place:

1) Witness – 1   2) Witness – 2

Signature ----------------------------   Signature -------------------------

Name: Name:

Address: Address:

Annexure V

प्रतिभागी सूचित सहमति फार्म

इस परीक्षण के लिए प्रतिभागी की पहचान संख्या: _____

परियोजना का शीर्षक: लिम्फोमा मंचन में पूरे शरीर एमआरआई की भूमिका: 18-एफ एफडीजी-पीईटी / सीटी सहित समग्र संदर्भ मानक के साथ तुलना।

प्रधान अन्वेषक का नाम: डॉ। लूणावत वीरन्ना
संपर्क नंबर 9493293808

सूचना पत्र की विषय-सूची दिनांक ....। यह प्रदान किया गया था कि मुझे मेरे द्वारा सावधानीपूर्वक पढ़ा गया / मुझे विस्तार से समझाया गया, जिस भाषा में मैं समझता हूं, और मैं पूरी तरह से विषय-सूची को समझ गया हूं। मैं पुष्टि करता हूं कि मुझे सवाल पूछने का अवसर मिला है। अध्ययन की प्रकृति और उद्देश्य और इसके संभावित जोखिम / लाभ और अध्ययन की अपेक्षित अवधि, और अध्ययन के अन्य प्रासंगिक विवरण मुझे विस्तार से बताए गए हैं। मैं समझता हूं कि मेरी भागीदारी स्वैच्छिक है और मैं बिना किसी कारण के किसी भी समय वापस लेने के लिए स्वतंत्र हूं, बिना मेरी चिकित्सा देखभाल या कानूनी अधिकार प्रभावित हुए बिना।

मैं समझता हूं कि इस शोध में मेरी भागीदारी से मेरे बारे में एकत्र की गई जानकारी और मेरे किसी भी मेडिकल नोट के वर्गों को एम्स के जिम्मेदार व्यक्तियों द्वारा देखा जा सकता है। मैं इन व्यक्तियों को अपने रिकॉर्ड तक पहुंचने की अनुमति देता हूं।

मैं उपरोक्त अध्ययन में भाग लेने के लिए सहमत हूं।

दिनांक: _ _ _ _ _ _ _ _ स्थान: _ _ _ _ _ _ _ _

(हस्ताक्षर / बाएं अंगूठे का निशान):

प्रतिभागी का नाम: _____

पुत्र / पुत्री / पति / पत्नी: _____

पूरा डाक पता: _____

यह प्रमाणित करता हूं कि मेरी उपस्थिति में उपरोक्त सहमति प्राप्त की गई है: _____

प्रधान अन्वेषक का हस्ताक्षर:

दिनांक: स्थान:

1) गवाह - 1   2) गवाह - 2

हस्ताक्षर ----------------------------   हस्ताक्षर ------------------------

नाम: नाम:

पता :   पता:

<u>ANNEXURE – VI</u>

<u>PATIENT PROFORMA</u>

Name :   Age/Sex:

Patient ID   Date

<u>Imaging findings:</u>

Lymph nodal staions

Nodal site	STIR	DWI	WB-MRI	PET/CT	CRS
Cervical station					
Suparaclavicular					
Mediastinal					
Hilar station					
Liver hilar					
Para-aortic					
Mesenteric					
Iliac station					
Inguinal station					
Axillary station					

<u>Extra nodal site or organ involvement.</u>

Extra-nodal site	Imaging modality					Other features
	STIR	DWI	Wb-mri	PET	CRS	Encasement of vessels / Calcification / Hemorrhage / Necrosis
Lung						
B marrow						
Liver						
Spleen						
Kidney						
Stomach						
Pancreas						
Bowel						
PLEURA						
PERICARDI						
CHEST WALL						

STAGING

	STIR	DWI	WB-MRI	PET/CT	Composite
Stage					

Histopathology report:

Bone marrow biopsy report:

Liver size :   cm, Spleen size: cm.

<u>ANNEXURE – VII</u>
<u>MASTER CHART</u>

CERVICAL / SUPRACLAVICULAR / AXILLARY / MEDIASTINAL / HILAR / MESENTERIC / LIVER HILAR / PARA-AORTIC / ILIAC / INGUINAL STATIONS

Each station group has columns: STIR, DWI, WB-MRI, PET-CT, Composite. Right-most columns: Bulky disease, STIR stage, DWI stage, WB-MRI stage, PET-stage, Composite stage.

SL. NO	Age/Sex	HPE	Bulky disease	STIR stage	DWI stage	WB-MRI stage	PET-stage	Composite stage
1	39Y/M	DLBCL	YES	IV	IV	IV	IV	IV
2	55Y/F	Mantle cell Lymphoma- Classical variant	NO	II	II	II	II	II
3	29Y/F	Hodgkin's lymphoma	NO	IV	IV	IV	IV	IV
4	55Y/M	Follicular lymphoma	YES	IV	IV	IV	IV	IV
5	7Y/M	Classical HL - Nodular sclerosis.	NO	IIIS	IIIS	IIIS	IV	IV
6	10Y/F	Classic Hodgkin's lymphoma	YES	II	II	II	II	II
7	41Y/M	DLBCL	NO	IV	IV	IV	IV	IV
8	12Y/F	Anaplstic large cell lymphoma	NO	IIIE	IIIE	IIIE	IIIE	IIIE
9	38Y/M	NHL -CLL	NO	IV	IV	IV	IV	IV
10	31Y/M	Primary mediastinal large B cell lymphoma.	YES	IV	IV	IV	IV	IV
11	60Y/F	CLL / Small lymphocytic lymphoma	NO	IV	IV	IV	IV	IV
12	16Y/F	Lymphocytic predominance - classical HL.	NO	I	I	I	I	I
13	11Y/M	Classic HL - mixed cellularity	NO	II	IIIS	IIIS	IIIS	IIIS
14	49Y/M	FNAC - HODGKIN'S LYMPHOMA	NO	III	TkI	III	III	II
15	43Y/M	PLHA, DLBCL	YES	IV	IV	IV	IV	IV
16	28Y/M	Classical HL - mixed cellularity	NO	IIIS	IIIS	IIIS	IIIS	IIIS
17	29Y/F	Primary mediastinal large B-cell lymphoma.	YES	IV	IV	IV	IV	IV
18	56Y/M	Hodgkin's lymphoma	NO	IV	IV	IV	IV	IV
19	13Y/M	Burkitt lymphoma.	NO	IV	IV	IV	IV	IV
20	70Y/M	DLBCL - germinal centre type	NO	IV	IV	IV	IV	IV
21	44Y/M	HL nodular sclerosis type.	NO	IV	IV	IV	IV	IV
22	45Y/M	Classic HL - Nodular sclerosis	NO	III	IV	IV	IV	IV
23	17Y/M	Nodular lymphocyte predominant HL	NO	IV	IV	IV	IV	IV
24	9Y/F	Classical HL - mixed cellularity	YES	IIIS	IIIS	IIIS	IIIS	IIIS
25	47Y/M	Classical Hodgkin's lymphoma	NO	IV	IV	IV	IV	IV
26	39Y/M	Gastric lymphoma - NHL - DLBCL	NO	IE	IIE	IIE	IIE	IIE
27	9Y/F	Classical HL -Mixed cellularity	YES	IV	IV	IV	IV	IV
28	70Y/F	DLBCL	NO	IV	IV	IV	IV	IV
29	14Y/M	Burkits lymphoma	YES	IV	IV	IV	IV	IV
30	22Y/M	NHL -CLL/SLL	NO	IV	IV	IV	IV	IV
31	38Y/M	DLBCL	NO	IV	IV	IV	IV	IV
32	64Y/F	DLBCL	YES	IV	IV	IV	IV	IV
33	68Y/F	NHL	NO	IIIE	IIIE	IIIE	IIIE	IIIE
34	54Y/M	Hodgkin's lymphoma	NO	IV	IV	IV	IV	IV
35	54Y/M	DLBCL	NO	IV	IV	IV	IV	IV
36	65Y/F	DLBCL - GCB TYPE	NO	II	II	II	II	II

EXTRA NODAL DISEASE

Stations: BONE MARROW, LUNG, LIVER, SPLEEN, KIDNEY, STOMACH, PANCREAS, BOWEL, PLEURA, PERICARDIUM, CHEST WALL. Each with columns: STIR, DWI, WB-MRI, PET-CT, Composite.

SL. NO	Age/Sex	HPE
1	39Y/M	DLBCL
2	55Y/F	Mantle cell Lymphoma- Classical variant
3	29Y/F	Hodgkin's lymphoma
4	55Y/M	Follicular lymphoma
5	7Y/M	Classical HL - Nodular sclerosis.
6	10Y/F	Classic Hodgkin's lymphoma
7	41Y/M	DLBCL
8	12Y/F	Anaplstic large cell lymphoma
9	38Y/M	NHL -CLL
10	31Y/M	Primary mediastinal large B cell lymphoma.
11	60Y/F	CLL / Small lymphocytic lymphoma
12	16Y/F	Lymphocytic predominance - classical HL.
13	11Y/M	Classic HL - mixed cellularity
14	49Y/M	FNAC - HODGKIN'S LYMPHOMA
15	43Y/M	PLHA, DLBCL
16	28Y/M	Classical HL - mixed cellularity
17	29Y/F	Primary mediastinal large B-cell lymphoma.
18	56Y/M	Hodgkin's lymphoma
19	13Y/M	Burkitt lymphoma.
20	70Y/M	DLBCL - germinal centre type
21	44Y/M	HL nodular sclerosis type.
22	45Y/M	Classic HL - Nodular sclerosis
23	17Y/M	Nodular lymphocyte predominant HL
24	9Y/F	Classical HL - mixed cellularity
25	47Y/M	Classical Hodgkin's lymphoma
26	39Y/M	Gastric lymphoma - NHL - DLBCL
27	9Y/F	Classical HL -Mixed cellularity
28	70Y/F	DLBCL
29	14Y/M	Burkits lymphoma
30	22Y/M	NHL -CLL/SLL
31	38Y/M	DLBCL
32	64Y/F	DLBCL
33	68Y/F	NHL
34	54Y/M	Hodgkin's lymphoma
35	54Y/M	DLBCL
36	65Y/F	DLBCL - GCB TYPE